Local delivery strategies for nitric oxide and gene therapy delivery

Mario López Moya

http://hdl.handle.net/10803/670610

ADVERTIMENT. L'accés als continguts d'aquesta tesi doctoral i la seva utilització ha de respectar els drets de la persona autora. Pot ser utilitzada per a consulta o estudi personal, així com en activitats o materials d'investigació i docència en els termes establerts a l'art. 32 del Text Refós de la Llei de Propietat Intel·lectual (RDL 1/1996). Per altres utilitzacions es requereix l'autorització prèvia i expressa de la persona autora. En qualsevol cas, en la utilització dels seus continguts caldrà indicar de forma clara el nom i cognoms de la persona autora i el títol de la tesi doctoral. No s'autoritza la seva reproducció o altres formes d'explotació efectuades amb finalitats de lucre ni la seva comunicació pública des d'un lloc aliè al servei TDX. Tampoc s'autoritza la presentació del seu contingut en una finestra o marc aliè a TDX (framing). Aquesta reserva de drets afecta tant als continguts de la tesi com als seus resums i índexs.

ADVERTENCIA. El acceso a los contenidos de esta tesis doctoral y su utilización debe respetar los derechos de la persona autora. Puede ser utilizada para consulta o estudio personal, así como en actividades o materiales de investigación y docencia en los términos establecidos en el art. 32 del Texto Refundido de la Ley de Propiedad Intelectual (RDL 1/1996). Para otros usos se requiere la autorización previa y expresa de la persona autora. En cualquier caso, en la utilización de sus contenidos se deberá indicar de forma clara el nombre y apellidos de la persona autora y el título de la tesis doctoral. No se autoriza su reproducción u otras formas de explotación efectuadas con fines lucrativos ni su comunicación pública desde un sitio ajeno al servicio TDR. Tampoco se autoriza la presentación de su contenido en una ventana o marco ajeno a TDR (framing). Esta reserva de derechos afecta tanto al contenido de la tesis como a sus resúmenes e índices.

WARNING. The access to the contents of this doctoral thesis and its use must respect the rights of the author. It can be used for reference or private study, as well as research and learning activities or materials in the terms established by the 32nd article of the Spanish Consolidated Copyright Act (RDL 1/1996). Express and previous authorization of the author is required for any other uses. In any case, when using its content, full name of the author and title of the thesis must be clearly indicated. Reproduction or other forms of for profit use or public communication from outside TDX service is not allowed. Presentation of its content in a window or frame external to TDX (framing) is not authorized either. These rights affect both the content of the thesis and its abstracts and indexes.

C.I.F. G: 59069740 Universitat Ramon Llull Fundació Rgtre. Fund. Generalitat de Catalunya núm. 472 (28-02-90)

UNIVERSITAT RAMON LLULL

DOCTORAL THESIS

Title	Local delivery strategies for nitric oxide and gene therapy delivery
Presented by	Mario López Moya
Centre	IQS School of Engineering
Department	Bioengineering
Directed by	Dr. Víctor Ramos Dr. Salvador Borrós

ACKNOLEDGMENTS

En primer lugar, al Dr. Salvador Borrós y a mi padre por prestarme su apoyo incondicional.

Al Dr. Víctor Ramos, por su inestimable ayuda, afecto e inigualable condición humana.

A todos mis compañeros de esta aventura, por haber compartido tantos buenos momentos haciéndola única e irrepetible.

A la futura doctora Ana López, por ayudarme siempre y esperarme durante tantas y tantas horas.

A los miembros del Institut Químic de Sarrià y la Universitat Ramon Llull, por su comprensión y apoyo durante la realización de este trabajo.

A todos los voluntarios que han participado en el estudio clínico, simplemente agradecerles su participación altruista y, en especial, al Dr. Emili Masferrer.

Al grupo del Dr. Wladimiro Jiménez, por hacer posible el desarrollo de esta investigación.

Finalmente, a mi querida Carlota por su paciencia esperándome durante innumerables noches y días festivos dedicados a la investigación.

This research has been financially supported by SUR (Secretaria d'Universitats i Recerca) of the DEC (Departament d'Empresa i Coneixement) of the Government of Catalonia and the European Social Fund (grants 2016FI_B 00703; 2017FI_B1 00113; 2018FI_B2 00136).

ABSTRACT

Over the last decades a great deal of expectation has been generated on the translation of RNA technology into clinical practice. Although an initial fast translation was foreseen some decades ago, complexities related to administration and delivery have limited introduction as an available therapeutic option. When compared to traditional drugs, RNA technologies require vectors to allow distribution, internalization and ultimately alteration of expression. Mainly, viral and non-viral vectors have been proposed as viable strategies to enhance efficiency. However, use of synthetic vectors have advantages such as versatility, scale-up capabilities and reproducibility. Among the best polymeric vector families are pBAE, a family of biodegrade polymers specifically developed to be non-toxic, form stable nanoparticles and facilitate endosomal scape.
Although RNAs hold a great therapeutic potential, treatment of complex multistage diseases usually requires a multifactor approach to improve clinical outcomes. Nitric oxide plays a deep effect on epithelial biology and development of dual therapies may hold a strong potential to improve outcomes of complex diseases.
Introduction of nitric oxide to pBAE has been accomplished both by adding organic nitrates and thionitrites. Organic nitrate containing pBAE nanoparticles have been found to form stable and effective nanoparticles while showing vasodilation effects *in vivo*. On the other hand, use of thionitrites as NO releasing moieties, shows a stronger nitric oxide release pattern, self-crosslinking and limited toxicity. Its applications have been directed towards local antimicrobial applications. One of the studied applications has been the coating of airway stents, showing a promising decrease of bacterial colonization. Similar results have been obtained in dermal applications were antimicrobial and dermal vasodilation effects have been observed in preclinical models and early stage clinical trials.

In conclusion, this thesis demonstrates that local treatments combined with a new family of pBAE based polymers with integrated capabilities to deliver nitric oxide could be a potential useful tool to treat cardiovascular and epidermal diseases.
An additional family of polymers containing nitric oxide, has successfully dedicated to antimicrobial applications.

RESUMEN

Durante las últimas décadas se han generado grandes expectativas sobre la translación de la tecnología del ARN a la práctica clínica. Aunque inicialmente se previó una transferencia rápida, las complejidades relacionadas con la administración y biodistribución han limitado la disponibilidad como herramienta terapéutica. En comparación con los fármacos tradicionales, las tecnologías de ARN requieren vectores para permitir la distribución, internalización y, en última instancia, alteración de la expresión proteica. Principalmente, vectores virales y no virales han sido propuestos como estrategias viables para mejorar la eficiencia de expresión. Sin embargo, el uso de vectores sintéticos tiene varias ventajas, como versatilidad, capacidad de escalado y reproducibilidad. Entre las mejores familias de vectores poliméricos se encuentran los poly(β-aminoesteres), una familia de polímeros específicamente desarrollados para formar complejos con ácidos nucleicos en forma de nanopartículas estables, biodegradarse y facilitar el escape de endosomas.

Aunque los ARN tienen un gran potencial terapéutico, el tratamiento de enfermedades complejas de múltiples etapas generalmente requiere un enfoque multifactorial para mejorar los resultados clínicos. El óxido nítrico tiene un profundo efecto en la biología epitelial teniendo el desarrollo de terapias duales un gran potencial para mejorar los resultados de enfermedades complejas.

La introducción de óxido nítrico al pBAE se ha logrado mediante la adición de nitratos orgánicos y tionitritos. Se ha descubierto que las nanopartículas de pBAE que contienen nitratos orgánicos forman nanopartículas estables y eficaces a la vez que muestran efectos vasodilatadores *in vivo*. Por otro lado, el uso de tionitritos como grupos liberadores de NO, muestra un patrón de liberación de óxido nítrico mas rápido y directo, auto-recirculación y toxicidad limitada. Sus aplicaciones se han dirigido a terapias antimicrobianas locales. Una de las aplicaciones estudiadas ha sido el recubrimiento de stents de las vías respiratorias, mostrando una prometedora disminución de la colonización bacteriana en la superficie de los dispositivos. Del mismo modo se han obtenido resultados similares en aplicaciones dérmicas donde se han observado efectos vasodilatadores dérmicos y antimicrobianos en modelos preclínicos y ensayos clínicos.

En conclusión, esta tesis demuestra que los tratamientos locales combinados con una nueva familia de polímeros basados en pBAE con capacidades integradas para administrar óxido nítrico podrían ser una herramienta potencialmente útil para tratar enfermedades cardiovasculares y epidérmicas.

Una familia adicional de polímeros que contienen óxido nítrico se ha dedicado con éxito a aplicaciones antimicrobianas.

RESUM

Durant les últimes dècades s'han generat grans expectatives sobre la translació de la tecnologia de l'ARN a la pràctica clínica. Encara que inicialment es va preveure una transferència ràpida, les complexitats relacionades amb l'administració i biodistribució han limitat la disponibilitat com a eina terapèutica. En comparació amb els fàrmacs tradicionals, les tecnologies d'ARN requereixen vectors per permetre la distribució, internalització i, en última instància, alteració de l'expressió proteica. Principalment, vectors virals i no virals han estat proposats com a estratègies viables per millorar l'eficiència d'expressió. No obstant, l'ús de vectors sintètics té diversos avantatges, com versatilitat, capacitat d'escalat i reproductibilitat. Entre les millors famílies de vectors polimèrics es troben els poly (β-aminoesteres), una família de polímers específicament desenvolupats per formar complexos amb àcids nucleics en forma de nanopartícules estables, biodegradar-se i facilitar l'escap de l'endosoma.

Tot i que els ARN tenen un gran potencial terapèutic, el tractament de malalties complexes amb múltiples etapes generalment requereix un enfoc multifactorial per millorar els resultats clínics. L'òxid nítric té un profund efecte en la biologia epitelial tenint el desenvolupament de teràpies duals un gran potencial per millorar els resultats de malalties complexes.

La introducció d'òxid nítric als pBAE s'ha aconseguit mitjançant l'addició de nitrats orgànics i tionitrits. S'ha descobert que les nanopartícules de pBAE que contenen nitrats orgànics formen nanopartícules estables i eficaces alhora que mostren efectes vasodilatadors *in vivo*. D'altra banda, l'ús de tionitrits com a grups alliberadors de NO, mostra un patró d'alliberament d'òxid nítric més ràpid i directe, auto-recirculació i toxicitat limitada. Les seves aplicacions s'han dirigit a aplicacions antimicrobianes locals. Una de les aplicacions estudiades ha estat el recobriment de stents de les vies respiratòries, mostrant una prometedora disminució de la colonització bacteriana en la superfície dels dispositius. S'han obtingut resultats similars en aplicacions dèrmiques on s'han observat efectes vasodilatadors dèrmics i antimicrobians en models preclínics i assajos clínics.

En conclusió, aquesta tesi demostra que els tractaments locals combinats amb una nova família de polímers basats en pBAE amb capacitats integrades per administrar òxid nítric podrien ser una eina potencialment útil per tractar malalties cardiovasculars i epidèrmiques.

Una família addicional de polímers que contenen òxid nítric s'ha dedicat amb èxit a aplicacions antimicrobianes.

TABLE OF CONTENTS

INDEX OF FIGURES

LIST OF ABREVIEATIONS

AAV	Adeno associated virus
ALDH	Aldehyde dehydrogenase
AMI	Acute myocardial infarction
C32	Aminopentanol-1,4-butanodioldiacrilate polybetaamino ester
C32-CK3	Trilysine oligopeptide terminated aminopentanol-1,4-butanodioldiacrilate polybetaamino ester
CEIC	Clinical ethical investigation committee
CFU	Colony forming units
cGMP	Cyclic guanosine monophosphate
CK3	Cys-Lys-Lys-Lys peptide
CVD	Cardiovascular disease
DAF	Fluorescein diacetate
DAF-FM	Diacetate (4-Amino-5-Methylamino-2',7'-Difluorofluorescein Diacetate)
DCC	N,N'-Dicyclohexylcarbodiimide
DCU	Dicyclohexylurea
DES	Drug eluting stent
DEB	Drug eluting balloon
DEA	diethyleneamine
DETA	diethylenetriamine
DLS	Dynamic Light Scattering
DMSO	Dimethylsulfoxide
DMAP	Dimethylaminopyridine
DNA	Deoxyribonucleic Acid
EDRF	Endothelial derived relaxing factor
EMA	European Medicines Agency
FACS	Fluorescence-Activated Cell Sorting
FBS	Fetal Bovine Serum
FDA	Food and Drug Administration
FTIR	Fourier Transformer Infrared spectroscopy
HDNF	Human Dermal Neonatal Fibroblast
HF	Heart Failure
iRNA	interfering Ribonucleic acid
IC50	Half maximal inhibitory concentration
K72-NO	pBAE based of 1,5-aminopanyl 6-nitrooxyhexanoate polymerized with butanodiacrilate and end-modified with Cys-Lys-Lys-Lys peptide.
LC50	Half lethal concentration
LDPM	Laser doppler perfusion monitoring
LNP	Lipid nanoparticles
MDA	Epithelial human breast cancer cell line MDA-MB-231

MTS	3-(4,5-dimethylthiazol-2-yl)-5-(3-carboxymethoxyphenyl)-2-(4-sulfophenyl-2H-tetrazolium
miRNA	micro-interference ribonucleic acid
MVTR	Mobile vapor transfer rate
MYBPC	Cardiac myoglobin binding protein
NAcGal	N-Acetyl-Galactosamine
NADPH	Nicotinamide adenine dinucleotide phosphate
NMR	Nuclear magnetic resonance
NO	Nitric oxide
NONOate	Diazeniumdiolate
NOS	Nitric oxide synthase
NP	Nanoparticle
eNOS	endothelial isoform of nitric oxide synthase
iNOS	induced nitric oxide synthase
nNOS	neural nitric oxide synthase
PAMAM	Poly(amidoamine)
PBAE	Polybetaaminoesther
PBS	Phosphate buffer saline
pDMAEMA	Poly(2-(dimethylamino)ethyl methacrylate)
PEG	Poly Ethylene Glycol
PCI	Percutaneous Coronary Intervention
PCL	Polycaprolactone
PLA	Polylactic acid
PLGA	Polylactic-co-glycolic acid
PLLA	Poly-L-Lactic acid
PGA	Polyglycolic acid
RISC	RNA-induced silencing complex
RNA	Ribonucleic acid
SARTI	stent-associated respiratory tract infection
siRNA	small-interfering Ribonucleic acid
SNAP	S-nitroso-N-acetylpenicillamine
SNO	S-nitrosothiol/thionitrite
TEWL	Trans epidermal water loss
THF	Tetrahydrofuran
TMS	Tetramethylsilane
T64-SNO	pBAE based of 1,5-aminopanyl 6-S-nitrosomercaptohexanoate polymerized with butanodiacrilate.
VSMC	Vascular smooth muscle cell

CHAPTER 0. MOTIVATION AND AIMS

During the last century, pharmacology has emerged as one of the major tools in modern medicine. Classical pharmacology has been based on the topological interference of enzymes in order to produce alterations in metabolic pathways and ultimately alterations of physiologic events.

Pharmacology has been traditionally based in small molecule approaches facing major hurdles associated to the enormous complexity of three-dimensional interference of proteins mediated by organic molecules. Those difficulties are related to synthesis complexity, pharmacokinetics and hard to expect off-target pharmacodynamics or side-effects. Small organic molecules can be decent allosteric modulators, enzyme inhibitors or ligands, but many physiologic events are based in interactions between large biomolecules being hard to alter by a small organic molecule. Small drugs have a size related thermodynamic drawback compared to large macromolecular interactions, implying that only a small number of targets that are druggable using small molecules [1], See Figure I. Those limitations have contributed to show pharmacology as an efficient way to treat some symptoms but an inefficient system to treat complex illnesses after treatment.

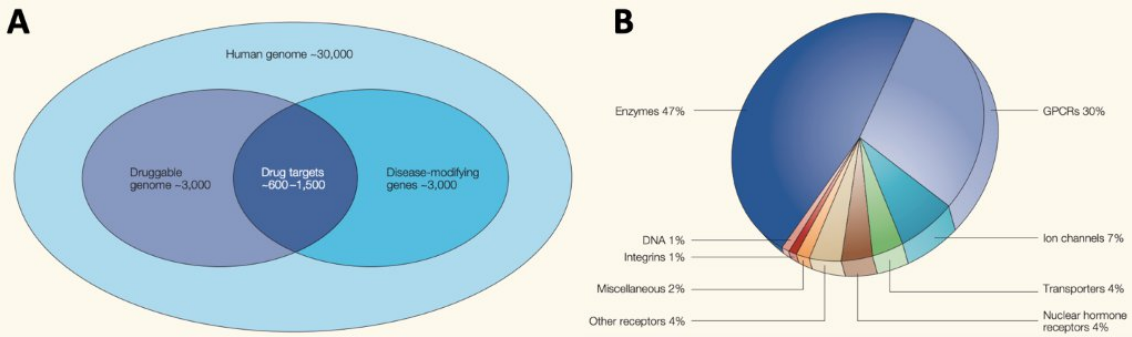

Figure I. Limitations of small molecule drugs. A, Biomolecules affordable by small-molecule drugs. B, Biomolecular targets of current small molecular drugs[1].

During the last decades, the appearance of immunology has boosted the development of new drug strategies based on a "simplification" of three-dimensional docking interactions of molecules and using the potency of the innate immune response mechanisms [2]. Those advances are being reflected in an economic success boosting antibodies as major blockbuster drugs nowadays [3].

Besides the advances of immunology, many targets are still undruggable or extremely complex to treat by small molecules or macromolecule based chemical interference. It is estimated that only 2% to 10% of proteins are potentially druggable by the traditional topological mechanisms [4]. Discoveries and understanding of how biological information is stored, regulated and expressed have opened tremendous opportunities for sequence-based therapeutic strategies. Those systems allow to face new targets that

were not approachable using classical pharmacology, making a whole new field to emerge for advancing therapies [5].
This higher potential is specially boosted by the solid phase synthesis simplicity of polynucleotides compared to traditional organic synthesis. Traditional synthesis of small organic molecules requires a great deal of effort, imagination, scalable challenges and cost, while nowadays oligonucleotide synthesis is fully computerized potentially producing any oligonucleotide in a few hours by a few hundred dollars. DNA or RNA synthesis has been automated thanks to solid synthesis technics that basically attach one monomer after the other while the molecule is attached to a solid support [6]. In comparison synthesis of organic chemistry requires a unique strategy and tools for every molecule making each job completely different.

Using foreign genetic material represents a serious biological and ethical threaten due to potential lack of reversibility and permanent modification of human beings [7]. For those reasons, current work only faces temporal modification of the expression profile, preferably trough RNA (ribonucleic acid) treatments interfering in expression of genes such as siRNA, miRNA or mRNA. RNA interference uses innate mechanisms based in the sequence-based specific catalytic mechanisms discovered by Craig and Mello[8] in the late 90s. This interference uses a reaction between small oligonucleotides and RNA inducing silencing complex (RISC) complex to specifically degrade mRNAs complementary to small siRNA or miRNA limiting its further expression.

Using iRNA has several advantages such as potentially facing any target, having predictable pharmacokinetics or higher potency with a lower dependency on daily administration. That translates into therapies that usually last for 5 days to more than 6 months after a single injection [9] compared to daily intake of small molecules that are rapidly renal or hepatically cleared.

Besides the apparent simplicity of using polynucleotides as therapeutic agents, there are several key factors that have limited the development of its potential, in Figure II schemes of the technique limitations are presented. Due to the core importance of DNA expression in cell survival, living organisms have adapted many mechanisms to avoid “uncontrolled” introduction of polynucleotides making the extracellular space ubiquitously hostile to DNA and specially to RNA by catalytic enzymes. The high structural negative charge of polynucleotides represents an enormous counterpart to cross cellular membranes and develop its therapeutic functions making almost inevitable the use of vectors to facilitate internalization and endosomal escape. Viral vectors have been naturally evolved during pass of time to survive infecting host cells while smuggling the immune system and are usually highly efficient in transfection of nucleic material. Synthetic vectors have been developed to protect oligonucleotides from nuclease activity, allow efficient internalization and targeting different tissues. In current work, non-viral polymers are attempted to be used due to its simple

composition, scalability and characterization making it potentially easier to translate into clinical practice. Non-viral vectors also allow modifications to guide delivery and targeting of specific tissues. Non-viral systems usually interact with RNA to form nanoparticles that flow suspended through the body. Encapsulation of particles gives sterical protection against enzymatic activity, lowers the immune response and reduces immunogenicity of siRNA. Particles need to be in a diameter range that allows efficient internalization, endosomal escape and bypasses renal clearance, usually falling in the few hundreds nanometer range [10].

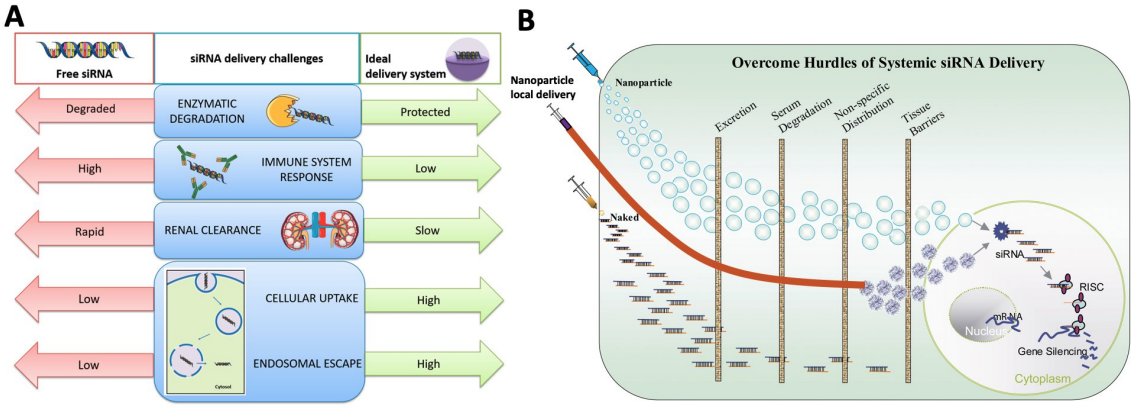

Figure II. Complexity of RNA delivery. A, Vectors requisites to efficiently deliver RNAs, adapted from [11]. B, Potential of Local delivery to bypass some pharmacology barriers, boosting the clinical translation of RNAs into clinical practice, adapted from [12].

Although the tremendous potential of RNA interference therapies, translation into clinical practice have been a path plenty of hurdles. Only a few products have reached FDA or EMA approvals besides more than 3000 clinical trials started and its theoretical predictability of pharmacokinetics and pharmacodynamics. This lack of translation may be related to the impediments mentioned above, drug related regulations and an excessive focus of exploiting the intravenous systemic delivery as the preferred route of administration.

Local delivery of therapeutic agents has the following advances that motivate the introduction into the project. First, using systems to deliver therapeutic agents right where they are needed allows to get advantage of diffusion diluting the concentration away from the insertion point. Lowering the concentration allows to use systems that may present off-target toxicity or undesired side effects if a systemic injection would have been used. Secondly, using non-viral vectors usually requires encapsulating heavily charged nucleotides with positively charged molecules to compensate nucleotide charges making particles cell adhesive. Surface proteins are negatively charged, making it easier for positively charged molecules to adhere to the cell surface [13,14] increasing the internalization efficiency and making nanoparticles less sensitive to protein corona adhesion of plasma proteins and retention of internalization properties [15].

Access by minimal invasive therapies have been rapidly evolving during the last decades to treat peripheral vascular diseases, structural and acquired heart diseases, neurological diseases, pneumological, gastrointestinal, hepatic or eye diseases among many others. In Figure III, a scheme of some of the multiple minimally invasive therapies that could be used is presented.

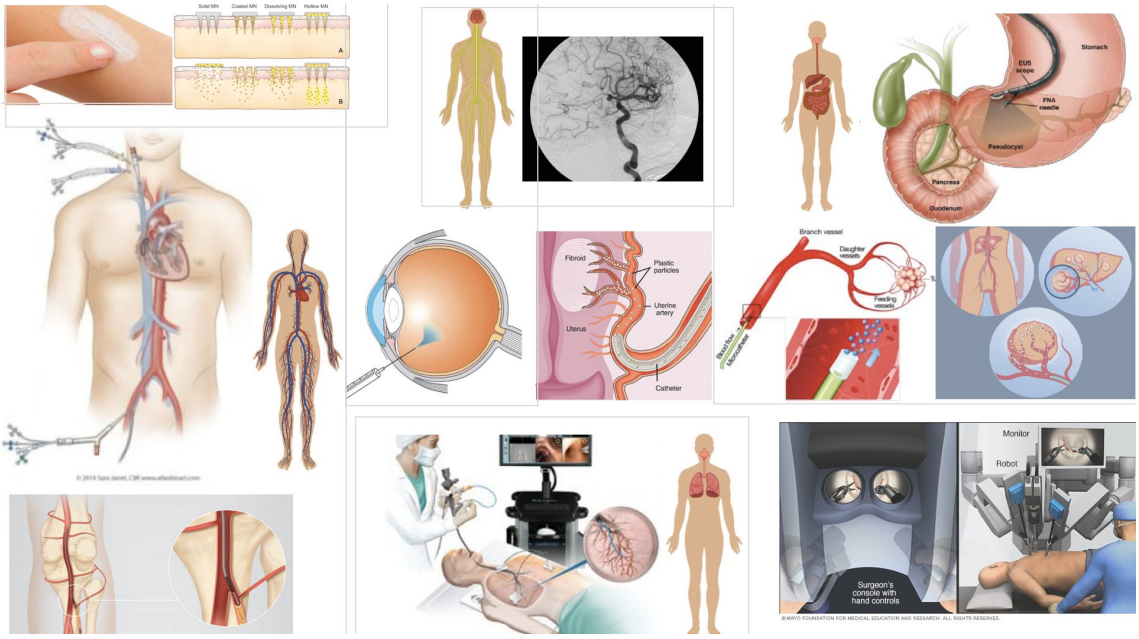

Figure III. Minimally invasive therapies useful to locally deliver RNAs therapies. Skin and ocular local delivery has been used since ancient times due to organ exposure and are great candidates to exploit RNA potential. Interventional cardiology, radiology and interventional pneumology are well established techniques to diagnose, treat, repair and deliver drugs. Endoscopy has also strong potential. Nowadays a combination of minimally invasive surgery and imagining technics also allows new delivery options to combine.

Disturbance of expression based therapeutics has great translation potential into clinics, in spite of slower pace than initially expected. Drug development has been traditionally focused into single metabolic pathway inhibition while cells, tissues and organs are regulated as complex adaptive systems with multiple cross-regulations[16,17] taking place simultaneously to keep homeostasis. This is clearly seen in diseases with multiple sequential stages such vessel or cutaneous diseases were injury response by clotting, immune response mediated inflammation and extracellular remodeling usually take place in a sequence with multiple different regulators working at the same time. Even though RNA interference has the potential to multitarget or treat previously undruggable targets in metabolic pathways, we aim to introduce vectors that co-deliver nucleic acids with potent signaling molecules to have a multimodal approach. It allows to have both a control on expression profile alteration of selected genes and using a potent signaler like NO that is strongly associated with central and peripheral vascular homeostasis, reduction of immune response and anticoagulant strategies. Due to the core importance of nitric oxide as a regulator of the vasculature and epithelial tissues in

many disorders, it is believed that synergistic effects between NO delivery and RNA could be found and exploited by co-delivery.

Proper vector delivery system design is of key importance to translating therapies into clinical environment due to the intrinsic sequence advantages of RNAs. Appropriate validation of delivery platform combined with a focus into local and controlled delivery may boost the predictability pharmacokinetics potentially reducing the times from target identification to clinical trials.

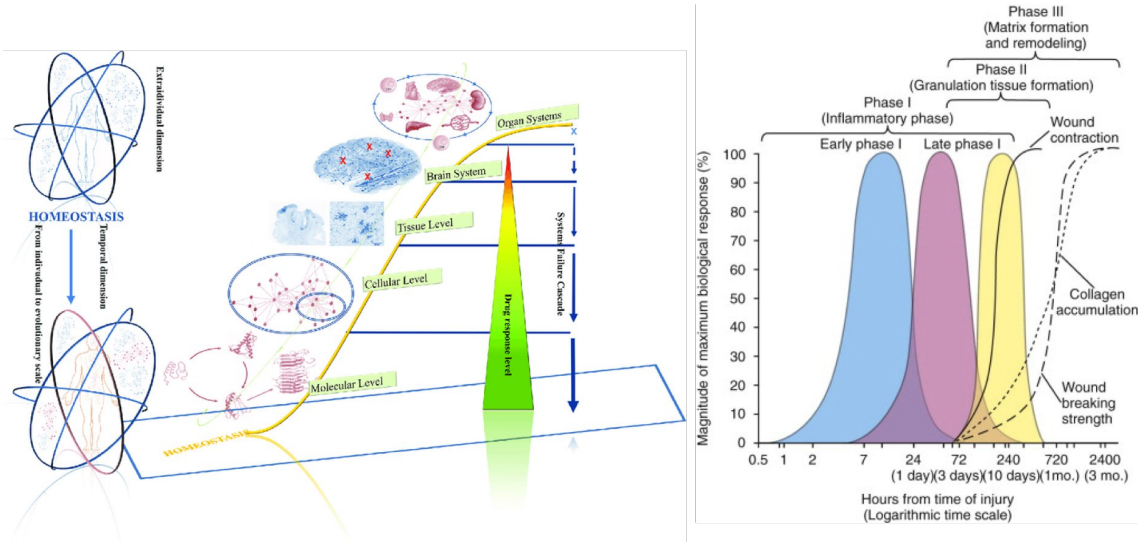

Figure IV. Multimodal strategy to face diseases. Decreasing drug effectiveness in the molecular, cellular, tissue, organ and individual level and example of a multimodal stage of wound healing, adapted from [18]. Potentially there may be a link between the decreasing activity of a single target focused designed drug and diseases with multiple stages and coordination of different events requiring different targeting at different moments.

In the present work, it is hypothesized that careful design of vectors and focusing in local drug-delivery may smooth the way to fully exploit the potential of iRNA and nitric oxide codelivery into selected human diseases.

Through this doctoral thesis the following objectives are aimed;

1.Synthetize a library of efficient non-viral polymers with integrated nitric oxide releasing and RNA complexation properties.

2.Validate the stability, cytotoxicity, transfection efficiency and nitric oxide function of the developed polymers through a large set of polynucleotides.

3.Develop strategies to locally deliver the RNA polyplexes developed.

4.Explore alternative applications of the developed polymers for antibacterial applications.

REFERENCES

[1] Imming P, Sinning C, Meyer A. Drugs, their targets and the nature and number of drug targets. Nat Rev Drug Discov. 2006 Oct;5(10):821-34. doi: 10.1038/nrd2132. Erratum in: Nat Rev Drug Discov. 2007 Feb;6(2):126. PMID: 17016423.

[2]Tiligada E, Ishii M, Riccardi C, Spedding M, Simon HU, Teixeira MM, Cuervo ML, Holgate ST, Levi-Schaffer F. The expanding role of immunopharmacology: IUPHAR Review 16. Br J Pharmacol. 2015 Sep;172(17):4217-27. doi: 10.1111/bph.13219.

[3] Philippidis, A. Top 15 Best-Selling Drugs of 2018 GEN - Genetic Engineering and Biotechnology News. 2019-03-11.

[4] Hopkins AL, Groom CR. The druggable genome. Nat Rev Drug Discov. 2002 Sep;1(9):727-30. doi: 10.1038/nrd892.

[5] Editorial Board. Delivering the promise of RNA therapeutics. Nat Med. 2019 Sep;25(9):1321. doi: 10.1038/s41591-019-0580-6

[6] Guzaev AP. Solid-phase supports for oligonucleotide synthesis. Curr Protoc Nucleic Acid Chem. 2013 Jun;Chapter 3:Unit3.1. doi: 10.1002/0471142700.nc0301s53.

[7] Rabino I. Gene therapy: ethical issues. Theor Med Bioeth. 2003;24(1):31-58. doi: 10.1023/a:1022967623162.

[8] Fire A, Xu S, Montgomery MK, Kostas SA, Driver SE, Mello CC. Potent and specific genetic interference by double-stranded RNA in Caenorhabditis elegans. Nature. 1998 Feb 19;391(6669):806-11. doi: 10.1038/35888.

[9]Ray KK, Landmesser U, Leiter LA, Kallend D, Dufour R, Karakas M, Hall T, Troquay RP, Turner T, Visseren FL, Wijngaard P, Wright RS, Kastelein JJ. Inclisiran in Patients at High Cardiovascular Risk with Elevated LDL Cholesterol. N Engl J Med. 2017 Apr 13;376(15):1430-1440. doi: 10.1056/NEJMoa1615758

[10] Blanco E, Shen H, Ferrari M. Principles of nanoparticle design for overcoming biological barriers to drug delivery. Nat Biotechnol. 2015 Sep;33(9):941-51. doi: 10.1038/nbt.3330.

[11] Serrano-Sevilla I, Artiga Á, Mitchell SG, De Matteis L, de la Fuente JM. Natural Polysaccharides for siRNA Delivery: Nanocarriers Based on Chitosan, Hyaluronic Acid, and Their Derivatives. Molecules. 2019;24(14):2570. Published 2019 Jul 15. doi:10.3390/molecules24142570.

[12]Woodle MC, Lu PY.(2005) Nanoparticles deliver RNAi therapy. Materials today;8-8 2005 34-41

[13] Mislick KA, Baldeschwieler JD. Evidence for the role of proteoglycans in cation-mediated gene transfer. Proc Natl Acad Sci U S A. 1996;93(22):12349-12354. doi:10.1073/pnas.93.22.12349

[14] Wagner E. Polymers for siRNA delivery: inspired by viruses to be targeted, dynamic, and precise. Acc Chem Res. 2012 Jul 17;45(7):1005-13. doi: 10.1021/ar2002232.

[15] Kaczmarek JC, Patel AK, Kauffman KJ, Fenton OS, Webber MJ, Heartlein MW, DeRosa F, Anderson DG. Polymer-Lipid Nanoparticles for Systemic Delivery of mRNA to the Lungs. Angew Chem Int Ed Engl. 2016 Oct 24;55(44):13808-13812. doi: 10.1002/anie.201608450.

[16] Hulsen T., Jamuar S.S., Moody A.R., KarnesJ.H., Varga O., Hedensted S., Spreafico R., Hafler D.A., McKinney E.F. (2019) Frontiers of Medicine. 2019 Mar 1;6:34

[17]Novikoff AB. THE CONCEPT OF INTEGRATIVE LEVELS AND BIOLOGY. Science. 1945 Mar 2;101(2618):209-15. doi: 10.1126/science.101.2618.209.

[18] Hampel H, Vergallo A, Perry G, Lista S; Alzheimer Precision Medicine Initiative (APMI). The Alzheimer Precision Medicine Initiative. J Alzheimers Dis. 2019;68(1):1-24. doi: 10.3233/JAD-181121.

CHAPTER 1. DEVELOPMENT OF NO-RELEASING NON-VIRAL VECTORS FOR iRNA DELIVERY

1.1 INTRODUCTION

During the last century, enormous advances have been accomplished towards the rationalization of molecular mechanisms behind living systems. One of the main milestones has been achieved by understanding the central role of DNA into physiology and molecular biology. Although the central dogma of molecular biology seems to be an elegant process of transcription and translation of DNA information into functional proteins, the regulation of gene expression has emerged as a highly regulated system with multiple levels. Especially fruitful have been the last 40 years, where major advances have been found in unraveling multiple expression mechanisms such as iRNA. Interference of mRNA was serendipity discovered by Fire and Mello[1], opening a new era where RNA molecules did not only served as DNA messengers into proteins but also had a deep effect on gene expression regulation through silencing, playing an essential role in mammalian biology.

Interference RNA are endogenous mechanisms that allow modulation of gene expression though degradation of mature mRNAs present in the cytoplasm. This system starts when small RNA molecules are processed by the Dicer enzyme yielding RNA molecules of around 22 base pairs with 2 overhanging nucleotides on the 3' end. Then the siRNA sense strand is incorporated into the RNA-induced silencing complex (RISC), activating the complex and allowing the cleavage of messenger RNAs with complementary sequences, ultimately blocking protein production. In Figure 1.1.1 a scheme of the mechanisms involved in the molecular biology of miRNA and siRNA are presented.

Both siRNA and miRNA are naturally occurring double stranded oligonucleotides of about 20-27 base pairs. The main difference between siRNAs and miRNA are cellular origin and specificity; siRNAs are extracellular molecules specifically compatible to a single mRNA target while miRNAs are intracellular molecules produced in the nucleus that interfere with a high number of messenger RNAs. Around 1600 human endogenous coded miRNAs [3] seem to target more than 50% of human genes playing an essential role modulating gene expression [4].

iRNA has a unique potential to revolutionize pharmacology by modifying expression patterns through a sequence-based approach. This system may be simpler to develop, adding novel and promising approaches for traditional complex fields such as vaccination[5] and viral infections[6]. Plenty of human effort and capital resources have been invested to bringing iRNA technology to pharmacological use. Nowadays after 20 years of intense research, major hurdles have been found yielding a slower pace than initially glimpsed.

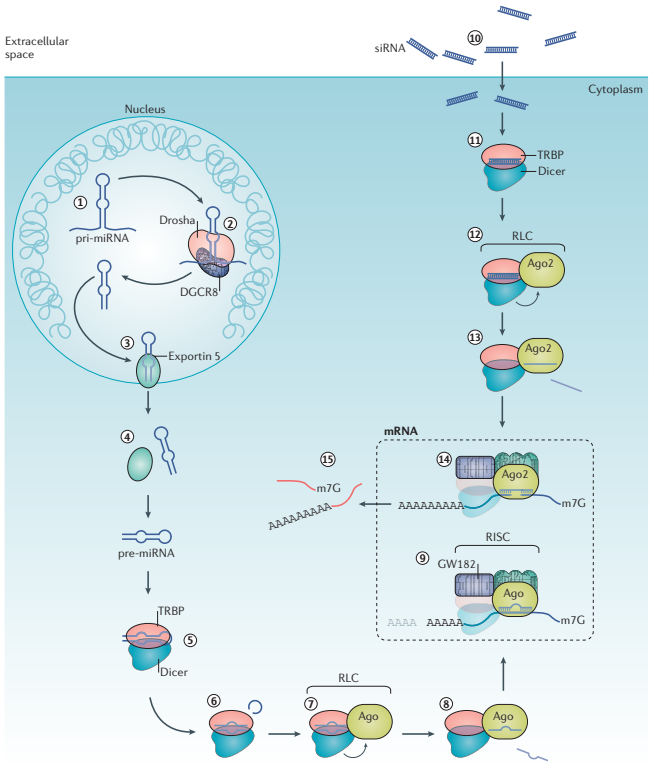

Figure 1.1.1 Mechanism of siRNA and miRNA silencing of mRNAs. Scheme of how exogenous siRNA and endogenous miRNA take advantage of the RISC complex to cut down mRNA expression through lysis, adapted from [2].

Although the elegance and initial highly expectations of iRNA use in medicine, delivery to the right cells and tissues have been major obstacles to overcome. What one day seemed an easy translation from bench to bedside, has taken more than 20 years to complete the first steps. Nowadays the first iRNA based drug has been approved, renewing expectations in the field. In Figure 1.1.2 the main achieved milestones of the last 30 years are presented.

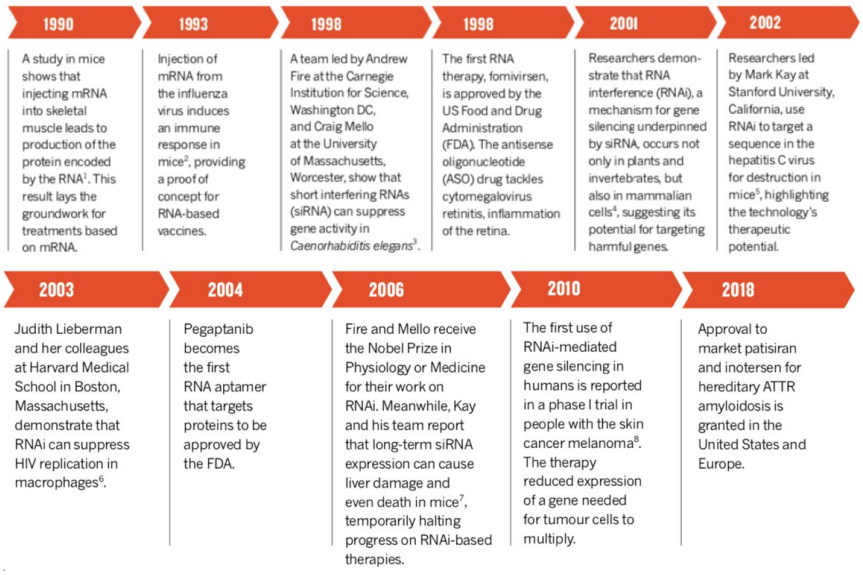

Figure 1.1.2 Main steps in the evolution of RNA therapeutics during the last 30 years.[7]

Besides intrinsic complementary complexities such as off-target effects, iRNAs have to be internalized trespassing the cellular membrane and face a harsh environment full of proteases. DNA and RNA have a strong negative backbone making it difficult to pass the lipophilic cellular membrane. Furthermore, naked double stranded RNA molecules are usually recognized by the innate immune system as a signal of viral presence triggering immune response when present at high concentrations.

As a first step, systemic delivery of naked RNA was attempted, yielding very poor results. Lack of initial positive results was due to the presence of ribonucleases in bloodstream, difficulties to diffuse across the cellular membrane and triggering of the immune system [8]. Partial improvement of those hurdles have been bypassed by incorporation of modifications in the RNA backbone such as 2'-O-methyl or 2'-fluoro, locked nucleic acids or phosphorothioate linkages[9]. A decent level of success has been achieved by conjugation of molecules in the 3' end of the sense strand such as cholesterol or N-Acetylgalactosamine achieving IC50 silencing at doses in the range of 5-50mg/kg[10][11] both *in vivo* and in clinical trials. Besides the improvements achieved by modification of the backbone and coupling conjugates, further systems are needed to bypass the multiple barriers present in biological systems and reduce overall doses.

To overcome delivery complexities and poor activity, several strategies such as encapsulation have been proposed to shield nucleic material in circulation and avoid endosomal degradation. In Figure 1.1.3 several strategies to complex and internalize RNA or DNA are presented.

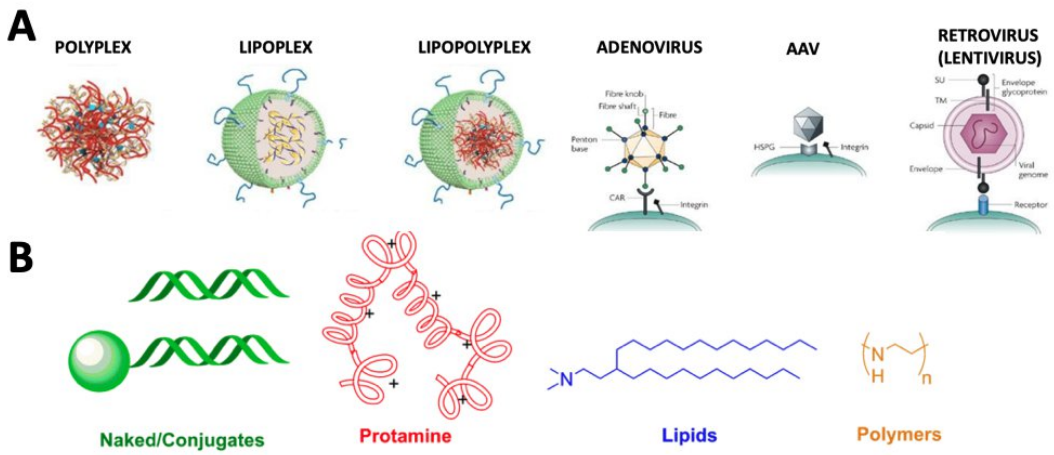

Figure 1.1.3 Main vector types and delivery materials for DNA, iRNA and mRNA delivery. A, Main non-viral vectors and viral vectors used for the delivery of nucleic acids. B, main materials used in for the delivery of nucleic acids.[12][13]

Pharmacological potency of RNAs have been greatly improved by encapsulation of nucleic acids through viral and non-viral vectors reducing several folds the doses needed

to achieve equivalent IC50s to naked RNAs. Encapsulation of nuclear material is a strategy to produce small particles in the nanoscopic range, allowing; shielding of nucleic acids, neutralization of negative charge, surface derivatization and internalization. Viral encapsulation is inspired in the intrinsic capabilities of virus to transport and selectively inject nucleic material into mammalian cells. Viral vectors have widely shown its transfection capabilities in multiple treatments [14] both *in vitro* and *in vivo* with positive results. However, use of viral vectors have associated challenges such as immunogenic reactions, scale-up limitations [15][16] and historical bad press associated with previous clinical applications [17] in the 80s. Those facts have limited its translation to clinics in favor of synthetic vectors. On the other hand, non-viral vectors are highly versatile constructs, ease to modify and scale-up. Two main groups of non-viral vectors have predominated the field; lipid nanoparticles (LNP) and polyplexes. Lipid nanoparticles are usually spherical vesicles that have at least one lipid bilayer or lipoplexes were positively charged lipids interact with the RNA forming a stable nanoparticle. Initially, lipids used such as lipofectamine® showed extensive *in vitro* use but poor *in vivo* performance due to its toxicity and poor transfection capabilities. New developments have introduced mixtures of cationic, cholesterol and small molecular weight lipids showing nanoparticle pKa, size and surface modification as the main factors to boost transfection. Those systems have also been conjugated with ligands such as folate, PEG, NAcGal or antibodies to increase stability in blood and improve cell specificity. Many applications using second generation Lipid nanoparticles have shown to be 10.000 times more efficient than naked siRNA delivery[18][19]. Although lipid nanoparticles have evolved extensively being one of the preferred strategies for RNA delivery, oxidation, stability and long-term storage may limit future translation.

On the other hand, polymers have been proposed as alternatives for RNA delivery, focusing on the use of positively charged molecules trying to balance charge and ease cell internalization.

Initial attempts in the early 60s tried to improve the RNA delivery by complexation with positive charged polymers such as protamine. Protamine is an arginine rich oligopeptide with positive charge derived from fish sperm. When bound to RNA or DNA form stable complexes capable of reducing immune response and protect nucleic acid from hydrolytic enzymes. Use of other cationic polymers such as poly(L-lisine), pDMAEMA or polyethyleneimine have been studied with different levels of success in transfection but translation has been complex due to high cytotoxicity and lack of degradability. Polyethyleneimine has also been widely used in its commercial form jetPEI® mainly for *in vitro* and animal trials. Chitosan, a natural polysaccharide containing repeating units of N-acetyl-D-glucosamine has been described to form stable nanoparticles and allow endosomal scape due to its positive charge at acidic pH[20].

Several polymers have been specially designed to be used in RNA delivery, see Figure 1.1.4 for details, among the widely studied are poly(β-amino esters). Those synthetic

polymers are designed to form stable nanoparticles, biodegrade, conjugate with ligands and show buffering effect capabilities to facilitate endosomal escape. pBAEs are obtained from a simple reaction between a diamine and a diacrylate, thus multiple combinations have been explored and screened [21] finding successful complexation of nucleic materials, low toxicity both *in vivo* and *in vitro* and high transfection efficacies [22][23]. Its mechanisms of endosomal scape have been also studied showing the internalization and delivery mechanisms as initially hypothesized [24]. Poly(β-amino ester) polyplexes comply with most of the expected properties of an ideal vector; easy to synthesize and scale-up, low toxicity, biodegradability and high chemical derivatization but high surface charge has limited its translation into clinical use. Many hybrid applications using both polymers, lipidoids, lipids and conjugates have been proposed trying to combine the advantages of the two technologies. Those complexes are called lipopolyplexes and have shown promising results[25] *in vivo* achieving high activity at low RNA doses 0.05mg/kg and promising stability results.

Many other polymers have been studied to deliver RNA or DNA material such as PAMAM dendrimers, gold nanoparticles or cyclodextrins. Those systems will not be considered for the present work that focuses into using synthetic polymers based in pBAE with nitric oxide releasing capabilities and intends to apply local delivery strategies.
Although RNA delivery has a promising future, the innumerable amount of effective small molecule therapeutic agents should not be undervaluated to face new therapeutic strategies. Some synthetic vectors have introduced co-delivery of drugs specially for oncological[26][27] applications. Co-delivery of RNA plus synthetic agents may give more therapeutical tools to face complex illnesses such as cancer, degenerative diseases and vascular diseases. Usually multistage physiological processes are biologically modulated through various interdependent pathways. For those situations having several therapeutic agents that actuate through several routes may increase chances to get improvements. One of the most interesting small signaling molecule that may be interesting to complement RNA activity is nitric oxide.

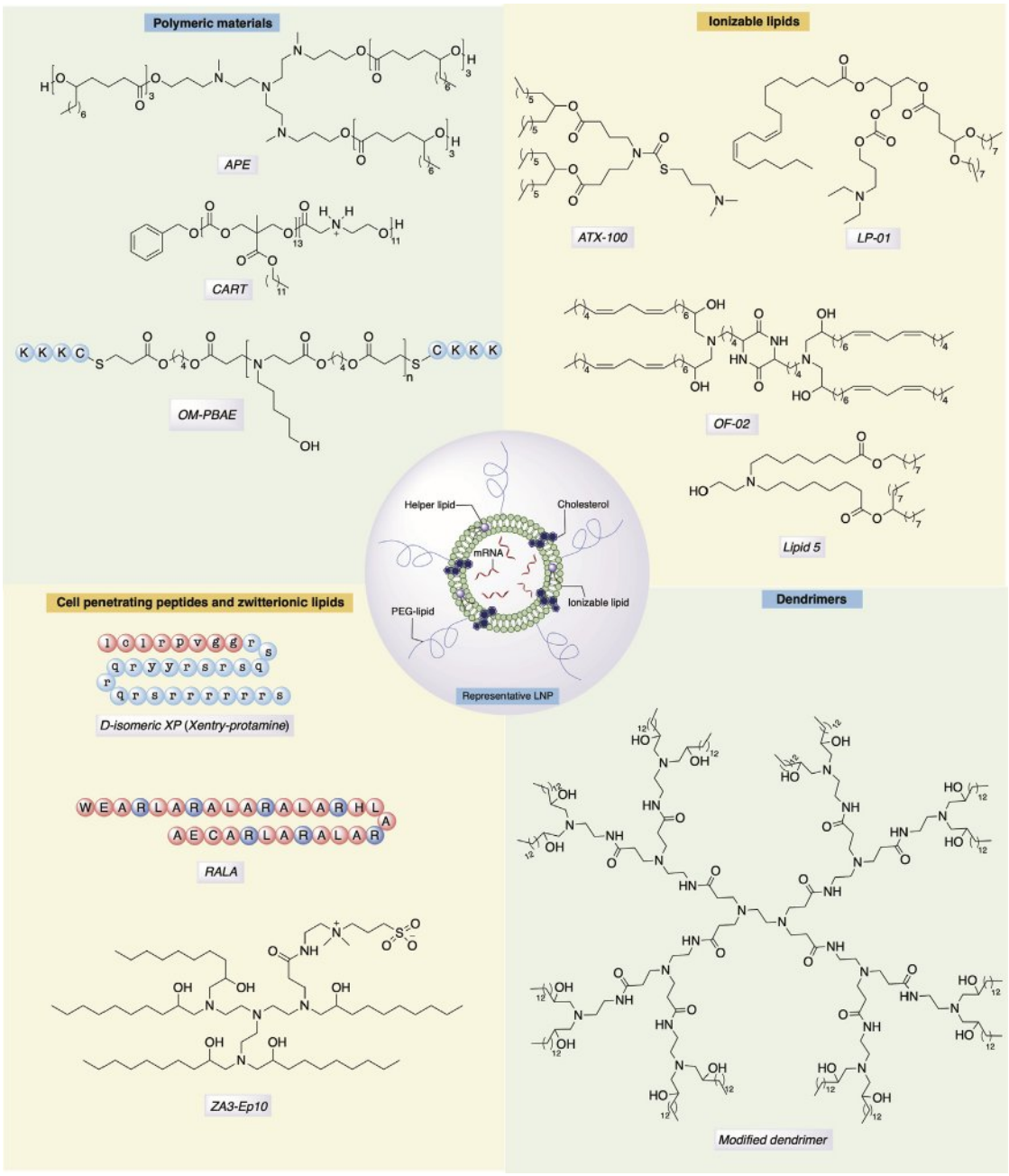

Figure 1.1.4 Non-viral vectors proposed for RNA delivery.[28] Main strategies of synthetic polymers and molecules proposed for RNA delivery comprising dendrimers derived with lipophilic tails, lipids with zwitterionic and protonable moieties and hydrophobic polymers with amines in the backbone.

NO has multiple functions in cell biology and its use together with RNA or other agents has not been deeply studied. Nitric oxide is a highly potent and small molecule with deep ubiquitous effect with remarkable importance in the vascular, dermal and hepatic tissues among others.

Nitric oxide is a simple diatomic molecule with a remarkable role in mammalian physiology, it was recognized as molecule of the year and the discovery of its biological importance granted a Nobel price of medicine in 1998. Chemical properties of nitric

oxide would suggest being an unstable molecule in physiologic environment with affinity to complex transition metal ions like heme, causing an equivalent toxicity to carbon monoxide [29]. Nitric oxide has biologically evolved being a key signaling molecule with multiple physiologic roles due to its unique chemical properties. NO is biosynthetized by a family of enzymes called Nitric Oxide Synthases (NOS), those molecules transform L-arginine into nitric oxide and citrulline by reducing NADPH. NO is naturally produced by nearly all cell types of the body by multiple NOS isoforms that have adapted its nitric oxide output to specific environments and responses.

The key properties of nitric oxide are related to its unique chemical half-life in the 1-10s and its ability to diffuse freely thorugh cell membranes making it an ideal signaling molecule functioning as a paracrine and autocrine signaler. Moreover at high concentrations It behaves as a toxic agent being useful as a defensive strategy against hosts.

Nitric Oxide plays several key biological processes; in the vascular system nitric oxide is produced by the endothelium in the pico to nanomolar range to control the vascular tone, proliferation of smooth muscle cells, reducing platelet adhesion and aggregation [30], contributing to balance and keep vascular hemostasis[31].

In other tissues like the central and peripheral nervous system it has been found that nitric oxide plays a key role in mediating synapsis by stimulating the release of neurotransmitters to nerve cells. For this role nitric oxide is exclusively produced by neural nitric oxide synthase (nNOS), an isoform that is almost exclusively present in central nervous system cells.

Introduction of nitric oxide releasing moieties into polymers has been extensively explored using several chemical strategies, see Figure 1.1.5. One of the oldest moieties used in pharmacology has been the organic nitrate, used since the XIX century. Organic nitrates have been deeply studied due to early adoption in pharmacology of nitroglycerine. It is indirectly converted to nitric oxide in vascular or hepatic cells through enzymatic mechanisms. Its synthesis can be achieved by a nucleophilic substitution using silver nitrate or direct nitration using nitric acid in anhydrous conditions.

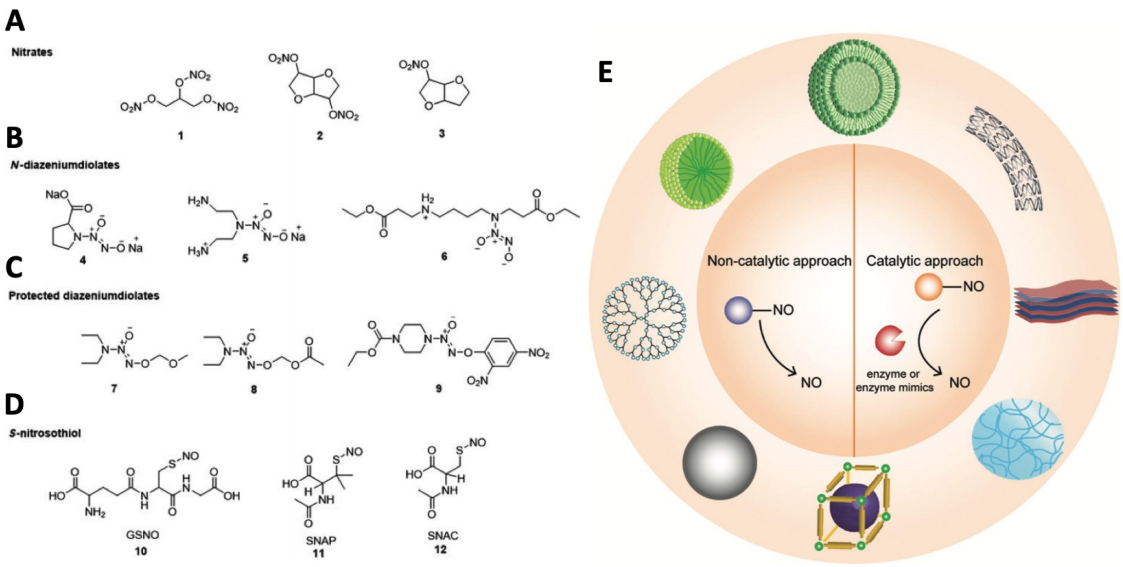

Figure 1.1.5 Main synthetic moieties used for nitric oxide release. A, Organic Nitrates an enzymatic dependent moiety. B, non-catalytic unprotected NONOates and protected C. D, S-Nitrosolothiol groups, a non-enzymatic NO delivery group. E, types of NO releasing moieties and potential applications[32].

N-diazenium diolates or NONOates are chemical groups produced by reacting gaseous nitric oxide at high pressure with secondary amines, generating a nitric oxide adduct that becomes unstable with temperature and specially under acidic conditions. Those moieties do not require any enzymatic pathway to deliver nitric oxide being its half-life highly dependent on the chemical environment. The half-life can be tuned from a few seconds up to a few days[33]. One of the main drawbacks of NONOate use is its lack of long-term stability of other NO chemical releasing groups.

Thionitrites or S-nitrosothiols (SNO) also have an interesting capability of storing nitric oxide chemically and releasing it later on, S-nitrosothiols are broadly present in the biological systems to stabilize NO by intermediary molecules such as S-Nitrosoglutathione. The chemical groups are produced by reacting thiols with a nitric oxide donating agents yielding indistinguishable colored thionitrites that releases nitric oxide as a response to heat, light and copper ions. Those moieties are usually slowly converted into nitric oxide in physiologic environments[34]. The delivery range can be tuned from highly unstable molecules up to several weeks depending on chemical environment. Many other chemical strategies have been explored to store chemically nitric oxide such as organic nitrites, metallic adducts or furoxan groups among others. Although main applications to chemical structures have been focused in the previously described groups[35].

In present chapter, the synthesis of pBAE based non-viral vectors for nucleic acid delivery and NO co-delivery are intended to be synthetized, exploring in further chapters its potential clinical applications.

1.2 MATERIALS AND METHODS

1.2.1 Materials: Unless noted all reagents were used from Sigma-Aldrich. CK3 was obtained from GL biochem without further purification. A large single batch of C32 was formed by the reaction of butanodiol diacrylate(1 eq) and 5-aminopentanol(1.08 eq) at 80 degreees reacting for 24 hours.

1.2.2 Synthesis of pBAEs containing organic nitrites: Nitrate containing pBAE was synthetized by reaction of n-bromoaliphatic carboxylic acid(1 eq) with $AgNO_3$(1.05 eq) in acetonitrile for 24h protected from light. Formed AgBr was filtered and the remaining solution was washed with ethyl acetate and water extraction and evaporation of the solvent. Esterification was undergone using C32 (1eq), DCC (1.05 eq) and the n-nitrooxyaliphatic carboxylic acid (1eq) in THF with DMAP as catalyst(0.05eq). Reaction was kept in ice for 30 minutes and further kept at room temperature for 48 hours. Solid DCU was filtered and yielded polymer was purified in ether and reacted with CK3 in DMSO overnight and purified in Acetone/diethyl ether and kept in DMSO at -20 ^oC until use . ^{1}H-RMN (400 MHz, CD_3OD, TMS) (ppm): δ= 7.26 (ddd, *J* = 17.3, 2.4, 1.5 Hz), 6.18 (dd, *J* = 10.4, 2.1 Hz), 5.87 (s), 4.59 – 4.44 (m), 4.28 – 4.16 (m), 4.18 – 4.05 (m), 3.56 (t, *J* = 6.6 Hz), 2.94 – 2.76 (m), 2.61 – 2.48 (m), 2.38 (qd, *J* = 7.6, 7.0, 4.6 Hz), 1.83 – 1.72 (m), 1.70 – 1.65 (m), 1.55 (dd, *J* = 15.6, 8.2 Hz), 1.37 (dt, *J* = 8.7, 4.4 Hz), 1.24 (td, *J* = 7.1, 2.4 Hz). FTIR-ATR: 1619 cm^{-1} (NO stretch), 1704 cm^{-1} (C=O stretch), 1275cm^{-1} (N-O stretch).

1.2.3 Synthesis of SNO containing pBAE polymers: SNO containing pBAE was synthetized by reacting tert-butyl nitrite and thiol containing organic acids at 1:1.05 excess in acetone, reacted for 5 minutes and then rotavapored at low temperature protected from light. Esterification was conducted by reaction of C32 (1 eq), DCC (1.0 eq), S-nitrosomercapto-organic acid (1.0 eq) and DMAP (0.02 eq) as catalyst in DCM. Reaction was bubbled in argon, protected from light and allow to react in an ice bath for 2 hours. Purification was concluded by centrifugation at room temperature and further crystallization of DCC at -80 ^oC followed by DCU filtration. Purification was conducted by precipitation in ether of the polymers, dissolving in acetone and bubbling .Polymers were kept in acetone solution in the freezer until further use, color was used as a quick check for stability.^{1}H-RMN (400 MHz, CD_3OD, TMS) (ppm): δ= 6.38 (ddd, *J* = 17.3, 2.4, 1.5 Hz, 0H), 6.18 (dd, *J* = 10.4, 2.1 Hz, 0H), 5.87 (s, 0H), 4.59 – 4.44 (m, 0H), 4.28 – 4.16 (m, 0H), 4.18 – 4.05 (m, 1H), 3.56 (t, *J* = 6.6 Hz, 0H), 2.94 – 2.76 (m, 0H), 2.61 – 2.48 (m, 1H), 2.38 (qd, *J* = 7.6, 7.0, 4.6 Hz, 0H), 1.83 – 1.72 (m, 1H), 1.70 – 1.65 (m, 0H), 1.55 (dd, *J* = 15.6, 8.2 Hz, 0H), 1.37 (dt, *J* = 8.7, 4.4 Hz, 0H), 1.24 (td, *J* = 7.1, 2.4 Hz, 0H). UV-Vis: 339 max, 506 max. FTIR-ATR: 1650 cm^{-1} (NO stretch), 1124 cm^{-1} (C=O stretch).

1.2.4 Synthesis of pBAEs containing organic nitrites: C32-CK3 (1 eq) was treated with tert-butyl nitrite (1.5 eq) at room temperature, reaction rapidly generated a phase of dark red and nitrogen oxide gases discouraging further exploration. C32 (1 eq) dissolved

in chloroform and tertbutyl nitrite (5 eq) was added and allow to react for 30 minutes first in ice bath and then at room temperature, further addition of CK3 and polyamines was added in DMSO.

1.2.5 Synthesis of pBAEs containing diazeniumdiolates: C32 (1.0 eq) was reacted in 10% DMSO with spermidine (2.2 eq) and DETA (2.2 eq) for 24h. Purification was performed by precipitation in diethylether/acetone mixture. The polymers were dried and dissolved in acetonitrile 10% and reacted in a high-pressure reactor (10 bar) with NO for 10 days, then solvent was evaporated and solid was further analyzed.

1.3 RESULTS AND DISCUSION

1.3.1. Synthetic strategy

Among the many possibilities to develop non-viral vectors with nitric oxide delivery capabilities a strategy based on pBAE polymers has been chosen. pBAE are simple to synthetize, versatile and specially designed polymers for RNA delivery applications. At present work the base polymer selected has been C32-CK3, a small molecular weight polymer derived from 5-aminopentanol 1,4-butanodiol diacrylate and terminated with oligopeptides rich in lysine (Figure 1.3.2.ii). Polymers based in this structure can be derived through modification of the side chain hydroxyl to add multiple nitric oxide moieties. Although polyplexes have a high-associated surface charge, it may enhance adhesiveness of particles to stay anchored in the environments of delivery site.

Introduction of nitric oxide delivery capabilities can be developed through many strategies, to select different types of chemical groups many aspects have been considered. Basically; stability, conditions for conversion to nitric oxide and previous experience in pharmacological use have been selected as main factors for cribbage. Although many strategies are potentially useful, it does not exist a preferred strategy and the introduction of moieties may depend on the final application, desired dose and chemical compatibility. In Figure 1.3.1. a scheme with different strategies, advantages and disadvantages is presented.

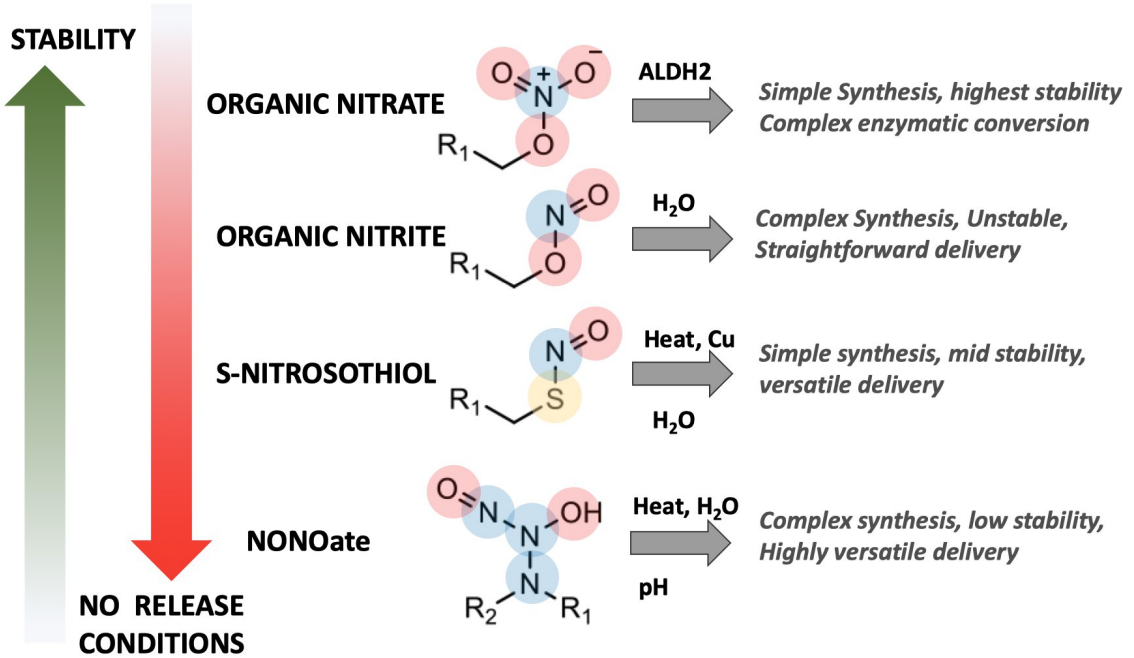

Figure 1.3.1. Panel of proposed strategies to introduce NO to RNA delivery polymers.

Organic nitrates have been used widely since the discovery of nitroglycerin[36] and are one of the preferred strategies due to its stability, lack of chemical reactivity and proven pharmacological usefulness. In the other hand pharmacodynamics of organic nitrates are dependent on specific aldehyde dehydrogenases that may complicate the deliverability of nitric oxide in different tissues.
Organic nitrites in contrast, are molecules that have a much simpler predictability of NO delivery due to its rapid conversion in aquose medium. During the last 100 years use as recreational substances with vasodilation effect has been extended. Higher instability and nitrosyl transfer between alcohols may limit the use as a real-life therapy.
Finally, S-nitrosothiols and diazeniumdiolates are also studied due to the extended research under those moieties undergone in the last 50 years[37].
NONOates are considered by its unique and clean NO delivery under acidic pH that could work in a symbiotic way with the pBAE design for endosomal disruption, on the other hand synthesis is reasonably more complex and stability is significantly lower. It remains unclear how stable SNO and NONOates will be achieved and if those groups will be unstable in contact with the polymer backbone or the synthesis conditions.

1.3.2. Synthesis of pBAE containing organic nitrates

Organic nitrates have been one of the preferred moieties to deliver nitric oxide to patients during the last century. It presents excellent stability, except for explosive environments and slight photosensitivity, lack of reactivity with other moieties and biotransformation to nitric oxide requiring ALDH2 or highly specified enzymes. Nitrooxy groups have a great potential to generate mid to long-term delivery strategies due to nitric oxide release depends on exposure to enzymes rather than environmental conditions such as temperature, pH or catalysis.
First attempts to introduce the nitro group were focused into nitrosation of 1-amino-5-pentanol to generate 5-nitrooxypentamine following by reaction with a diacrylate to form a C32-NO. This route was abandoned due to complexities in the synthetic pathway and doubts about the ability of the moiety be able to reach the enzymatic active sites required to convert organic nitrates to nitric oxide. Alternative molecules such as aminoethanol were also attemted without success, in Figure 1.3.2.1 the attempted structures are presented.

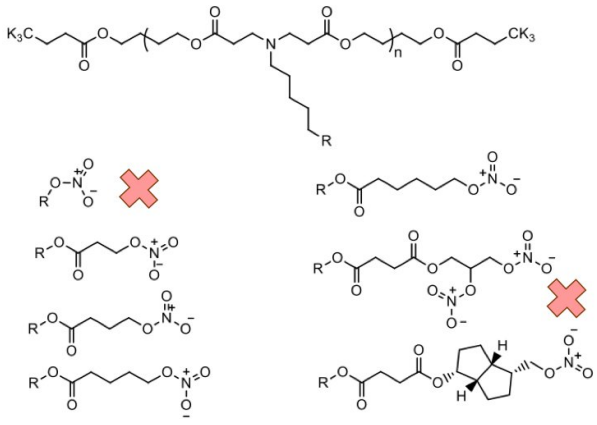

Figure 1.3.2.1 Attempted structures studied to introduce organic nitrates into C32 Backbone.

Introduction of nitrooxy moieties can also be introduced by reaction of silver nitrate with primary halides. Reaction occurs by a SN_2 substitution reaction of negatively charged nitrate to the alpha carbon to the halide. The reaction is strongly driven by the high insolubility of silver halides that contributes to equilibrium displacement. Availability of organic acids terminated in bromine or iodide moieties contributed to simplify the synthesis. A set of nitrooxy-terminated organic acids was synthetized ranging from 2 to 6 carbon atoms, selecting hexanoic (named as K72-NO in present work) as the preferred strategy based on previous experimentation. After modification of the hydroxyl moiety derivatization with amine or thiol containing amines allowed to end-modify the base polymers to complex with nucleic acids. Further modification with amine reactive fluorophores yielded polymers tagged. Besides completing the chemical synthesis, it is complex to predict if the added groups will be active or will remain unable to undergo the enzymatic reaction.

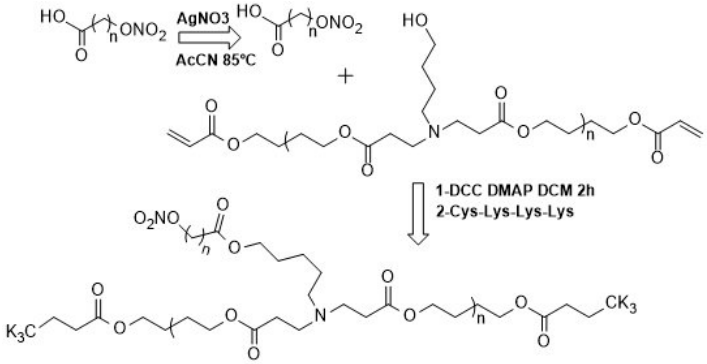

Figure 1.3.2.2 Panel of strategy followed to generate a pBAE containing an organic nitrate group.

1.3.3. Diazeniumdiolate introduction into pBAE

Nitric oxide adducts are great candidates to store and deliver nitric oxide into non-viral vectors. Its destabilization directly delivers pure nitric oxide without any catalyst or enzymatic action involved.

Diazeniumdiolate show destabilization in neutral pH solutions that increase as pH lowers. This property is attractive to incorporate into polymers for nanoparticle delivery due to the sudden decrease of pH during endocytosis. Delivery of nitric oxide during endocytosis may enhance the potency of nitric oxide, due to is preferably delivered intracellularly where it may play a stronger action avoiding dilution on extracellular fluids.

In the other hand, NONOates have a net negative charge, making it a potential drawback due to nanoparticle stabilization if derivatization levels are significantly high.

Stability of the adducts, besides pH is also strongly influenced by temperature and chemical environment. Chemical environment can modify the half-life in neutral pH from a few seconds to almost a day, in Figure 1.3.3.1 a scheme of the structure of diazeniumdiolates and its half-life is presented.

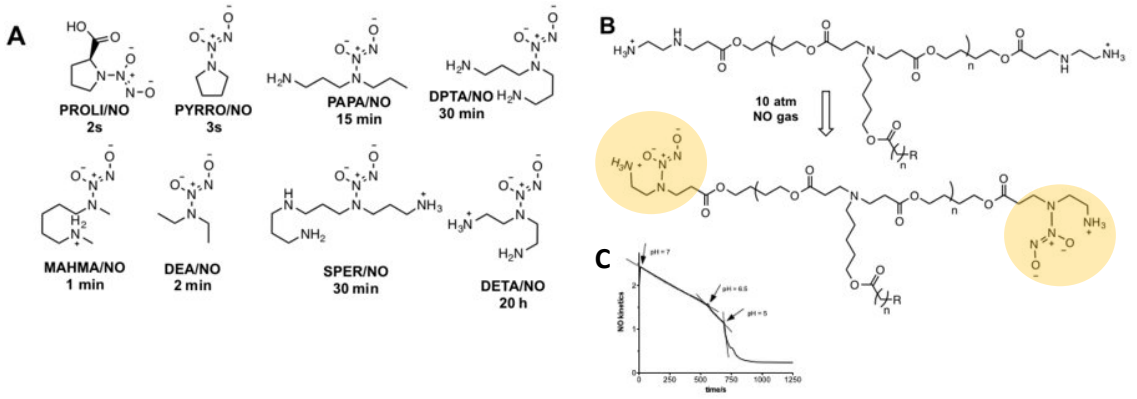

Figure 1.3.3. Examples of diazeniumdiolates with extreme half-lifes, its characteristic synthesis and typical NONOate degradation kinetics. A, characteristic NONOates and its half-life approximation of aquose decomposition at neutral pH and 20 °C.B, Attempted chemical strategies and C, Results of Spermidine-NONOate in function of pH.

The high difference in stability is strongly influenced by the intermolecular charge compensation by protonated amines at specific geometries. One of the difficulties of making NO adducts rely in the difficulty to have secondary amines with available amine groups within 3 positions in both sides limiting the extension of the half-life of the NO donating species.

At present work target half-life and NO-delivery may be in the weeks to even months timeframe, being the largest single molecule reported DETA/NO with a $t_{1/2}$ of 20h [38]. Complexing NONOates into micelles, films or nanoparticles has been reported to extend

delivery for over a few days to a week [39][40], but probably being still not enough for local therapy single dose applications.

The first attempt to introduce NONOate into pBAE was based in adding spermine-NO and DETA-NO directly to C32, unfortunately no solvent was found to dissolve polymer and NONOate to facilitate the reaction. DETA-NO show solubility only in basic water while those conditions are not compatible with pBAE chemistry. Lack of direct bonding of NONOate to polymers forced to change strategy towards adding the secondary amine to the polymer backbone and then trying to incorporate the nitric oxide adducts.
Derivatization of the side chains to incorporate secondary amines was also intended by tosylation of C32 hydroxyl and then reacting with DETA and finally incorporation of nitric oxide. Unfortunately, incorporation of side secondary and primary amines was found to be non-viable at high pressures of NO and this strategy was abandoned. Further information can be found in ANNEX I.

Low stability of diazeniumdiolates, risk of incorporation negative charge of the nanoparticle that may lower stability when mixed with RNA and complexity in synthesis directed other synthetic methods to add nitric oxide into pBAE.

1.3.4. Thionitrite introduction into pBAE

S-nitrosothiols are interesting moieties to incorporate nitric oxide delivery because of its important biological roles in nitric oxide metabolism. S-nitrosothiols are synthetized by the reaction of thiols with nitric oxide or nitrosation compounds being an endogenous system to extend the effects of short living nitric oxide and stabilizing it into molecules such as S-Nitrosoglutathione that modulates nitric oxide expression, excretion and distribution.
S-nitrosothiols are easily formed synthetically by reacting a thiol with a nitrosation agent such as tert-butyl nitrite[41] to form stable S-nitrosothiols with strong vivid colors such as red or green depending on α-carbon substituents.
Originally tertiary S-nitrosothiols were desired to be introduced into C32 base polymer by Steglich reaction. Direct introduction of a tertiary SNO such as SNAP was obtained but rapidly became unstable, probably due to decomposition driven by autocatalysis.
A set of primary mercapto terminated organic acids was synthetized with a stability that correlates with length between moieties. Introduction of those molecules using a carbodiimide, dimethylamino pyridine (DMAP) and the esterification reactions evolved without observed effect on SNO moiety. It was noted during the synthesis that gelation occurred relatively often. To overcome the polymerization of the base polymer the crude was bubbled with Argon, prepared at a higher dilution and rapidly kept in freezer. Further reaction to incorporate primary amines was successful for diamines but more challenging for CK3. S-nitrosothiols are not directly incompatible with amines as can be

seen in S-nitrosogluthatione where they coexist. Introduction of CK3 may involve a reaction between the thiol of the cysteine and the side S-nitrosothiols. Finally, T64-SNO, the condensation of S-nitrosoundecanoic acid and C32 was, not directly destined to compensate RNA and used without oligopeptide extension, but introduction of polyamines such as generation 2 or 3 PAMAM, spermidine or equivalent should have been feasible to synthetize and transfect.

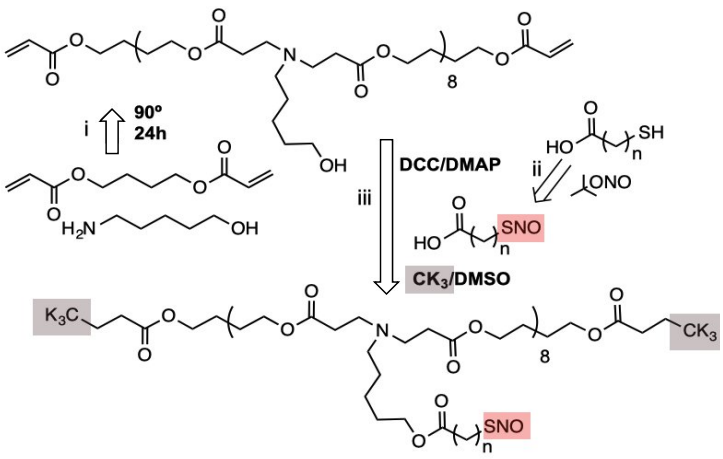

Figure 1.3.4. Panel of strategies followed to include thionitrites to C32 backbone.

1.3.5. Alkyl nitrite containing pBAE

Introduction of alkyl nitrite moieties to polymers may be a desirable route to introduce nitric oxide release properties. Unfortunately, alkyl nitrites also show rapid amine nitrosation and coexistence of amines and alkyl nitrites in the same molecule seem not possible [42].
In Figure 1.3.5 a scheme of the intended strategy is presented. For all experiments tertiary alkyl nitrites have been used due to better exchange ratio[43].

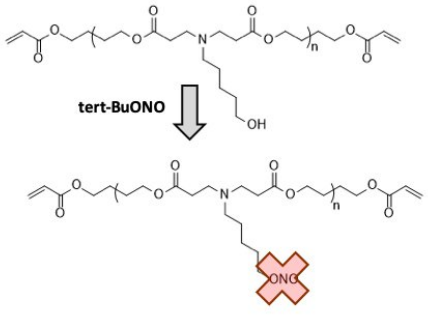

Figure 1.3.5. Panel of studied strategies of organic nitrite synthesis on C32 based pBAE.

Initially direct nitrosation of C32-CK3 was intended by direct reaction with tert-butylnitrite, but evolved rapidly into colorful species lacking the characteristic IR bands of alkyl nitrites.

1.4 CONCLUDING REMARKS

In the present chapter, a series of strategies have been explored to develop poly(beta-amino ester)s based in C32-CK3 introducing moieties that may potentially add nitric oxide deliverability *in vivo*.

K72-NO, a polymer based on C32-CK3 with side hydroxyls esterified by a 6-nitroxoy hexanoic acid has been successfully synthetized together with polymers with shorter side chain extensions. Polymer seem to be stable and suitable for nitric oxide and RNA delivery. Introduction of S-nitrosothiols have been also completed generating a whole set of polymers based on C32 with the sidechains esterified with primary SNO-terminated organic acids between 3 and 16 carbons in length. Stability of the polymers depends strongly on the length of chain extenders. Extension of polymers, such as T64-SNO, with polyamines can be completed with diamines, being thiol containing-amines such as CK3 preferably avoided. Several strategies have been intended to introduce unsuccessfully tertiary SNO, such as SNAP. Organic nitrites and diazeniumthiolate have not been found viable to be introduced to C32 and were abandoned.

In the following chapters, the polymers developed will be studied to elucidate the nitric oxide delivering capabilities, RNA transfection capabilities and potential strategies to locally deliver them for localized therapies.

1.5 REFERENCES

[1] Fire A, Xu S, Montgomery MK, Kostas SA, Driver SE, Mello CC. Potent and specific genetic interference by double-stranded RNA in Caenorhabditis elegans. Nature. 1998;391(6669):806-811. doi:10.1038/35888

[2] Setten RL, Rossi JJ, Han SP. The current state and future directions of RNAi-based therapeutics. Nat Rev Drug Discov. 2019 Jun;18(6):421-446. doi: 10.1038/s41573-019-0017-4. Erratum in: Nat Rev Drug Discov. 2019 Mar 18;: Erratum in: Nat Rev Drug Discov. 2019 Apr 24;

[3] Kamanu, T., Radovanovic, A., Archer, J. et al. Exploration of miRNA families for hypotheses generation. Sci Rep 3, 2940 (2013). https://doi.org/10.1038/srep02940

[4] Friedman RC, Farh KK, Burge CB, Bartel DP. Most mammalian mRNAs are conserved targets of microRNAs. Genome Res. 2009;19(1):92-105. doi:10.1101/gr.082701.108

[5] Pardi N, Hogan MJ, Porter FW, Weissman D. mRNA vaccines - a new era in vaccinology. Nat Rev Drug Discov. 2018;17(4):261-279. doi:10.1038/nrd.2017.243

[6] Tan FL, Yin JQ. RNAi, a new therapeutic strategy against viral infection. Cell Res. 2004;14(6):460-466. doi:10.1038/sj.cr.7290248

[7] DeWeerdt, S. (2019). RNA therapies explained. Nature, 574(7778), S2–S3. doi:10.1038/d41586-019-03068-4

[8] Layzer JM, McCaffrey AP, Tanner AK, Huang Z, Kay MA, Sullenger BA. In vivo activity of nuclease-resistant siRNAs. RNA. 2004;10(5):766-771. doi:10.1261/rna.5239604

[9] Deleavey, G. F., Watts, J. K., Damha, M.J in Current Protocols in Nucleic Acid Chemistry (ed Beaucage, S. L. *et al) Ch 16, Unit 16.3 (2009)*

[10] Wolfrum C, Shi S, Jayaprakash KN, et al. Mechanisms and optimization of in vivo delivery of lipophilic siRNAs. Nat Biotechnol. 2007;25(10):1149-1157. doi:10.1038/nbt1339

[11] Nair JK, Willoughby JL, Chan A, et al. Multivalent N-acetylgalactosamine-conjugated siRNA localizes in hepatocytes and elicits robust RNAi-mediated gene silencing. J Am Chem Soc. 2014;136(49):16958-16961. doi:10.1021/ja505986a

[12] Waehler R, Russell SJ, Curiel DT. Engineering targeted viral vectors for gene therapy. Nat Rev Genet. 2007 Aug;8(8):573-87. doi: 10.1038/nrg2141.

[13] Kowalski PS, Rudra A, Miao L, Anderson DG. Delivering the Messenger: Advances in Technologies for Therapeutic mRNA Delivery. Mol Ther. 2019;27(4):710-728. doi:10.1016/j.ymthe.2019.02.012

[14] Lee SHS, Chang H, Kim JH, et al. Inhibition of mTOR via an AAV-Delivered shRNA Tested in a Rat OIR Model as a Potential Antiangiogenic Gene Therapy. Invest Ophthalmol Vis Sci. 2020;61(2):45. doi:10.1167/iovs.61.2.45

[15] Verma IM, Somia N. Gene therapy -- promises, problems and prospects. Nature. 1997;389(6648):239-242. doi:10.1038/38410

[16] Setten RL, Rossi JJ, Han SP. The current state and future directions of RNAi-based therapeutics [published correction appears in Nat Rev Drug Discov. 2019 Mar 18;:] [published correction appears in Nat Rev Drug Discov. 2019 Apr 24;:]. Nat Rev Drug Discov. 2019;18(6):421-446. doi:10.1038/s41573-019-0017-4

[17] Kurreck J. Rethinking Delivery: Viral vectors and RNA Interference. Journal of RNA and Genomics. 2017;13(1)

[18] Dong Y, Love KT, Dorkin JR, et al. Lipopeptide nanoparticles for potent and selective siRNA delivery in rodents and nonhuman primates [published correction appears in Proc Natl Acad Sci U S A. 2014 Apr 15;111(15):5753]. Proc Natl Acad Sci U S A. 2014;111(11):3955-3960. doi:10.1073/pnas.1322937111

[19] Dong Y, Eltoukhy AA, Alabi CA, et al. Lipid-like nanomaterials for simultaneous gene expression and silencing in vivo. Adv Healthc Mater. 2014;3(9):1392-1397. doi:10.1002/adhm.201400054

[20] Serrano-Sevilla I, Artiga Á, Mitchell SG, De Matteis L, de la Fuente JM. Natural Polysaccharides for siRNA Delivery: Nanocarriers Based on Chitosan, Hyaluronic Acid, and Their Derivatives. Molecules. 2019;24(14):2570. Published 2019 Jul 15. doi:10.3390/molecules24142570

[21] Lynn DM, Anderson DG, Putnam D, Langer R. Accelerated discovery of synthetic transfection vectors: parallel synthesis and screening of a degradable polymer library. J Am Chem Soc. 2001;123(33):8155-8156. doi:10.1021/ja016288p

[22] Fornaguera C, Guerra-Rebollo M, Lázaro MÁ, et al. In Vivo Retargeting of Poly(beta aminoester) (OM-PBAE) Nanoparticles is Influenced by Protein Corona. Adv Healthc Mater. 2019;8(19):e1900849. doi:10.1002/adhm.201900849

[23] Hattori Y, Arai S, Okamoto R, Hamada M, Kawano K, Yonemochi E. Sequential intravenous injection of anionic polymer and cationic lipoplex of siRNA could effectively deliver siRNA to the liver. Int J Pharm. 2014;476(1-2):289-298. doi:10.1016/j.ijpharm.2014.09.059

[24] Riera R , Feiner-Gracia N , Fornaguera C , Cascante A , Borrós S , Albertazzi L . Tracking the DNA complexation state of pBAE polyplexes in cells with super resolution microscopy. Nanoscale. 2019;11(38):17869-17877. doi:10.1039/c9nr02858g

[25] Kaczmarek JC, Patel AK, Kauffman KJ, et al. Polymer-Lipid Nanoparticles for Systemic Delivery of mRNA to the Lungs. Angew Chem Int Ed Engl. 2016;55(44):13808-13812. doi:10.1002/anie.201608450

[26] Xiao B, Ma L, Merlin D. Nanoparticle-mediated co-delivery of chemotherapeutic agent and siRNA for combination cancer therapy. Expert Opin Drug Deliv. 2017;14(1):65-73. doi:10.1080/17425247.2016.1205583

[27] Meng H, Mai WX, Zhang H, et al. Codelivery of an optimal drug/siRNA combination using mesoporous silica nanoparticles to overcome drug resistance in breast cancer in vitro and in vivo. ACS Nano. 2013;7(2):994-1005. doi:10.1021/nn3044066

[28] Kowalski PS, Rudra A, Miao L, Anderson DG. Delivering the Messenger: Advances in Technologies for Therapeutic mRNA Delivery. Mol Ther. 2019;27(4):710-728. doi:10.1016/j.ymthe.2019.02.012

[29] McCleverty JA. Chemistry of nitric oxide relevant to biology. Chem Rev. 2004;104(2):403-418. doi:10.1021/cr020623q

[30] Wang GR, Zhu Y, Halushka PV, Lincoln TM, Mendelsohn ME. Mechanism of platelet inhibition by nitric oxide: in vivo phosphorylation of thromboxane receptor by cyclic GMP-dependent protein kinase. Proc Natl Acad Sci U S A. 1998;95(9):4888-4893. doi:10.1073/pnas.95.9.4888

[31] Farah C, Michel LYM, Balligand JL. Nitric oxide signalling in cardiovascular health and disease. Nat Rev Cardiol. 2018;15(5):292-316. doi:10.1038/nrcardio.2017.224

[32] Yang T, Zelikin AN, Chandrawati R. Progress and Promise of Nitric Oxide-Releasing Platforms. Adv Sci (Weinh). 2018;5(6):1701043. Published 2018 Apr 23. doi:10.1002/advs.201701043

[33] Keefer LK. Fifty years of diazeniumdiolate research. From laboratory curiosity to broad-spectrum biomedical advances. ACS Chem Biol. 2011;6(11):1147-1155. doi:10.1021/cb200274r

[34] Kevil CG, Patel RP. S-Nitrosothiol biology and therapeutic potential in metabolic disease. Curr Opin Investig Drugs. 2010;11(10):1127-1134.

[35] Liang H, Nacharaju P, Friedman A, Friedman JM. Nitric oxide generating/releasing materials. Future Sci OA. 2015;1(1):FSO54. doi:10.4155/fso.15.54

[36] Murrell, William (1879). "Nitro-glycerine as a remedy for angina pectoris". The Lancet. 113 (2894): 80–81, 113–115, 151–152, 225–227. doi:10.1016/s0140-6736(02)42404-x

[37] Keefer LK (2011) Fifty years of Diazeniumdiolate Research. From Laboratory Curiosity to Broad-Spectrum Biomedical Advances. ACS Chem. Biol. 2011, 6, 1147-1155.

[38] Davies KM, Wink DA, Saavedra JE, Keefer LK (2001) Chemistry of the diazeniumdiolates. 2. Kinetics and mechanism of dissociation to nitric oxide in aqueous solution. J Am Chem Soc. 2001 13;123(23):5473-81

[39] Jeong H, Park K, Yoo JC, Hong J (2018) Structural heterogeneity in polymeric nitric oxide donor nanoblended coatings for controlled release behaviors. RSC Adv., 2018, 8, 38792–38800

[40] Jo YS, van der Vlies AJ, Gantz J, Thacher TN, Antonijevic S, Cavadini S, Demurtas D, Stergiopulos N, Hubbell JA (2009) Mielles for Delivery of Nitric Oxide. J. Am. Chem. Soc. 2009, 131, 40, 14413-14418

[41] Roy B; Hardemare AM; Fontecave M. (1994) New thionitrites: Synthesis, stability, and Nitric Oxide Generation. J. Org. Chem 1994, 59, 7019-7026.

[42] Friedman L, JBayless JH. (1969) Aprotic diazotization of aliphatic amines. Hydrocarbon products and reaction parameters. J. Am. Chem. Soc. 1969, 91, 7, 1790-1794

[43] Doyle MP, Terpstra JW, Pickering RA, LePoire DM (1983) Hydrolysis, nitrosyl exchange, and synthesis of alkyl nitrites. J. Org. Chem. 1983, 48, 20, 3379-3382

CHAPTER 2. DEVELOPMENT OF DUAL NO AND RNA NON-VIRAL VECTORS

2.1 INTRODUCTION

After exploring the synthesis and successfully obtaining several non-viral vectors with integrated nitric oxide moieties, it is aimed to validate its RNA complexing properties, transfection performance and explore the effect of nitric oxide contained in the vectors to vascular biology. It is hypothesized that a non-viral vector with ability to efficiently co-deliver nitric oxide and RNAs would be of great interest to treat cardiovascular diseases.

During the last decades, cardiovascular disease (CVD) has accounted one out of every three deaths worldwide[1]. CVD encompasses all the disfunctions of blood vessels and the heart leading to illnesses, such as coronary heart diseases, peripheral arterial and vascular disease, structural heart disease or cerebrovascular disease among others. Those dysfunctions are strongly related to risk factors such as smoking, hypertension, diabetes, dyslipidemia and age[2]. Those risk factors usually have strong effects on different dysregulations, such as abnormal flow patterns, hypertension, excessive oxidative stress and atherosclerosis, leading to the development of several cardiovascular disease. During the last decades great efforts have been carried out to understand and overcome the syndromes caused by the illnesses. Many therapies have also been developed to successfully treat major symptomatically events related to CVD by means of surgical, percutaneous[3] and pharmacological therapies.

Although such a vast disease has complex causalities, most of them are governed by dysregulations that end up in sudden alterations of blood flow causing severe symptoms such as stroke or heart attack. Development of revascularization therapies, prosthetics or current pharmacology has shown an improvement of survival but lacks the potential to reverse the dysregulations causing the disease progression and ultimately the acute and life-threating events.

Major efforts have been dedicated to unravel the mechanisms under cardiovascular disease attempting to improve treatments. Two tremendous milestones were recognized by the Nobel prices in medicine of 1998 and 2006 [4][5]. One of the milestones was related to the unraveling of the mystery originated after discovery in 1977 of an unknown agent, named by that time Endothelium derived relaxing factor (EDRF). After years of intense research, it was found to be nitric oxide, a simple diatomic molecule that play an almost providential role in vascular biology, in Figure 2.1.1 a scheme of the role in vascular biology is presented.

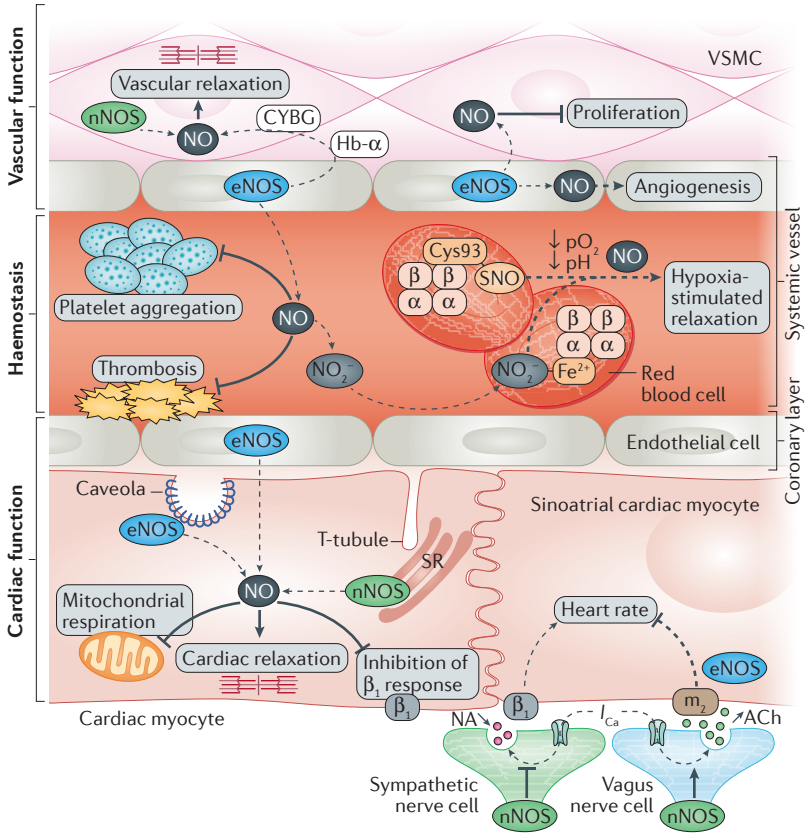

Figure 2.1.1 Effect of nitric oxide in vascular biology. Nitric oxide is synthetized by nitric oxide synthases and plays a key local role. In endothelium eNOS has key roles in the lumen preventing platelet aggregation and ultimately thrombosis. Abluminal NO promotes generation of cGMP activation of PKG lowering calcium intracellularly leading to VSMC hyperpolarization followed by relaxation and ultimately vasodilation. Similarly in myocardiocytes NO induces the increase of cGMP leading to myosin-binding protein C (MYBPC) phosphorylation reducing myophilament calcium sensitivity and ultimately cardiac relaxation[6].

NO has been found to be related to key processes in vascular biology, such as orchestrating vascular tone, inhibiting smooth muscle cell proliferation and its anti-inflammatory/anticlotting properties. It is nowadays well stablished that cardiovascular risk factors impact on the bioavailability of nitric oxide in the vasculature enhancing smooth muscle cell proliferation, that provokes vasoconstriction and platelet aggregation ultimately leading to thrombosis. This lack of bioavailability has a core effect in the development of hypertension and ultimately the acute symptoms of CVD.

Besides the essential role of nitric oxide, miRNAs have been found to be key endogenous modulators of CVD gene expression [7]. Many miRNAs have been found to keep homeostasis and play key roles in the progression of pathogenesis. miRNAs are intracellularly expressed RNA molecules that mature into single stranded RNAs that are partially complementary to mRNAs. MicroRNAs modulate post-transcriptionally gene expression by binding to commentary mRNAs and RISC complex reducing gene expression [8]. microRNAs have been identified as key regulators of important

cardiovascular diseases such as atherosclerosis[9], myocardial fibrosis[10], acute myocardial infarction[11] and heart failure among others. The use of gene expression modulators may be of high therapeutic potential due to versatility to revert pathological conditions by pro-healing miRNAs. In Figure 2.1.2. some miRNAs with key roles in vascular protection and illness progression are presented.

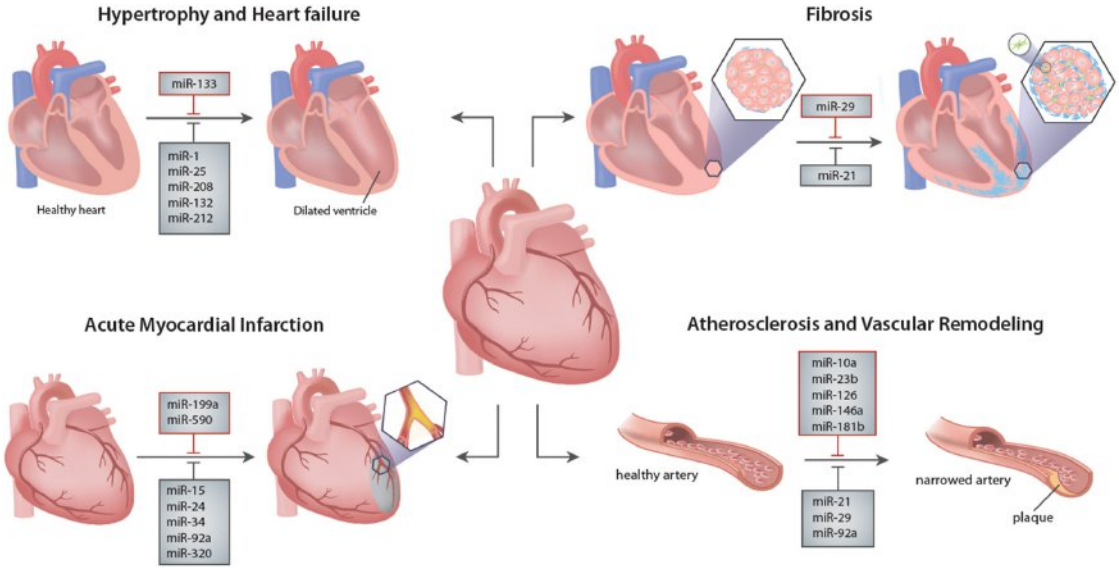

Figure 2.1.2. Role of miRNA in vascular biology as modulators of Heart Failure, fibrosis, AMI and Atherosclerosis.[12]

Many therapies have been proposed to treat vascular diseases by either RNA therapeutics[13] or treatment with NO[14]. Until nowadays, a RNA and NO dual system that can face cardiovascular dysregulations has not been explored. Using two more powerful pathways of vascular homeostasis may be an efficient way to promote new and better therapies for cardiovascular disease.

Nowadays specific vectors to co-deliver RNA and nitric oxide have not been reported having a theoretically high therapeutic potential. Present chapter aims to explore the nitric oxide activity, nanoparticle stability and performance in transfection of a pBAE containing an organic nitrate.

2.2 MATERIALS AND METHODS

2.2.1 Materials: Unless noted all reagents were used from Sigma-Aldrich and used as received. CK3 was obtained from GL biochem without further purification. Luciferase coding mRNA has been purchased from Trilink Biotechnologies(CleanCap® FLuc mRNA). Alexa Fluor™ 568 NHS Ester (Succinimidyl Ester) have been used as red fluorescent labels reactive to amines, purchased from ThermoFisher. 4-Amino-5-Methylamino-2',7'-Difluorofluorescein Diacetate have been purchased from ThermoFisher scientific as a cellular fluorescent marker sensitive to nitric oxide. Internalization studies have been studied with a Red fluorescent dye sensitive to pH; pHrodo™ Red, succinimidyl ester from Invitrogen.

2.2.2 Synthesis of K72-NO polymer: Nitrate containing C32 was synthetized as previously descrived in chapter 1 and used the same stock of materials for all the experiments described. K72-NO was kept in freezer dissolved in DMSO. As an example K72-NO spectral data is presented ^{1}H-RMN (400 MHz, CD_3OD, TMS) (ppm): δ= 6.38 (ddd, *J* = 17.3, 2.4, 1.5 Hz, 0H), 6.18 (dd, *J* = 10.4, 2.1 Hz, 0H), 5.87 (s, 0H), 4.59 – 4.44 (m, 0H), 4.28 – 4.16 (m, 0H), 4.18 – 4.05 (m, 1H), 3.56 (t, *J* = 6.6 Hz, 0H), 2.94 – 2.76 (m, 0H), 2.61 – 2.48 (m, 1H), 2.38 (qd, *J* = 7.6, 7.0, 4.6 Hz, 0H), 1.83 – 1.72 (m, 1H), 1.70 – 1.65 (m, 0H), 1.55 (dd, *J* = 15.6, 8.2 Hz, 0H), 1.37 (dt, *J* = 8.7, 4.4 Hz, 0H), 1.24 (td, *J* = 7.1, 2.4 Hz, 0H). FTIR-ATR: 1619 cm^{-1} (NO stretch), 1704 cm^{-1} (C=O stretch), 1275cm^{-1} (N-O stretch).

2.2.3 Synthesis of nanoparticles: K72-NO and polynucleotide nanoparticles were mixed at equal volumes in acetate buffer (25mM, pH=5). Polynucleotide stock solution was 0,01 µg/µL and K72NO amount was adapted from a 100 µg/µL stock solution. After mixing solution was vigorously mixed and left at room temperature for 30 minutes before further actions.

2.2.4 Nanoparticle lyophilization: Nanoparticle lyophilization was undertaken by adding sucrose to 20mg/mL and freezing in liquid nitrogen following lyophilization. Reconstitution was done by adding miliQ® water and vortexing for 1 minute.

2.2.5 Gel retardation assay: Nanoparticle stability was studied running retardation assays over2.5% Agarose gels in TAE balanced buffer (Tris-Acetate-EDTA) using SYBR green (1 µg/uL) as detection agent. Samples were run during 45 min at 80V and imaged over UV light.

2.2.6 Dynamic Light scattering: Particle size and Z-potential were determined using a Zetasizer Nano ZS (Malvern Instruments Ltd, UK) at 633nm and 4mW. Measurements were carried out mixing 100µL of Acetate buffer (25mM, pH 5) and 900 µL of PBS.

2.2.7 Buffering capacity: Acid-base titration was used to stablish the buffering capacity of polyplexes. 5 mg of polymer were diluted in 0.9M NaCl to 1 mg/mL. Subsequently pH was adjusted with 0.1M sodium hydroxide until a pH=10 was reached. The buffering capacity was measured by adding aliquots of 10 µL of 0.1HCl and recording the pH(Crison Basic 20+, Crison instruments) after each addition until pH=2.

2.2.8 Cell culture and nanoparticle transfection: COS-7 and MDA MB 231 (GFP+) have been used for all experiments between passage 3 and 8. Cells were cultured at 37□C in a 5% CO_2 atmosphere. The media used consisted in DMAEM supplemented with 10% FBS, penicillin/streptomycin and 1% glutamine. For transfection and viability experiments cells were seeded in a 96 well plate, suitable for cell culture during 12h. Prior to nanoparticle incubation, cells were washed with PBS and incubated with the nanoparticles prepared as previously described for 2h at 37□C prior to media change and further analysis.

2.2.9 Cytotoxicity: Cell viability was studied by using MTS and LiveDead assay. For MTS, cells cultured were washed with PBS, incubated in 20% of MTS (Celltiter 96, Promega) diluted in culture media for one hour and analyzed by optical absorbance at 490nm in 96 wp (Elx808 Biotek Instruments Ltd). Controls were selected as follow, positive control of viability were cells untreated, and negative controls were cells killed by 60 seconds incubation in ethanol and incubated with MTS. An alternative method to asses viability, Live/Dead® () was used to get images of morphology and viability. Cells were washed twice with PBS and incubated for 30 minutes with serum free media supplemented with Calcein-AM and propidium iodide following manufacturer instructions. Cells were washed with serum free media and imaged by fluorescence microscopy Calcein-AM (ex/em 490/525) and PI (ex/em 535/617).

2.2.10 FACS expression measurement: Transfection efficiency was measured by flow cytometry (FACS; in a BD Fortessa cell analyzer). After transfection, cells were incubated for 5 min with trypsin− ethylenediaminetetraacetic acid at 37 °Cin 5%CO2 atmosphere and fixed with previously filtered paraformaldehyde (0.22 µm, 2% in PBS). GFP expression was quantified and compared against a negative control of untreated cells.

2.2.11 Internalization experiment: Study of the internalization mechanisms were performed by derivatization of K72-NO polymer with a dye with variable fluorescence dependence on environmental pH, pHrodo™ Red, SE (Thermo Fisher). Derivatization of the polymer was performed at a 0.2 % molar ratio amine-NHS esther in DMSO. Polymer was purified by precipitation in diethylether/acetone and analyzed by TLC to check residual unbound dye. Nanoparticles were formed with pGFP at 100:1 ratio and incubated over COS-7 cells at 10kcells/96wp incubated with Hoetsch 33342 and imaged by epifluorescence/confocal microscopy every 15 minutes. Evaluation of Luciferase activity was studied by incubation with luciferin and image analysis after 2 minutes exposure.

2.2.12 in vivo hemodynamic study: This study was addressed to investigate the hemodynamic effects of PBAE NPs that includes a nitrooxy group acting as NO donor in healthy animals. Eight male Wistar rats (Charles-River, Saint Aubin les Elseuf, France) were randomly assigned to one of the following groups: 1) Intravenous bolus injection (30 mg/kg bw) of PBAE NO donor NPs (n=4). 2) Intravenous bolus injection of PBAE NPs without the nitrooxy group as negative control (n=4). Next, rats were anesthetized with Inactin® (100 mg/Kg bw, Sigma-Aldrich Chemie Gmbh, Steinherim, Germany) and

prepared with PE-50 polyvinyl catheters in the left femoral artery and vein for blood pressure recording and blood sampling and infusion of substances, respectively. The arterial catheter was connected to a highly sensitive transducer (Hewlett Packard, Avondale, PA) that was calibrated before each study. Hemodynamic parameters were recorded in a multichannel system (PowerLab®, ADInstruments, Sydney, Australia) after a 30 min stabilization period. Then, values of mean arterial pressure (MAP) and heart rate (HR) were continuously recorded in basal conditions and for 180 min after the intravenous administration of NO donor or negative control. At the end of the hemodynamic study the animals were sacrificed by an overdose of anesthesia (isofluorane).

2.2.13 Statistical analysis: Data were analyzed using GraphPad® Prism. Comparisons between groups were done by one-way ANOVA using Turkey *post-hoc* test. Differences were considered significant when $p<0.05$ *, $p<0.01$** and $p<0.001$***.

2.3 RESULTS AND DISCUSSION

2.3.1 K72-NO synthesis

A new set of polymers based on previously synthetized[15] non-viral vector and improved by end-modification of C32 pBAE[16] has been developed. Synthesis is based on the extension of the C32 hydroxyl terminated side chains with alkyl chains terminated with nitrooxy moieties (K72-NO) to incorporate nitric oxide releasing properties. The lack of reactiveness of organic nitrate altogether with the specificity of Steglich reaction yielded a robust and reliable coupling reaction, the synthetic scheme can be observed in Figure 2.3.1. Development of nitrooxy terminated carboxylic acids used for coupling was accomplished by modifying available halogen terminated carboxylic acids with silver nitrate. Total yield of K72-NO was in the 50-60% after purification. Polymers obtained are highly viscous materials that are stable under dry conditions.

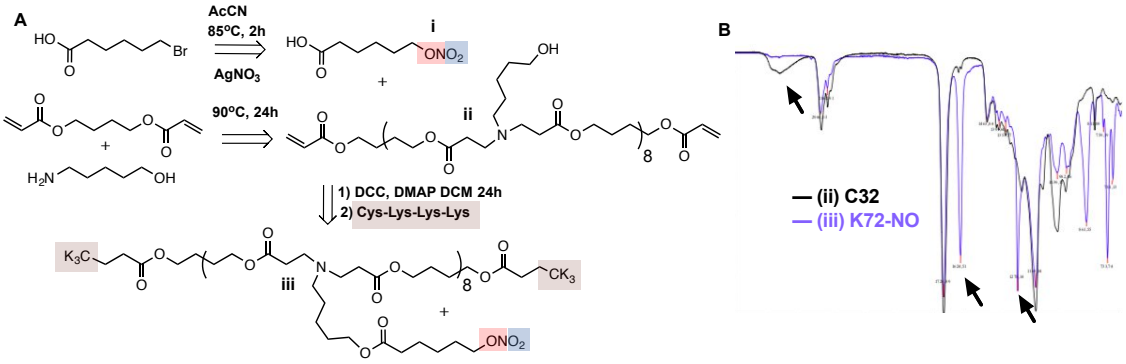

Figure 2.3.1. K72-NO synthesis scheme. A, Synthetic pathway to produce K72-NO by synthesis of nitrooxyhexanoic acid and further coupling it to C32 polymer by esterification of the hydroxyl groups. B, FTIR-ATR of C32 and K72-NO. Arrows show organic nitrate characteristic bands and hydroxyl bands.

2.3.2 Biophysical characterization of K72-NO based polyplexes

Poly(beta-amino esters) are biodegradable polymers designed to form stable nanoparticles (NP) with oligonucleotides and allow efficient endosomal escape to deliver nuclear material intracellularly. NP stability is of great importance to develop efficient RNA therapies due to importance of shielding nuclear material and compensate negative charge during internalization. Nanoparticles have been proposed as key vectors for systemic delivery due to unique size properties and internalization capabilities, those properties are also completely valid for local delivery under nanoparticle form. Modification of the C32-CK3 base polymer to incorporate organic nitrates through an extension of the side chains enhances hydrophobicity of base polymer, increases of hydrophobicity have been related to more stable nanoparticles[17]. A series of C32-CK3 side extended polymers have been synthetized using chain extenders of different length but current discussion is focused in the 6 carbon (K72-NO) due to better nanoparticle stability. In Figure 2.3.2 multiple

experiments are presented to characterize K72-NO polyplex stability with a broad range of polynucleotides. K72-NO is mainly compared to C32-CK3 due to previous data comparing it to best in class pBAE or well stablished non-viral vectors such as lipofectamine[18][19].

K72-NO characterization was started by screening the electrophoresis behavior in agar gel, results showed that ratios beyond 2-5 (polymer to nucleotide weight ratio) form stable complexes with a correlation between increasing polymer ratio and stability (Figure 2.3.2.L). Lack of fluorescence in the socket at high polymer ratios is probably due to dye exclusion from nanoparticles at high polymer ratios. The range of nucleotides used, allow to extrapolate that K72-NO does form stable nanoparticles with a broad range of polynucleotides such as small double stranded RNA, large single stranded RNA or large double stranded DNA.

After screening the nanoparticle stability, the hydrodynamic diameter of nanoparticles was studied using DLS and single-nanoparticle tracking. The whole set of complexes formed stable nanoparticles of polymer to nucleic acid weight ratios between 50 and 200, with diameters in the 150-250 nm range (Figure 2.3.2.B-D). The different methods used to evaluate hydrodynamic diameter and stability gave consistent results. Low Nanoparticle polydispersity also supported that stable nanoparticle sets were formed with lack of particle aggregation.
The study of surface charge shows a positive ζ-potential in correlation with polymer ratio (Figure 2.3.2.F-H). Surface charge represented by Z-potential has an important role in biophysical stability and biochemical compatibility. Particles with near neutral ζ-potential usually have a higher tendency to flocculate while in particle-cell and particle-protein interaction the potential leads to affinity for charged serum and cell surface proteins mediating internalization and potentially helping to direct particles to different organs[20]. Larger sets of nanoparticles were also studied beyond 200:1 but were discarded its use in the study due to strong positive charge and poor results obtained previously in the research group. Compatibility in blood media was simulated by adding fetal bovine serum to nanoparticles and tracking optical density, basically 50:1 polymer ratio showed stable particles besides the presence of serum proteins (data not shown) while 200:1 ratio rapidly coagulated. Interaction of serum protein with nanoparticles was intended to be studied by dynamic light scattering but measurements were not viable due to probable interference between serum proteins, nanoparticles and aggregates.

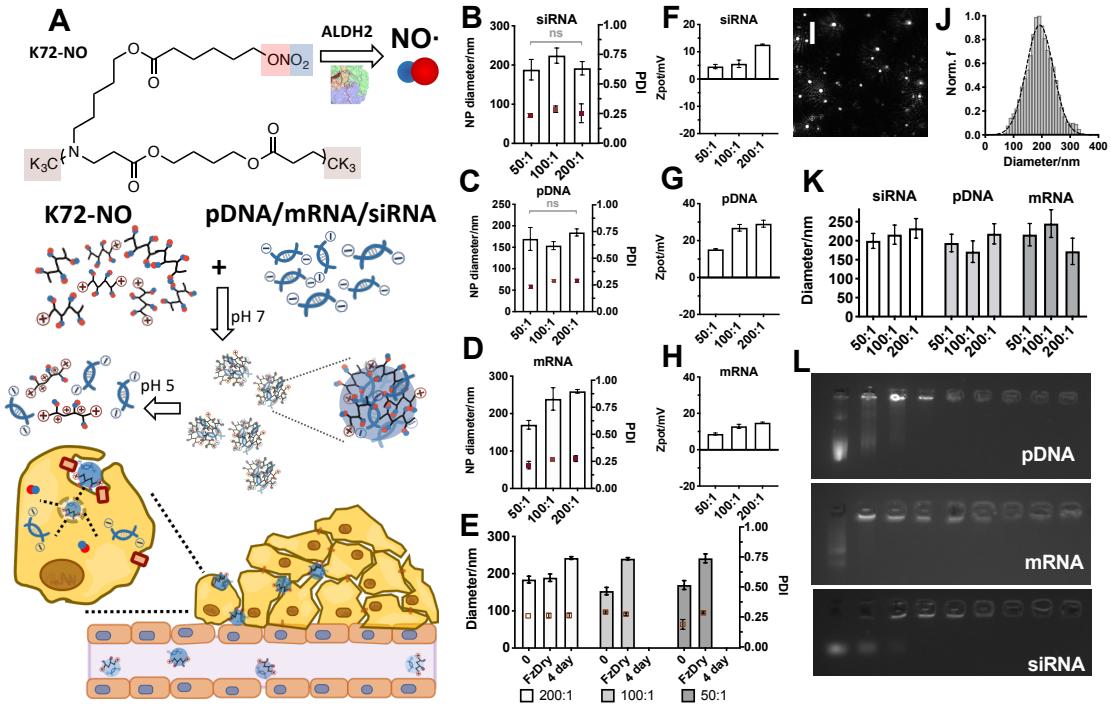

Figure 2.3.2. Nanoparticle characterization. A, K72-NO pBAE derivatized with oligopeptides (purple) and Organic Nitrates (blue-red) and its scheme of nanoparticle formation with RNA. B, C and D, Dynamic Light scattering measurement of nanoparticle diameter and polydispersivity index of K72-NO with siRNA, pGFP and mRNA respectively at 50 to 200 weight ratios (polymer to DNA/RNA). E, Effect of lyophilization and evolution of time to nanoparticle diameter at different weight ratios. F, G and H, z-Potential measurement of siRNA, pDNA and mRNA. I, Dynamic Light scattering microscopy image of single nanoparticles tracking using Nano particle tracking analysis. J, Example of K72-NO-pGFP 50:1 diameter population after nanoparticle formation, dashed line shows a gaussian fitting. K, Nanoparticle tracking analysis characterization of diameter using different nucleic acids. L, Gel electrophoresis of pDNA, mRNA, siRNA to polymer weight ratios of 0, 2, 5, 10, 25, 50, 100, 150 and 200. Retention of nucleic acids shows good complexation. All results are shown as mean plus minus the standard error mean. * $p<0.05$, ** $p<0.01$, ***$p<0.001$.

Developing polyplexes that are stable in blood media is of critical interest to allow high residence times in circulation. Surface coating of nanoparticles with non-fouling polymers such as PEG has been used successfully to increase stability[21] but also affects the potential of rapid particle internalization.

Although highly charged positive nanoparticles are not suitable for systemic administration due to coagulation it may have a potential interest in local delivery to exploit the adhesiveness and limited local effects of highly positively charged polymers.

Robustness of polyplex stability in nanoparticle form was also studied by checking the freeze-drying compatibility, freeze and thaw and nanoparticle stability after 4 days. Large Polymer to nucleotides ratios showed stable nanoparticles under all conditions.

Those results are probably explained by the larger ζ-potential of the polyplexes (Figure 2.3.2.E).

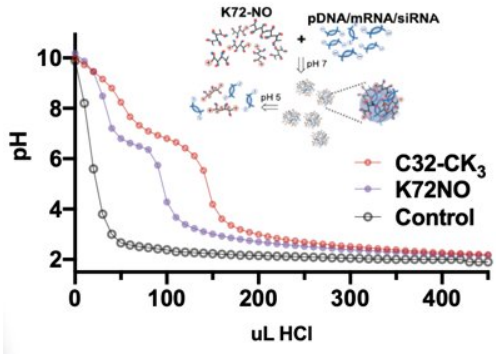

Figure 2.3.3. Buffering effect of K72-NO and control polymer.

The base polymer used is designed to destabilize in acid media due to the protonation of tertiary amines of the backbone. Destabilization should happen during endocytosis caused by the diminution of pH and positive charging of K72-NO followed by intracellular delivery of nucleic material. Results show a slightly lower nominal buffering compared CK3-C32 due to larger molecular weight of K72-NO, suggesting that intracellular delivery should not be significantly compromised (Figure 2.3.3). High polymer ratios were found to be more unstable in plasma-like media due to flocculation. Although it may not be a critical issue in local delivery strategies, tagging of nanoparticles with PEG molecules increased stability in plasma (data not shown).

Ability of K72-NO to deliver nitric oxide was studied *in vitro* by either chemical and enzymatic methods. Incubation of polymer suspensions in media supplemented with serum did not show any increase in nitric oxide or its metabolites. DAF-FM, a nitric oxide sensitive fluorescent dye was proposed as a reporter molecule to detect the *in situ* production of NO. Surprisingly, final results showed that there is not a real conversion and fluorescence was caused by interference of polymeric backbone with the dye rather than transformation into NO. Delivery of nitric oxide in the presence of aldehyde dehydrogenase was found to be unable to report biotransformation of the organic nitrates. At this point, it was unclear if NO delivery *in vitro* failed due to lack of enzymatic affinity or lack of enzymatic isoforms available for *in vitro* testing.

Incubation of cells with NO sensitive dye and K72-NO nanoparticles was suspected to slightly increase fluorescence although no conclusive results were found. It is possible that the cells used *in vitro* lack the isoforms of ALDH required to metabolize organic nitrates[22]. Conclusions related to NO release lead to require either complex biochemical tools or use *in vivo* experiments to unravel the potential of K72-NO to release nitric oxide.

2.3.3 Toxicity evaluation of K72-NO

The cellular toxicity of K72-NO has been studied by incubation of the polymer and nanoparticle suspensions of different concentrations. The evaluation of toxicity has been evaluated using at least two different cell lines and two different methods of cellular viability evaluation, seeking a more robust conclusions. Results obtained are presented in Figure 2.3.4, cytotoxicity patterns show a similar trend to well stablished C32-CK3 polymer and equivalent pBAEs[23]. K72-NO cytotoxicity (Figure 2.3.4.E) increased with concentration and polymer ratio as expected due to interaction with negatively charged surface proteins, both MTS and calcein-AM assays showed consistent results (Figure 2.3.4.A-C). Although MTS results seemed to be more sensitive than microscopy.
LC50 of nanoparticles showed an equivalent degree of toxicity for the two cell lines evaluated being the concentration close to 0.1mg/mL. The cellular toxicity profile of the polymer alone showed a 10- to 20-fold decrease compared to nanoparticles probably due to a faster interaction with cellular membrane proteins. The LC50 of nanoparticle suspension may give an extrapolation to dose toxicities as high as 100mg/kg (Figure 2.3.4.D). Those doses may be considerably larger due to a greater number of cells and potentially higher metabolic activity than in monocultures. Injection of doses in mice as high as 30mg/kg of K72-NO nanoparticles have been found to lack appreciable side effects reinforcing the low toxicity profile of the K72-NO polymer based nanoparticles (Figure 2.3.4.E).

A similar toxicity pattern to previously studied pBAE may imply that organic nitrate does not impact negatively in the biocompatibility, although cells studied *in vivo* probably lack the ability to biotransform organic nitrates into nitric oxide. All the experiments were conducted using siRNA coding to block GFP expression as a theoretical worst-case selection for nanoparticle stability. It is assumed that polynucleotide sequences used, do not have an influence in the toxicity being the polymer the leading cytotoxic component.

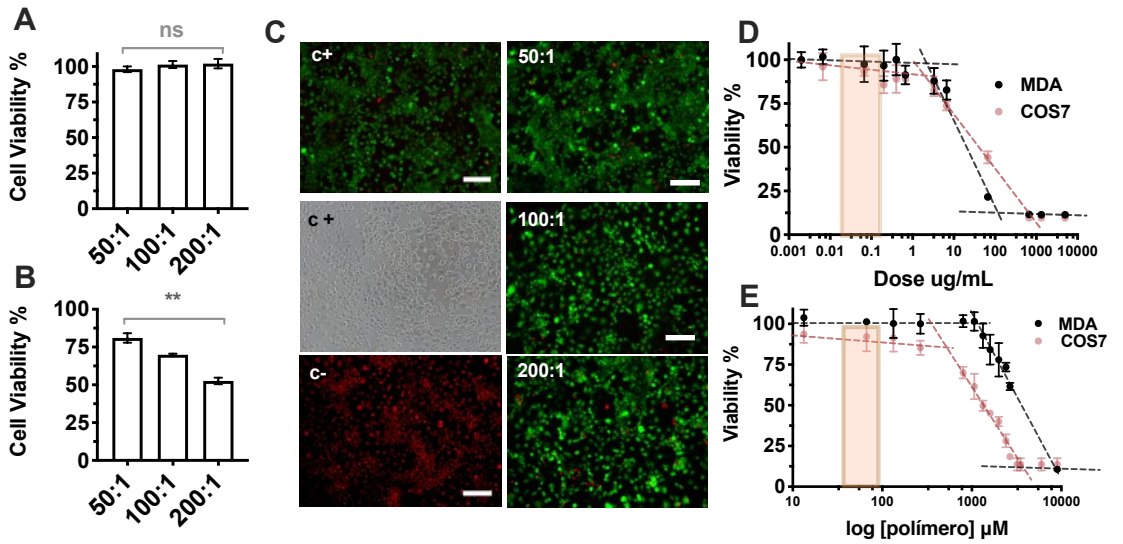

Figure 2.3.4 *In vitro* cell toxicity of K72-NO and K72-NO polyplexes. A, MDA MTS viability after treatment with nanoparticles. B, COS-7 MTS viability after treatment with nanoparticles. C, Cell viability of COS-7 after calcein-AM staining and PI at different polymer ratios, positive control were untreated cells, and negative control cells treated with ethanol. D, Dose response MTS viability after treating MDA and COS-7 with increasing nanoparticle concentration, highlighted area represents incubation ran. E, Dose response MTS viability after treating MDA and COS-7 with increasing K72-NO polymer alone. In red the range of detectable activity and usual treatment is highlighted. All results are shown as mean plus minus the standard error mean. * p<0.05, ** p<0.01, ***p<0.001.

2.3.4 Transfection efficiency

Modification of the expression patterns has been evaluated using a broad sample of polynucleotides (20 bp dual stranded siRNA, 996 base pair of single stranded mRNA and 5556 bp dual stranded DNA plasmid) in an attempt to proof the capacity of the system to deliver a broad spectrum of nucleic material to cells. Studying different mechanisms to alter gene expression and different cell lines. Results show equivalent results of expression modification following different approaches such as silencing, introduction of DNA and direct induction of mRNA, suggesting that the non-viral vector developed may be suitable to be used with different silencing/expression strategies. Analysis of expression by fluorescence microscopy, fluorescent activated cell sorting and luminescence imaging gave consistent results about the expression interference. Results can be observed in Figure 2.3.5.

Results show a dose-dependent response with equivalent or better results to previously reported C32-CK3 (Figure 2.3.5.D). The cellular cultures were able to induce the expression of reporter genes such as luciferase and GFP as well as silence the expression of a GFP expressing cell line. The use of siRNA showed a reduction of 75% of fluorescent dye (Figure 2.3.5.A) due to a complete fluorescence suppression may require a larger and longer lasting dosing. As a general trend, higher polymer ratio show better

transfection efficiency. It is probably due to a sequence of events induced by a higher affinity to surface proteins and a faster internalization and more efficient endosomal escape caused by a higher positive charge and destabilization of nanoparticles.

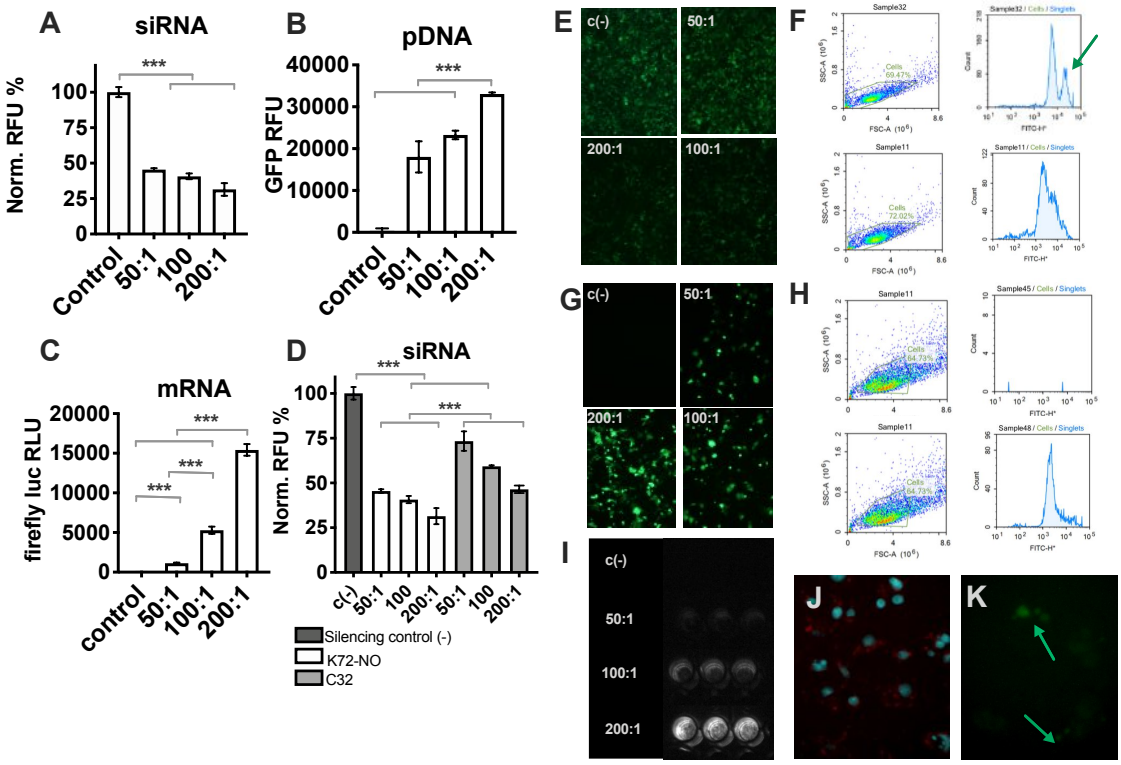

Figure 2.3.5 *In vitro* transfection efficacy. A, siRNA silencing effect of GFP positive MDA cells treated with nanoparticles at different ratios. B, GFP expression at different ratios of pDNA coding for GFP. C, luciferase expression by mRNA-K72-NO nanoparticles at different polymer ratios. D, Comparison of siRNA silencing effect of CK3-C32 and K72-NO polymers. E Images of GFP silencing effect at different polymer ratios. F, FACS silencing distribution of cells and fluorescence. G, GFP expression at different ratios of pDNA and K72-NO. H, FACS fluorescence distribution of control cells(top) and transfected cells(down). I, Light expression after mRNA coding for luciferase. J, Internalization of K72-NO nanoparticles labeled with acid pH-sensitive dye, K-Expression of GFP after 30 min incubation. All results are shown as mean plus minus the standard error mean. * $p<0.05$, ** $p<0.01$, ***$p<0.001$.

High polymeric ratios imply a more stable complexation and potentially better shielding nucleic material from catalytic enzymes of the serum, on the other hand the higher polymer ratios increase toxicity and lowers stability in serum-containing media due to flocculation risk.

After exploring the suitability of expression pattern disturbance through different pathways, a deeper insight into understanding the internalization mechanism was attempted. Nanoparticles are designed to be endocytosed and deliver the nucleic material under acidic pH due to positive charging and nanoparticle destabilization to allow nucleic material delivery into cytoplasm. To evaluate the endosomal escape K72-NO was labeled with a pH dependent fluorescence probe that becomes strongly fluorescence at acidic pH (Figure 2.3.5.J-K). It has been observed that after 15 minutes

a concentration in the cell surface followed to further concentration into vesicles with a fluorescent increase is observed being consistent with an endocytosis mechanism. Also, an increase of GFP was observed after 120 minutes in some cells. The results were limited by the use of an epifluorescence microscopy, the use of confocal microscopy may be of greater interest to further assess the localization of vesicles and the localization of reporter gene expression.

The best strategy to alter gene expression may depend strongly on the clinical situation to be explored, usually siRNA or miRNA are good candidates to temporarily suppress expression also low molecular weight allow a better dosing efficiency, DNA plasmids are only expressed though insertion into nuclear membrane in cell division phase what restricts the performance in non-dividing tissues and requires a significantly more complex peptide. Using a whole mRNA has also a great potential to induce the direct expression of proteins to target cells.

2.3.5 In vivo results

Limitations found to assess the capabilities of K72-NO to deliver nitric oxide, forced to study the biotransformation under hemodynamic conditions to ultimately determine whether the polymer had nitric oxide releasing properties. The hemodynamic study consisted in catheterizing the femoral artery of a rat with an intravascular pressure and heart rate sensor to see the effects of K72-NO nanoparticles administration. Results are presented in Figure 2.3.6. Injection of nanoparticles showed a sudden decrease of blood pressure (10 to 20 mmHg) that was sustained for at least 3 hours, control injection with C32-CK3 (polymer lacking the organic nitrate) did not show significant alteration of the blood pressure or heart rate. Probably, the sudden decrease is the result of the nitric oxide and the physiological response to compensate cardiac output. Usually, pressure decreases/drop/decline of 1 to 10 mmHg have been found to be clinically significant for blood pressure associated diseases[24], suggesting that current non-viral vectors may be potential candidates to improve outcomes of selected vascular treatments by the effect of nitric oxide.
During the experiments, heart rate was also rapidly increased and maintained high during the whole experiment. Drugs delivering nitric oxide are well described to produce systemic vasodilation that causes an arterial volume depletion that lowers pressure and ultimately lowers cardiac output[25]. To compensate blood supply, usually heart rate increases causing reflex tachycardia. Interestingly the effect of nitroglycerin is fast and clears within 5-10 minutes[26] after administration while the effect after administration of K72-NO was sustained for hours. Lower doses of polymer injection did show a dose dependent decrease of blood pressure and increase of heart rate. Nanoparticles injected had a fluorescent marker to check the distribution with a special focus to the

vasculature. It can be observed how polymer significantly attached to the surface of blood vessels when compared with non-labeled control (Figure 2.3.6.C-D).
Besides the hemodynamical effects, the doses in both NO delivering and control polymers showed good dose tolerability without any observed adverse events. Interestingly, the range of NO delivered was in the physiologic range of activity although it remains unclear what is the exact concentration needed[27].

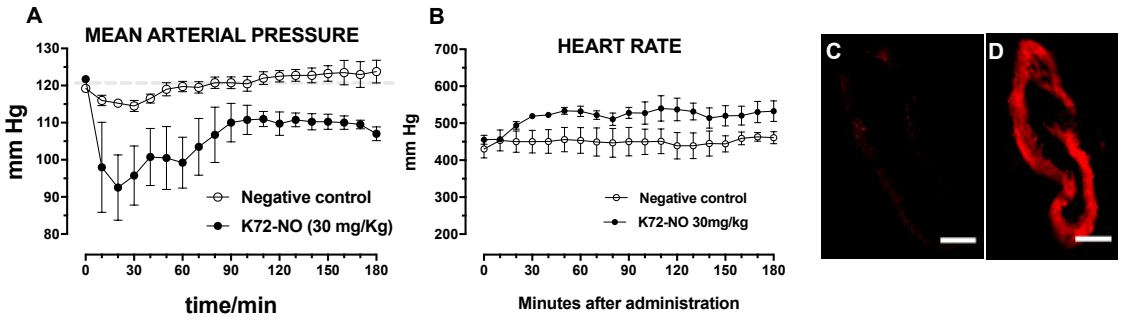

Figure 2.3.6 *In vivo* transfection and vasodilation effects. A. Hemodynamic effects induced by the intravenous administration of PBAE NO donor NPs in healthy rats. Changes in mean arterial pressure (MAP) and heart rate (HR) were recorded in baseline conditions and for 180 minutes after the intravenous administration of K72-NO donor NPs (30 mg/Kg bw) or the corresponding negative control to healthy rats. B, Effect of the NPs injection on heart rate showing an increase in the K72-NO coherent with vasodilation. C ,D, Aortic sections after injection of control NPs(left, C) and fluorescent labeled by Nanoparticle K72-NO labeled with Texas-Red.

Biotransformation of organic nitrates to nitric oxide and activation of cGMP dependent vasorelaxation has been a great deal of debate during the last decades[28]. Basically, organic nitrates are biotransformed both by hepatic tissue and blood vessels in humans or rodents, while porcine or bovine may lack this ability and only liver is able to transform organic nitrates to nitric oxide[29].
Esterase activity of ALDH2 plays an important role in the biotransformation of organic nitrates to active nitric oxide, this role is based on an active site thiol side reaction resulting in reductase activity of the mitochondrial chain. In figure 2.3.7 a scheme of the main pathways to biotransform NO from organic nitrates is presented.

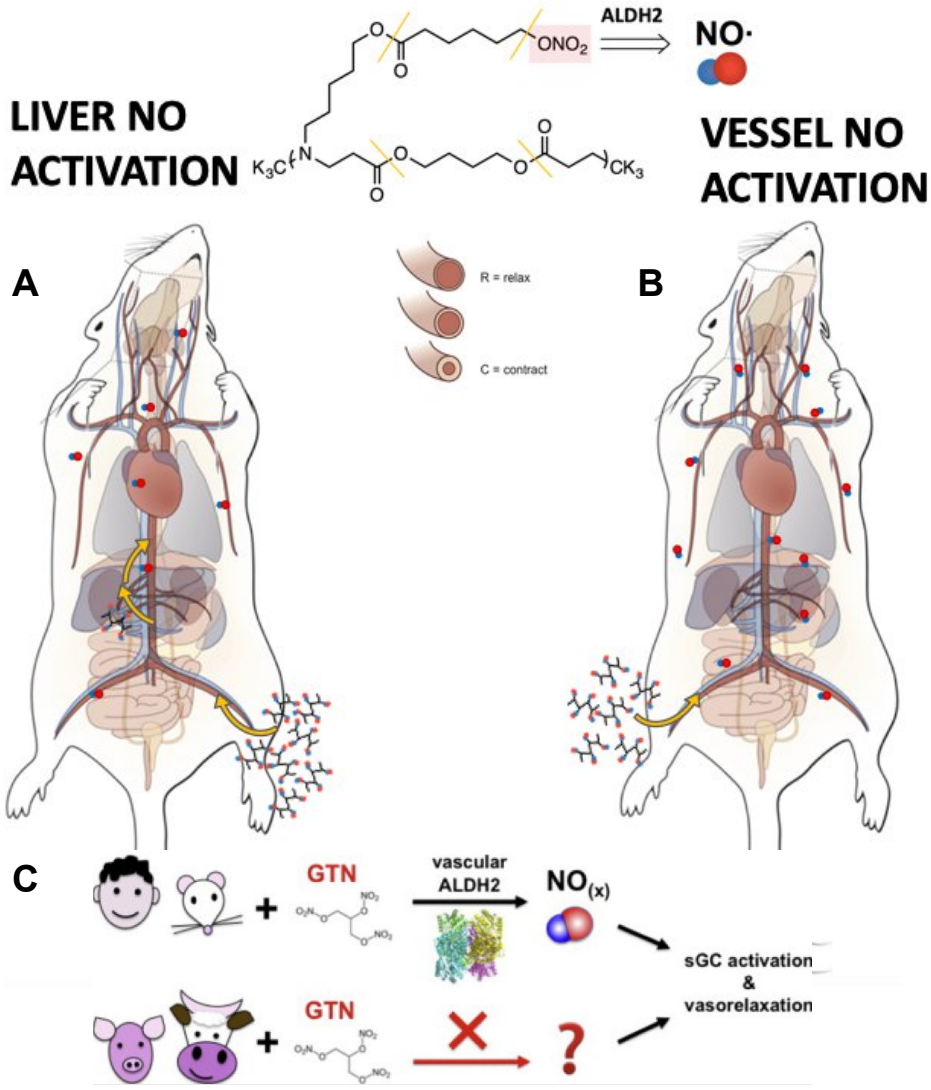

Figure 2.3.7. Mechanism of nitric oxide delivery from K72-NO nanoparticles. A, Hypothesis of nanoparticle degradation and/or nitric oxide biotransformation after hepatic internalization of nanoparticle or fragments. B, Activation of the C, Different schemes of organic nitrates biotransformation of different species by vascular ALDH2 or unknown routes.

Understanding the biotransformation pathway is of great interest to develop locally relevant therapeutic strategies to deliver both nitric oxide and modify expression patterns. Pharmacodynamics of the nitrate moieties are probably slower in biotransformation than nitroglycerin explaining partially why long effects are observed. Intravascular degradation to small K72-NO fragments may allow transformation in hepatic cells or in vascular cells being another plausible mechanism.

Assessing the route of biotransformation is complex due to interspecies variability of ALDH2 isoform and tissue expression. Isoform specificities are also found between different ethnic groups[30] with significant enzymatic activity.

It is possible that a mixture of the events take place, having a partial extravascular degradation and intracellular degradation, also primary organic nitrates have less affinity than secondary organic nitrates[31] contributing also to long-lasting effect that may extend to hours or days due to nanoparticle degradation and biotransformation of NO may be additive, reaching a sustained release of nitric oxide.
Understanding the pathways is of great importance to design local delivery strategies targeting the vasculature or other tissues.

2.4 CONCLUDING REMARKS

pBAE derivatized with cationic peptides and organic nitrate moieties (K72-NO) have been found to be an efficient way to co-deliver nitric oxide in a relevant physiological concentration and a broad spectrum of polynucleotides.
K72-NO has been proved to form stable nanoparticles of around 200 nm when complexing with a broad set of nucleotides such as 20-6000 base of RNA and DNA plasmids with more than 1000 bases. Stability increased with polymer ratio and different diameter characterization gave comparable values for all configurations. K72-NO presented a higher stability than C32-CK3 probably due to higher hydrophobicity.

Transfection efficiency and toxicity have been found to be equivalent to well stablished C32-CK3 non-viral system. The transfection is produced by endocytosis mechanism of the polymeric particles that previously attach to the cell membrane. Both pDNA, siRNA and mRNA have been found to alter gene expression by different analytical methods. As a general trend, higher ratio of polymer to nucleic material has a higher transfection efficiency but is also associated to higher toxicity.

Vasodilation and increase of heart rate have been observed after nanoparticles injection and a sustained effect was achieved compared to expectable results of an organic nitrate. Those results imply that the organic nitrate route is a viable way to co-deliver RNA and NO. It remains unclear which mechanism is undertaken by the nanoparticles to efficiently biotransform the nitric oxide.

In addition to the systemic effect of nitric oxide, nanoparticles labeled with fluorescent dye have been found to accumulate in the vascular wall of blood vessels encouraging the potential use in local delivery targeting vasculature. This role is of special importance to combine RNA therapeutics with NO delivery in local therapies, opening new opportunities for treatments with limited drug candidates or current solutions.

2.5 REFERENCES

[1] Wang et al. GBD 2015 Mortality and Causes of Death Collaborators. Global, regional, and national life expectancy, all-cause mortality, and cause-specific mortality for 249 causes of death, 1980-2015: a systematic analysis for the Global Burden of Disease Study 2015. Lancet. 2016 Oct 8;388(10053):1459-1544. doi: 10.1016/S0140-6736(16)31012-1. Erratum in: Lancet. 2017 Jan 7;389(10064):e1.

[2] O'Donell J.C., Elousa R. (2008) Factores de riesgo cardiovascular. Perspectivas derivadas del Framingham Heart Study. Rev Esp Cardiol. 2008 Mar;61(3):299-310. DOI: 10.1157/13116658.

[3] Sanghavi, M.D. (2013) The history of cardiac care: overtreatment or impressive gains. Lancet, 2013, 382, 759-760. DOI: 10.1157/13116658

[4] Koshland DE Jr. The molecule of the year. Science. 1990 Dec 21;250(4988):1637. doi: 10.1126/science.250.4988.1637. PMID: 17734689.

[5] Fire A, Xu S, Montgomery MK, Kostas SA, Driver SE, Mello CC. Potent and specific genetic interference by double-stranded RNA in Caenorhabditis elegans. Nature. 1998 Feb 19;391(6669):806-11. doi: 10.1038/35888.

[6] Farah C, Michel LYM, Balligand JL. Nitric oxide signalling in cardiovascular health and disease. Nat Rev Cardiol. 2018 May;15(5):292-316. doi: 10.1038/nrcardio.2017.224.

[7] Lucas T, Bonauer A, Dimmeler S. RNA Therapeutics in Cardiovascular Disease. Circ Res. 2018 Jul 6;123(2):205-220. doi: 10.1161/CIRCRESAHA.117.311311.

[8] Gebert LFR, MacRae IJ. Regulation of microRNA function in animals. Nat Rev Mol Cell Biol. 2019;20(1):21-37. doi:10.1038/s41580-018-0045-7.

[9] Lu Y, Thavarajah T, Gu W, Cai J, Xu Q. Impact of miRNA in Atherosclerosis. Arterioscler Thromb Vasc Biol. 2018 Sep;38(9):e159-e170. doi: 10.1161/ATVBAHA.118.310227.

[10] Yuan J, Liu H, Gao W, Zhang L, Ye Y, Yuan L, Ding Z, Wu J, Kang L, Zhang X, Wang X, Zhang G, Gong H, Sun A, Yang X, Chen R, Cui Z, Ge J, Zou Y. MicroRNA-378 suppresses myocardial fibrosis through a paracrine mechanism at the early stage of cardiac hypertrophy following mechanical stress. Theranostics. 2018 Apr 3;8(9):2565-2582. doi: 10.7150/thno.22878.

[11] Lima J Jr, Batty JA, Sinclair H, Kunadian V. MicroRNAs in Ischemic Heart Disease: From Pathophysiology to Potential Clinical Applications. Cardiol Rev. 2017 May/Jun;25(3):117-125. doi: 10.1097/CRD.0000000000000114

[12] Lucas T, Bonauer A, Dimmeler S. RNA Therapeutics in Cardiovascular Disease. Circ Res. 2018 Jul 6;123(2):205-220. doi: 10.1161/CIRCRESAHA.117.311311.

[13] Olson EN. MicroRNAs as therapeutic targets and biomarkers of cardiovascular disease. Sci Transl Med. 2014 Jun 4;6(239):239ps3. doi: 10.1126/scitranslmed.3009008.

[14] Kural MH1, Wang J2, Gui L2, Yuan Y2, Li G3, Leiby KL4, Quijano E4, Tellides G3, Saltzman WM5, Niklason LE6 (2019) Fas ligand and nitric oxide combination to control smooth muscle growth while sparing endothelium. Biomaterials. 2019 Aug;212:28-38. doi: 10.1016/j.biomaterials.2019.05.011

[15] Yang F1, Green JJ, Dinio T, Keung L, Cho SW, Park H, Langer R, Anderson DG. (2009) Gene delivery to human adult and embryonic cell-derived stem cells using biodegradable nanoparticulate polymeric vectors. Gene Ther. 2009;16(4):533-46. doi: 10.1038/gt.2008.182.

[16] Segovia N, Dosta P, Cascante A, Ramos V, Borrós S. Oligopeptide-terminated poly(β-amino ester)s for highly efficient gene delivery and intracellular localization. Acta Biomater. 2014 May;10(5):2147-58. doi: 10.1016/j.actbio.2013.12.054.

[17] Fenton OS, Kauffman KJ, McClellan RL, Kaczmarek JC, Zeng MD, Andresen JL, Rhym LH, Heartlein MW, DeRosa F, Anderson DG. Customizable Lipid Nanoparticle Materials for the Delivery of siRNAs and mRNAs. Angew Chem Int Ed Engl. 2018 Oct 8;57(41):13582-13586. doi: 10.1002/anie.201809056.

[18] Montserrat N1, Garreta E, González F, Gutiérrez J, Eguizábal C, Ramos V, Borrós S, Izpisua Belmonte JC. (2011) Simple generation of human induced pluripotent stem cells using poly-beta-amino esters as the non-viral gene delivery system. J Biol Chem. 2011 8;286(14):12417-28. doi: 10.1074/jbc.M110.168013

[19] Dosta P. Develpment of cell-specific RNAi delivery vectors based on poly(beta-amino ester)s with therapeutic applications. IQS-Universitat Ramon Llull, Barcelona 2017.

[20] Fornaguera, C., Guerra-Rebollo, M., Lázaro, M. Á., Cascante, A., Rubio, N., Blanco, J., & Borrós, S. (2019). In Vivo Retargeting of Poly(beta aminoester) (OM-PBAE)

Nanoparticles is Influenced by Protein Corona. Advanced Healthcare Materials, 1900849. doi:10.1002/adhm.201900849

[21] Kaczmarek JC, Patel AK, Kauffman KJ, Fenton OS, Webber MJ, Heartlein MW, DeRosa F, Anderson DG. Polymer-Lipid Nanoparticles for Systemic Delivery of mRNA to the Lungs. Angew Chem Int Ed Engl. 2016 Oct 24;55(44):13808-13812. doi: 10.1002/anie.201608450.

[22] Tsou PS, Page NA, Lee SG, Fung SM, Keung WM, Fung HL. Differential metabolism of organic nitrates by aldehyde dehydrogenase 1a1 and 2: substrate selectivity, enzyme inactivation, and active cysteine sites. AAPS J. 2011;13(4):548-555. doi:10.1208/s12248-011-9295-4

[23] Green JJ, Langer R, Anderson DG. A combinatorial polymer library approach yields insight into nonviral gene delivery. Acc Chem Res. 2008;41(6):749-759. doi:10.1021/ar7002336.

[24] Hardy ST, Loehr LR, Butler KR, Chakladar S, Chang PP, Folsom AR, Heiss G, MacLehose RF, Matsushita K, Avery CL. Reducing the Blood Pressure-Related Burden of Cardiovascular Disease: Impact of Achievable Improvements in Blood Pressure Prevention and Control. J Am Heart Assoc. 2015 Oct 27;4(10):e002276. doi: 10.1161/JAHA.115.002276

[25] Vatner SF, Pagani M, Rutherford JD, Millard RW, Manders WT. Effects of nitroglycerin on cardiac function and regional blood flow distribution in conscious dogs. Am J Physiol. 1978 Mar;234(3):H244-52. doi: 10.1152/ajpheart.1978.234.3.H244.

[26] Christensson B, Nordenfelt I, Westling H, White T. Intravenous infusion of nitroglycerin in normal subjects. Scand J Clin Lab Invest. 1969 Feb;23(1):49-53. doi: 10.3109/00365516909078085.

[27] Hall CN1, Garthwaite J. (2009) What is the real physiological NO concentration in vivo? Nitric Oxide. 2009;21(2):92-103. doi: 10.1016/j.niox.2009.07.002.

[28] Opelt M., Eroglu E., Waldeck-Weiermair M., Russwurm M., Koesling D., Malli R., Graier W.F., Fassett J.T., Schrammel A., Mayer B. (2016) Formation of Nitric Oxide by Aldehyde Dehydrogenase-2 Is Necessary and Sufficient for Vascular Bioactivation of Nitroglycerin. J Biol Chem. 2016 11;291(46):24076-24084.

[29] Neubauer R., Wölkart G., Opelt M., Schwarzenegger C., Hofinger M., Neubauer A., Kollau A, Schmidt K., Schrammel A., Mayer B. (2015) Aldehyde dehydrogenase-

independent bioactivation of nitroglycerin in porcine and bovine blood vessels. Biochem Pharmacol. 2015 15;93(4):440-8. doi: 10.1016/j.bcp.2014.12.021.

[30] Beretta M, Gorren AC, Wenzl MV, Weis R, Russwurm M, Koesling D, Schmidt K, Mayer B. (2010) Characterization of the East Asian variant of aldehyde dehydrogenase-2: bioactivation of nitroglycerin and effects of Alda-1. J Biol Chem. 2010 Jan 8;285(2):943-52. doi: 10.1074/jbc.M109.014548.

[31]Lang BS, Gorren CF, Oberdorfer G, Wenzl V, Furdui CM, Poole BL. Mayer B. and Gruber K. (2012) Vascular Bioactivation of Nitroglycerin by Aldehyde Dehydrogenase-2. J Biol Chem. 2012 2; 287(45): 38124–38134. doi: 10.1074/jbc.M112.371716.

CHAPTER 3. DEVELOPMENT OF LOCAL DELIVERY STRATEGIES FOR RNA DELIVERY

3.1 INTRODUCTION

A majority of diseases only affect small sections of the body while most therapies requiring pharmaceutical intervention are approached through systemic administration strategies. Generally, drugs can be administered locally or systemically pursuing either widespread or local effects, see Figure 3.1.1. Oral and intravenous administrations have been vastly used delivery routes, however facing off-target effects such as diarrhea, hepatic or renal toxicity are frequently common and limit the use of multiple potentially effective molecules. Furthermore, a systemic delivery requires the crossing of several biological barriers cutting down the ratio of molecules that could be successful using other administration strategies [1].

On the other hand, local administrations pursuing local activity such as ocular injections or skin applications generally lack off-site toxicity while allowing high local concentrations and a therapeutic localized effect. Local administrations also require significantly more complex systems to be delivered and a significantly higher level of medical intervention than systemic administrations.

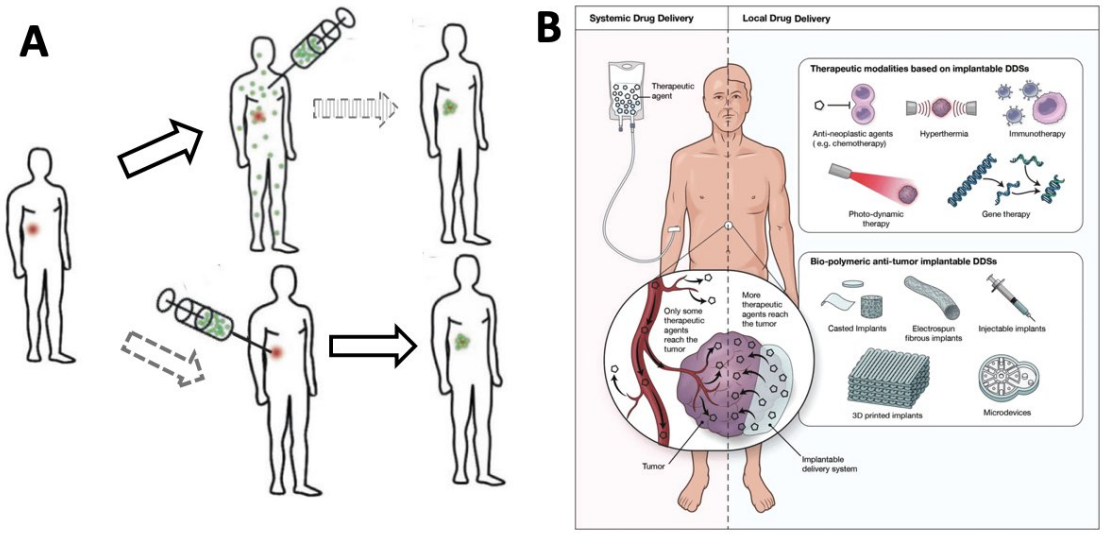

Figure 3.1.1 Representation of local and systemic delivery strategies. A, Scheme of targeted systemic delivery and local approach to treat a localized disfunction. B, General strategies followed for an intravenous systemic administration and strategies followed to accomplish local drug delivery[2].

When RNA therapeutics arrived into the pharmacological field, initial attempts pursued systemic administration as the preferred strategy in a similar way to traditional small molecule drugs[3]. However, as mentioned in previous chapters, the chemical nature of nucleic acids, lack the ease of crossing biological barriers commonly found in organic molecules with small size and versatile partition coefficients. Those facts lowered initial

expectations of obtaining a fast translation of RNA therapeutics into the clinics, revealing the initially expected translation to be a huge enterprise[4]. As mentioned in earlier chapters, pharmacokinetics and biodistribution have been one of the major limitations contributing to the delay in bringing targeted delivery strategies to real medicine[5]. It should not appear surprising that the only marketed RNA based drug or therapies in late stage trials are mainly in ocular, hepatic or renal fields. Those fields either benefit from local applications or take advantage from intrinsic filtration mechanisms that drive concentration.

In present chapter, a set of strategies will focus on trying to develop local delivery strategies for the RNA technologies developed. Attempting to develop the hypothesis that applying the RNA therapeutic strategies used in the past may be an erroneous approach to get a smooth translation into real life clinical products. To develop desirable local effects after local administrations, some systems to avoid uncontrolled diffusion must be available. Some strategies have been focused in release-controlled systems such as PLA based delivery, hydrogel matrix to control sustained elution[6][7] or adhesive properties of nanoparticles[8]. Local effects can also be obtained by active targeting specific tissues or cell types after systemic administration. It has been one of the preferred strategies pursued by researches, but multiple interactions and crossing biological barriers still limit its generalized success. However, developing hybrid strategies were a local administration is supplemented with targeting capabilities for specific cell types or tissues may be desirable strategy.

Although local delivery may find many advantages playing a close bet to the rules of thermodynamics, it is worth to mention that it cannot be generalized and should mainly be considered for niche applications.

Among the many potential applications that exploit the local advantages for iRNA, this chapter will focus on local treatment of cardiovascular therapies. Those, may be benefited from the vast amount of minimally invasive techniques, co-delivery of nitric oxide and the intrinsic potential of RNA therapeutics. Cardiovascular applications have “relatively” simple biological directly exposed to bloodstream structures to benefit from RNA therapies being studied in present application, furthermore in last decades several local administered drugs have strongly improved efficacy of therapies such as PCI[9].

One field that could benefit from RNA local delivery is acute myocardial infarction. Myocardial infarction is one of the main causes of death affecting yearly as large as 5% of population older than 75 years old[10]. Being especially dangerous for European and developed countries, due to its expected rise in incidence reaching to double in the next decades.

Management of myocardial infarction has revolutionized cardiology thanks to primary angioplasty massification in late 90s, reducing its overall mortality by a 15%[11] to around 5% net mortality nowadays. Besides the success of PCI, heart failure, a clinical disorder impairing the ability to eject blood[12], has emerged as an important

comorbidity of myocardial infarction due to lack of regeneration mechanisms over long ranges and aged tissues. Therapies to avoid heart failure (HF) would be highly valuable, to increase both the life expectancy and welfare of patients suffering from myocardial infarction.
Many strategies have been studied to improve regeneration focused in cell therapy with a great variety of results[13], probably associated to intrinsic complexities of using human cells in therapies[14]. Recently use of systemically administered adeno associated viruses (AAV) complexed with miRNA has been found to reduce infarct size in large mammals together with improving ventricular function[15], renewing expectations to translate results into clinical practice.

Among other potential therapies that could benefit from RNA technology is percutaneous coronary intervention PCI. PCI started in 1976 by Dr. Gruntzieg by inserting a balloon up to coronary arteries to allow for acute opening. Although a good short-term success was found it rapidly evolved into an incidence as high as 50% in revascularization. In 1986 introduction of the first bare metal stents allowed a reduction of revascularization up to 30%[16]. In early 2000 introduction of drug eluting stents further reduced the rate of complications up to 10%[17]. Further development of biodegradable drug eluting stents or other developments have failed to overcome recent best in class Sirolimus low profile drug eluting stents. Open questions and complex cases such as small diameter vessels, reiterative revascularization lesions or highly comorbidities such as diabetes, still remains as a field of improve where RNA delivery may benefit from the easier pharmacokinetics.
In the same age, drug eluting balloon have also been entered into the market as an alternative therapy for revascularization without the need for long-term implants[18] with potential associated long-term events, nowadays this technique provides a solution for avoiding revascularization of DES and BMS and holds the potential to improve restenosis “the aquilles heel” of PCI[19]. RNA delivery has been studied[20] and applied[21] holding the potential to introduce tailored therapies for complex scenarios like small vessels, bifurcation lesions, ACS and deliver better long-term therapies.

Present chapter aims to develop strategies to locally deliver the developed nanoparticle system and to cardiovascular diseases.

3.2 MATERIALS AND METHODS

3.2.1 Materials: Unless noted all reagents were used from Sigma-Aldrich and used as received. K72NO based nanoparticles have been used as described in previous chapters, the fluorescent version of the polymer has been prepared using amine reactive Alexa Fluor™ 568 NHS Ester (Succinimidyl Ester) in DMSO at 1:20. Fluorescently tagged siRNA have been obtained from Sigma (SIC007) and used to track nanoparticles. Formulations containing biodegradable polymers have been prepared by an emulsion method combining PLGA at 10% weight dissolved in dichloromethane and nanoparticles at polymer/RNA rate of 100:1 in the water phase and drying under vacuum.

3.2.2 Tissue Harvesting: Tissues to perform *ex vivo* experiments were harvested from local abattoir, washed with saline and kept refrigerated until use in a 72h frame. Coronary arteries have been dissected in sections of 2.5-3 mm and 50 mm for further experimentation. For coronary infusion or injection experiments, the whole heart have been used and directly punctured or canalization.

3.2.3 Ex vivo infusion system: A bioreactor for infusion of media has been developed, consisting of a double chamber, one for arterial flow and the outer to keep the environment wet. Flow has been set with a peristaltic pump (Baooding shenchen precision pump co.,LTD) at 30mL/min in pulsatile mode at a frequency of 1Hz. The system was closed using silicone tubing and standard connectors, 3-way valves and a hemostasis valve to introduce the devices. The arteries were secured to the connectors using nylon sutures (Arago Gama, Cardedeu, Spain). The whole system was inserted into an oven at 37 degrees using DMEM as medium supplemented with sodium azide (0.1mg/mL) and Penicillin/streptomycin (3U/mL).

3.2.4 Porous balloon development: A porous tube of ePTFE (Gore, Sacramento Ca, USA) was conformed over a perforated 3x20 mm semicompliant PTFE balloon(Fairway, Iberhospitex, Lliça de vall, Spain) and fix it using epoxy adhesive in the extremes.

3.2.5 Coating and implantion: Coronary stents 3x18mm (iChrom, Iberhospitex, Lliça de Vall, Spain) and 3x18 PTCA balloons (ihtEVOLVE®, iberhospitex, Lliça de Vall, Sapin) were spray coated using ultrasound dispersion technique at a dose of 3µg/mm^2 and dried at room temperature. Stents were further crimped using a manual crimping tool and stored until use. Expansion into arteries was performed at nominal pressure (atm) using an infusion pump.

3.2.6 Infusion of nanoparticles: A bolus of 5mg of nanoparticles containing fluorescent labelled siRNA at 1:200 ratio was prepared and infused through the porous balloon over a period of 10 minutes and further washed with 10 mL boluses of media. Same dose of nanoparticles were injected though the myocardium infusion catheter (Iberhospitex S.A., Lliçà de Vall, Spain).

3.2.7 Tissue histology&micrscopy: After the experiments, tissue samples have been dissected, washed in Saline and further embedded in OCT (Tissue-Plus, Fisher Scientific), frozen at -32 ^{o}C and frozen-sectioned using a cryostat(Leica CM1800) and stored in a glass slide until further analyzed.

3.2.8. Fluorescence evaluation: Nanoparticle retention was evaluated by mapping the fluorescence of the whole tissue using a microplate reader (SpectraMax, Molecular devices, San Jose CA, USA) and mapping wavelengths of the dyes used to tag polymer and/or the RNA molecules, further evaluation has been performed using a fluorescence microsope.

3.2.9 Statistical analysis: Data were analyzed using GraphPad® Prism. Comparisons between groups were done by one-way ANOVA using Turkey *post-hoc* test. Differences were considered significant when $p<0.05$ *, $p<0.01$** and $p<0.001$***.

3.3 RESULTS AND DISCUSSION

3.3.1 Balloon angioplasty infusion and drug eluting balloon strategies

Evolution in angioplasty techniques has allowed to reduce significantly the events after intervention from 50% in the 80s down to 7-10% nowadays. However, in absolute numbers in-stent restenosis carries back annually more than half a million patients to back to the cathlab or surgery room. For those patients, intervention with current DEB has not surpassed the results of DES claiming for further developments that bring better outcomes. Current DEB use both paclitaxel or sirolimus, those drugs although efficient in limiting restenosis, lack the ability of boost reendothelialization and recover natural mechanisms that keep homeostasis. New RNA based therapies could exploit the limits of current drugs to improve outcomes due to the following reason:
First, vascular pharmacokinetics are quite straightforward allowing dosing in the desired point, second RNA holds the hope to either use intrinsic mechanisms, such as miRNA, or develop multitarget strategies to keep low neointima growth, boost endothelial growth and avoid thrombosis simultaneously. And lastly, a co-delivery of nitric oxide should enhance a pro-homeostasis state. In Figure 3.3.1, a set of strategies have been developed to attempt the delivery of RNA and NO to vascular tissues.

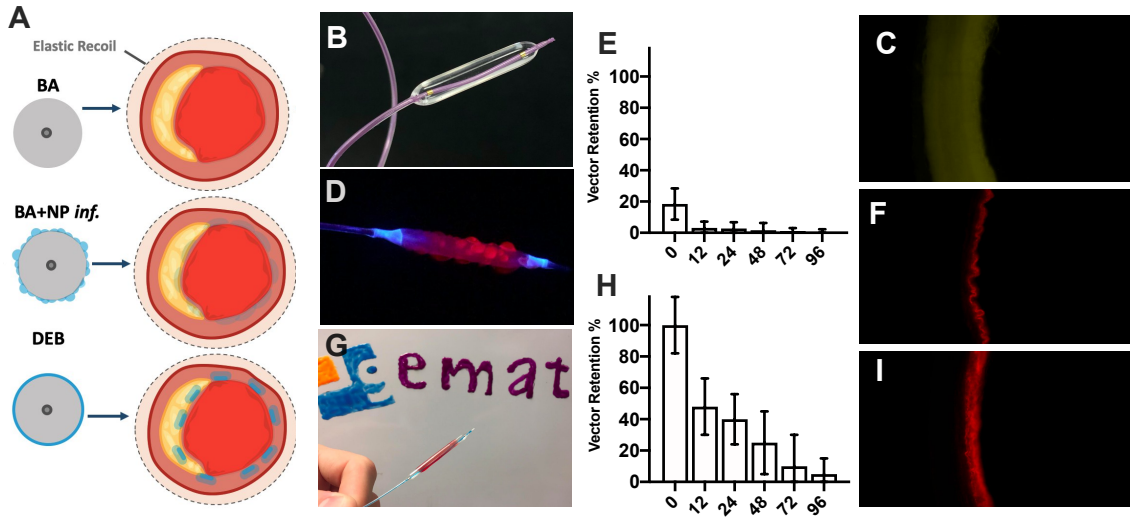

Figure 3.3.1 Strategies developed to include RNA therapeutics to drug eluting balloons. A, Scheme of balloon, porous balloon to infuse nanoparticles and drug eluting balloon with polymeric coating. B, Traditional balloon for angioplasty. C, control autofluorescence porcine coronary artery after PTCA balloon expansion. D, image of porous balloon for infusion of nanoparticles. E, retention of fluorescent labeled nanoparticles after nanoparticle infusion through porous balloon. F, Coronary artery after infusion of nanoparticles. G, Example of colored drug eluting balloon. H, Retention of fluorescence after DEB expansion. I, coronary artery fluorescence after DEB expansion.

Local delivery strategy has been developed to apply RNA with the developed nanoparticles directly to vascular lesions through a porous balloon. This strategy holds the advantage of directly applying potentially unstable nanoparticles by direct infusion with a minimal preparation. It has been shown that developed nanoparticles hold a great potential to stay attached to vascular cells due to the hydrophobic and positive charge. Although stability has not been directly evaluated, both polymer and siRNA stayed adhered to the endothelial surface in a similar manner, assuming that decomposition was driven by a hydrolysis mechanism and not nanoparticle degeneration. In Figure 3.3.1.F, it can be seen how NP only attaches to the surface of the vessel wall, because of the limited endothelium denudation and complexity to cross biological barriers. High adhesiveness of nanoparticles is coherent with previously observed adherence to blood vessels after intravascular infusion in chapter 1, and it is coherent with the hydrophobic and positive charged surface of nanoparticles making it complementary to the negative surface charge of endothelial cell glycocalyx[22].

Although directly applying a nanoparticle load to a vascular lesion could potentially result beneficial, it is also possible that therapy needs to be extended for longer periods to be effective. For those situations it is proposed to include a biodegradable polymer such as PLGA to extend the treatment for a period up to a few months. Introduction of nanoparticles is produced by an emulsion method that allows for modification of the polymer degradation speed, dose and vector-RNA ratio relatively easily. Enlargement of the delivery could be obtained by changing the polymer to PLLA or polycaprolactone. It has been observed that using a drug eluting balloon with biodegradable polymers as excipients does extend significantly the retention in the vessel wall.
How stable are nanoparticles inside the matrix has been previously explored in similar applications with positive results[23]. Balloon expansion leads to arterial denudation and deep penetration of the treatment, leading also to a better retention of the Nanoparticles in the vessel wall. Both strategies developed should be useful delivery options to improve transfer of RNA to vascular structures for either short periods or longer periods of time depending on the application requirements. A first set of porcine experiments led to well tolerated but non-conclusive expression results, probably due to lack of location markers. Currently experiments to evaluate further the *in vivo* vascular response to nanoparticles with active RNA molecules are under approval, hoping to bring new solutions to the interventional field.

Introduction of RNA technology to the clinical world could potentially bring new therapies to the real world focused into healing disfunctions that currently are only treated when acute syndromes occur. As an example, development of treatments to induce regeneration of unstable plaque or heavily calcified lesions could be theoretically possible in the following years. Development of personalized medicine for challenging

patient groups such as diabetics, high bleeding risk factors or young patients could be possible in the following decades.

3.3.2 Evaluation of RNA eluting stent

Another field that could benefit from dual RNA and nitric oxide delivery is treatment of vascular lesions requiring from vascular scaffolding such as drug eluting stents, stent grafts, carotid stents or peripheral stents. During the last decades combination of scaffolding and pharmacological treatment has brought a great success into the field. Furthermore, a great deal of knowledge has been generated about the roles of miRNA molecules in the progression of vascular disease and restenosis. Micro RNAs play critical roles in restenosis generating plenty of candidates to be introduced into novel treatments of vascular disease[24]. In Figure 3.3.2 several *in vitro* and *ex vivo* experiments assessing the drug transfer and coating characteristics are presented.

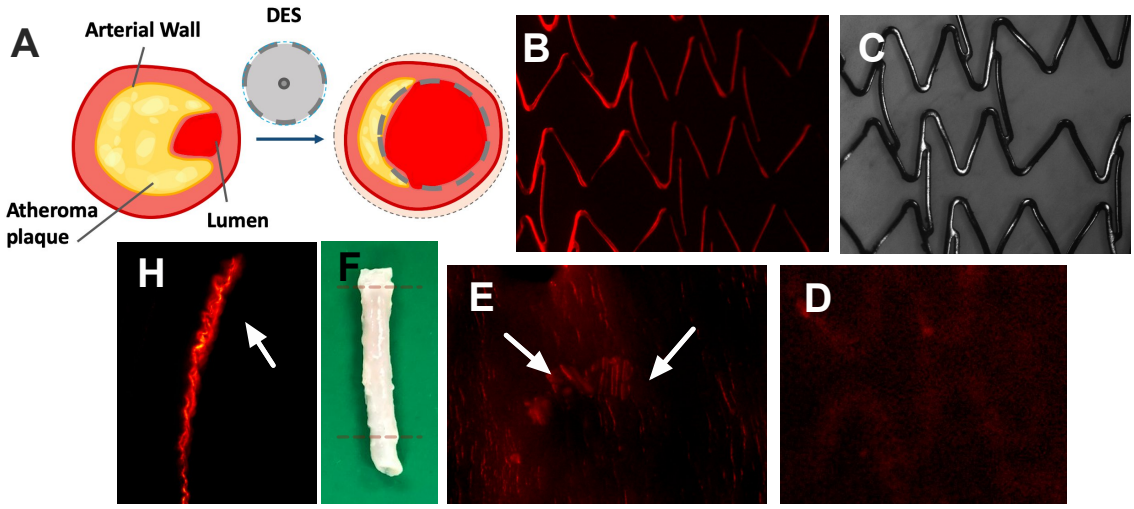

Figure 3.3.2. Evaluation of K72-NO polymers into drug eluting stents. A, Scheme of arterial stenting. B, Image of a drug eluting stent coated with RNA-pBAE-PLGA system. C, image of the stent over arterial wall. D, image of the drug delivery system to the arterial wall after 1 day. E, detail of the drug transfer in a bending strut zone. F, Detail of a stent implanted in an artery and H, detail of polymer transfer after stent expansion.

A first approach of RNA loading was achieved by directly coating drug eluting stents, the coating characteristics were found to be stable after simulation of drug eluting stent use in a silicone mock vessel. RNA and vector load has been observed to efficiently transfer into blood vessel cell wall *ex vivo*. It is highly possible that *in vivo* a much more efficient transfer would be obtained due to active migration and colonization by vascular cells would benefit from diffusion. Drug delivery profiles can be tuned by either modifying the PLGA-pBAE ratio or by using other biodegradable polymers such as PLLA or PCL as previously stated.

Several applications have been proposed using multiple strategies focused towards inhibiting smooth muscle cell proliferation, boosting endothelial response or limiting growth factor expression[25]. Some strategies such as miR21 and miR221 have been reported to be strongly related to inhibit smooth muscle cell proliferation[26]. Similar results have been achieved by enhancing the expression of 7ND gene, being selective towards smooth muscle cells but having no effect on endothelial cell proliferation[27]. Interestingly, overexpression of eNOS for enhancing the production of nitric oxide has been associated to accelerate endothelial proliferation[28]. Current work aims to combine the delivery of nitric oxide with a miRNA or siRNA specifically selected to block smooth muscle proliferation for further animal experiments, suggesting that would be a great candidate to improve results associated to vascular implants such as drug eluting stents.

Currently experiments to proof the expression of miRNA in porcine arteries and to check the capabilities to include active miRNA or siRNA to boost reendothelialization and reduce neointima ingrowth are under evaluation. Models using challenging locations such as small vessels or bifurcations will be selected to challenge the delivery system.

3.3.3 Catheter for minimally invasive controlled infusion of RNA and NO

Heart failure after myocardial infarction still remains as one of the big therapeutic areas to be covered in cardiology besides the multiple attempt strategies. Those strategies have attempted to use stem cells or tissue engineering with limited success. Although holding a great therapeutic potential, cell therapies lack many critical issues to successfully translate into real life clinics. Immunogenic issues, patient variability, logistics and regulatory constraints of cell-based therapeutics are among the most complex issues to bypass[29].

In an attempt to introduce a new minimally invasive therapy involving local delivery of RNA therapeutics, a new catheter has been adapted to the application. The catheter is designed to reach almost any location in either the left or right ventricles. Left ventricles can be approached through either femoral or radial approaches. It could also be inserted through femoral vein and reach either the right ventricle or the left ventricle though a transeptal puncture. The features of the catheter can be observed in Figure 3.3.3.1

The catheter has an integrated system to deflect the tip as much as 120 degrees that allow reaching almost any point through combination of deflection and axial rotation. A flexible coaxial needle is integrated allowing for puncture and injection once the catheter is oriented in the ventricle wall.

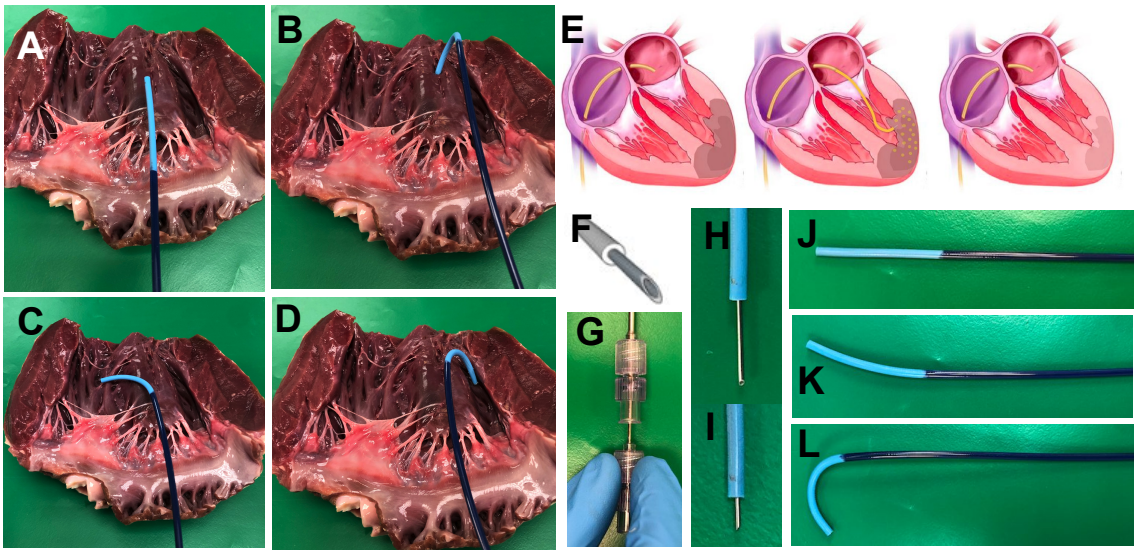

Figure 3.3.3.1 Delivery catheter for intraventricular infusion. A-D, *ex vivo* experiments of injection location in porcine myocardium. E, Scheme of the trans-septal injection of particles into infarcted area. F, Scheme of catheter tip. G-I, needle injection system. J-L, Deflection detail of the catheter.

Orientation in the ventricles should be guided by transesophageal echocardiography and fluoroscopy to locate the catheter to affected zones. Introduction and navigation have been evaluated in silicone vasculature vessels trough transaortic approach, reaching left ventricle without further complications. The needle lumen can be used to guide the catheter to the ventricle if needed, using a 0.032" guide wire. Once in the ventricle reaching multiple locations was accomplished easily. Results obtained in silicone mock vessels have also been reproduced *in vivo* in acute porcine models to establish the intravascular technique.

Currently *ex vivo* experiments using porcine hearts have shown the feasibility of reaching the ventricle and successfully locating the punctures and inject RNA load. Potentially this strategy could be directly applied in those patients that arrive with ventricle compromised function using miRNA and NO co-injections in compromised areas. It could also be combined with intravascular coronary injection of nanoparticles, but retention and prolonged action could limit its effectiveness.

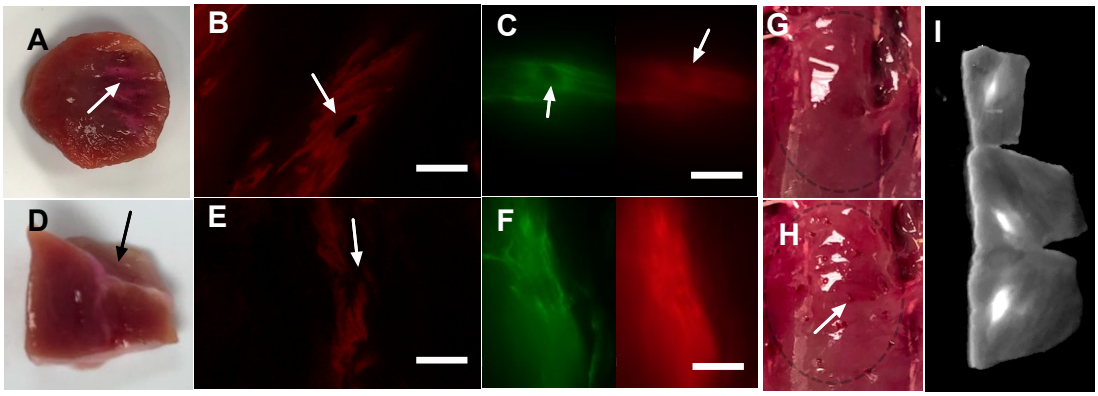

Figure 3.3.3.2 Intraventricular injection of fluorescently labeled K72NO NP. A, Example of a 10mm transversal cut after multiple injections, white arrow marks the injection point.B-C, Detail of injection in perpendicularly cut section of myocardium and control section. D, Macroscopic cut of a longitudinal fluorescent injection in myocardium, arrow point the injection point. E-F, Detail of the fluorescent loaded injection longitudinally and control tissue. G-H, Example of simulated infarcted zone and injections details after intervention. I, 10 mm Macroscopic fluorescent image section cut after 72h nanoparticle injection. Scale bar 500µm.

Direct injection and delivery of nanoparticles inside the ventricle, should increase the chances to obtain the desired activity from RNA. Direct administration does not require nanoparticles to be stable in circulation, deal with excretion or cross multiple biological barriers. It is just injected in the location where action is desired with the help of imagining techniques such as echography and fluoroscopy or even fusion images techniques if possible. Sustained releasing systems could also be applied by inclusion of nanoparticles in microspheres or co-injecting of gelling liquids with the NP or simply with high viscose excipients. Equivalent strategies could be used including the nanoparticles in PLGA microspheres for delivering nitric oxide and RNAs from days to months, se detail in Figure 3.3.3.2. Also, multiple injection series could be completed after several interventions.

Use of nitric oxide in myocardial infarction has been shown to increase synergistically the regeneration effect of stem cells[30][31], being possible that NO can also stimulate intrinsic mechanisms for recovery when used simultaneously with RNAi. Among the many potential therapeutic strategies chosen, it could appear as a straightforward approach to use the intrinsic mechanisms encoded by miRNAs to modulate myocardial cellular response to physiological stimuli. Using miRNAs coded to tune myocardial functions could be exploited to direct physiological modification in infarcted areas thanks to the potential of miRNAs to tune phenotype expression towards cardiomyocyte proliferation, fibroblast reprogramming or stem cell dedifferentiation[32]. Among many potential candidates, delivery of miRNA-199a and/or miRNA-29 could be of great potential due to its stimulation of cardiac myocytes repair [33] and inhibition of fibrotic response, miRNA-29 acts downregulating several genes responsible for synthesis of extracellular proteins that overexpress after myocardial infarction[34].

Currently permissions for the feasibility experiments in large animals are being requested and we hope to explore in the near future therapeutic potential of co-Delivery of nitric oxide and iRNA to reduce infarcted area.

3.4 CONCLUDING REMARKS

In present chapter several strategies to deliver locally the RNA containing nanoparticles developed in previous chapters have been explored. RNA containing nanoparticles can be directly delivered using developed porous balloon that directly delivers nanoparticles to vasculature for those vectors that present adhesive properties against vascular tissues. A balloon coated with RNA containing nanoparticles and PLGA as excipient has been found to extend for longer periods of time and higher doses of RNA to the vascular walls. Balloons have been tested using an *ex vivo* model with perfusion to explore retention of nanoparticles in arterial tissue both using whole tissue fluorescence and histologic distribution of particles. Similar findings have been found in drug eluting stents using RNA and PLGA as excipients.

A therapeutic strategy to treat heart failure after myocardial infarction has been developed using a catheter for directly injecting RNA containing nanoparticles to ventricles. It has been found to be useful for injecting and retaining vectors into the ventricle through a transaortic approach. Therapy could also be used to inject nanoparticles to tissues adjacent to vascular structures such as hepatic tissue or even tumors.

Potential to exploit pharmacokinetics using *ex vivo* models seem to be promising for further experimentation *in vivo* to demonstrate effectiveness of the local delivery strategies.

3.5 REFERENCE

[1] Ji T, Kohane DS. Nanoscale systems for local drug delivery. Nano Today. 2019;28:100765. doi:10.1016/j.nantod.2019.100765

[2] Talebian S, Foroughi J, Wade SJ, et al. Biopolymers for Antitumor Implantable Drug Delivery Systems: Recent Advances and Future Outlook. Adv Mater. 2018;30(31):e1706665. doi:10.1002/adma.201706665

[3] Park J, Park J, Pei Y, Xu J, Yeo Y. Pharmacokinetics and biodistribution of recently-developed siRNA nanomedicines. Adv Drug Deliv Rev. 2016;104:93-109. doi:10.1016/j.addr.2015.12.004

[4] Wang F, Zuroske T, Watts JK. RNA therapeutics on the rise. Nat Rev Drug Discov. 2020;19(7):441-442. doi:10.1038/d41573-020-00078-0

[5] Targeting for delivery. Nat Biomed Eng. 2019;3(9):671-672. doi:10.1038/s41551-019-0457-5

[6] Wang LL, Burdick JA. Engineered Hydrogels for Local and Sustained Delivery of RNA-Interference Therapies. Adv Healthc Mater. 2017;6(1):10.1002/adhm.201601041. doi:10.1002/adhm.201601041

[7] Segovia N, Pont M, Oliva N, Ramos V, Borrós S, Artzi N. Hydrogel doped with nanoparticles for local
sustained release of siRNA in breast cancer. Adv Healthc Mater. 2015;4(2):271-280. doi:10.1002/adhm.201400235

[8] Lesniak A, Salvati A, Santos-Martinez MJ, Radomski MW, Dawson KA, Åberg C. Nanoparticle adhesion to the cell membrane and its effect on nanoparticle uptake efficiency. J Am Chem Soc. 2013;135(4):1438-1444. doi:10.1021/ja309812z

[9] Bangalore S, Kumar S, Fusaro M, et al. Short- and long-term outcomes with drug-eluting and bare-metal coronary stents: a mixed-treatment comparison analysis of 117 762 patient-years of follow-up from randomized trials. Circulation. 2012;125(23):2873-2891. doi:10.1161/CIRCULATIONAHA.112.097014

[10] Vázquez-Oliva G, Zamora A, Ramos R, et al. Acute Myocardial Infarction Population Incidence and Mortality Rates, and 28-day Case-fatality in Older Adults. The REGICOR Study. Rev Esp Cardiol (Engl Ed). 2018;71(9):718-725. doi:10.1016/j.rec.2017.10.019

[11] Cahill TJ, Kharbanda RK. Heart failure after myocardial infarction in the era of primary percutaneous coronary intervention: Mechanisms, incidence and identification of patients at risk. World J Cardiol. 2017;9(5):407-415. doi:10.4330/wjc.v9.i5.407

[12] Yancy CW, Jessup M, Bozkurt B, et al. 2013 ACCF/AHA guideline for the management of heart failure: a report of the American College of Cardiology Foundation/American Heart Association Task Force on Practice Guidelines. J Am Coll Cardiol. 2013;62(16):e147-e239. doi:10.1016/j.jacc.2013.05.019

[13] Madigan M, Atoui R. Therapeutic Use of Stem Cells for Myocardial Infarction. Bioengineering (Basel). 2018;5(2):28. Published 2018 Apr 6. doi:10.3390/bioengineering5020028

[14] Madonna R, Van Laake LW, Davidson SM, et al. Position Paper of the European Society of Cardiology Working Group Cellular Biology of the Heart: cell-based therapies for myocardial repair and regeneration in ischemic heart disease and heart failure. Eur Heart J. 2016;37(23):1789-1798. doi:10.1093/eurheartj/ehw113

[15] Gabisonia K, Prosdocimo G, Aquaro GD, et al. MicroRNA therapy stimulates uncontrolled cardiac repair after myocardial infarction in pigs. Nature. 2019;569(7756):418-422. doi:10.1038/s41586-019-1191-6

[16] Meier B, Bachmann D, Lüscher T. 25 years of coronary angioplasty: almost a fairy tale. Lancet. 2003;361(9356):527. doi:10.1016/s0140-6736(03)12470-1

[17] Bernhard M, Forty years of percutaneouscoronary intervention.Cardiovascular Medicine. 2018 ;21(11):278–281 doi: 10.4414/cvm.2018.00589

[18] Jeger RV, Eccleshall S, Wan Ahmad WA, et al. Drug-Coated Balloons for Coronary Artery Disease: Third Report of the International DCB Consensus Group. JACC Cardiovasc Interv. 2020;13(12):1391-1402. doi:10.1016/j.jcin.2020.02.043

[19] de la Torre Hernandez JM, Puri R, Alfonso F. Drug-Coated Balloon: "Scoring to Win". JACC Cardiovasc Interv. 2017;10(13):1341-1343. doi:10.1016/j.jcin.2017.05.019.

[20] Gareri C, De Rosa S, Indolfi C. MicroRNAs for Restenosis and Thrombosis After Vascular Injury. Circ Res. 2016;118(7):1170-1184. doi:10.1161/CIRCRESAHA.115.308237

[21] Hossfeld S, Nolte A, Hartmann H, et al. Bioactive coronary stent coating based on layer-by-layer technology for siRNA release. Acta Biomater. 2013;9(5):6741-6752. doi:10.1016/j.actbio.2013.01.013

[22] Vargas FF, Osorio MH, Ryan US, De Jesus M. Surface charge of endothelial cells estimated from electrophoretic mobility. Membr Biochem. 1989;8(4):221-7. doi: 10.3109/09687688909026816.

[23] Devulapally R, Paulmurugan R. Polymer nanoparticles for drug and small silencing RNA delivery to treat cancers of different phenotypes. Wiley Interdiscip Rev Nanomed Nanobiotechnol. 2014;6(1):40-60. doi:10.1002/wnan.1242

[24] Varela N, Lanas F, Salazar LA, Zambrano T. The Current State of MicroRNAs as Restenosis Biomarkers. Front Genet. 2020;10:1247. Published 2020 Jan 10. doi:10.3389/fgene.2019.01247

[25] Lekshmi KM, Che HL, Cho CS, Park IK. Drug- and Gene-eluting Stents for Preventing Coronary Restenosis. Chonnam Med J. 2017;53(1):14-27. doi:10.4068/cmj.2017.53.1.14

[26] Wang D, Deuse T, Stubbendorff M, et al. Local MicroRNA Modulation Using a Novel Anti-miR-21-Eluting Stent Effectively Prevents Experimental In-Stent Restenosis [published correction appears in Arterioscler Thromb Vasc Biol. 2015 Oct;35(10):e51]. Arterioscler Thromb Vasc Biol. 2015;35(9):1945-1953. doi:10.1161/ATVBAHA.115.305597

[27] Egashira K, Nakano K, Ohtani K, Funakoshi K, Zhao G, Ihara Y, Koga J, Kimura S, Tominaga R, Sunagawa K. Local delivery of anti-monocyte chemoattractant protein-1 by gene-eluting stents attenuates in-stent stenosis in rabbits and monkeys. Arterioscler Thromb Vasc Biol. 2007 Dec;27(12):2563-8. doi: 10.1161/ATVBAHA.107.154609. Epub 2007 Sep 20. PMID: 17885211.

[28] 73. Sharif F, Hynes SO, McCullagh KJ, Ganley S, Greiser U, McHugh P, et al. Gene-eluting stents: non-viral, liposome-based gene delivery of eNOS to the blood vessel wall in vivo results in enhanced endothelialization but does not reduce restenosis in a hypercholesterolemic model. Gene Ther. 2012;19:321–328.

[29] Ghaemi RV, Siang LC, Yadav VG. Improving the Rate of Translation of Tissue Engineering Products. Adv Healthc Mater. 2019;8(19):e1900538. doi:10.1002/adhm.201900538

[30] Yao X, Liu Y, Gao J, et al. Nitric oxide releasing hydrogel enhances the therapeutic efficacy of mesenchymal stem cells for myocardial infarction. Biomaterials. 2015;60:130-140. doi:10.1016/j.biomaterials.2015.04.046

[31] Rainer Schulz, Malte Kelm, Gerd Heusch, Nitric oxide in myocardial ischemia/reperfusion injury, Cardiovascular Research, Volume 61, Issue 3, February 2004, Pages 402–413, doi: 10.1016/j.cardiores.2003.09.019

[32] Sun T, Dong YH, Du W, et al. The Role of MicroRNAs in Myocardial Infarction: From Molecular Mechanism to Clinical Application. Int J Mol Sci. 2017;18(4):745. Published 2017 Mar 31. doi:10.3390/ijms18040745

[33] Gabisonia K, Prosdocimo G, Aquaro GD, Carlucci L, Zentilin L, Secco I, Ali H, Braga L, Gorgodze N, Bernini F, Burchielli S, Collesi C, Zandonà L, Sinagra G, Piacenti M, Zacchigna S, Bussani R, Recchia FA, Giacca M. MicroRNA therapy stimulates uncontrolled cardiac repair after myocardial infarction in pigs. Nature. 2019 May;569(7756):418-422. doi: 10.1038/s41586-019-1191-6. Epub 2019 May 8. PMID: 31068698; PMCID: PMC6768803.

[34] van Rooij E, Sutherland LB, Thatcher JE, DiMaio JM, Naseem RH, Marshall WS, Hill JA, Olson EN. Dysregulation of microRNAs after myocardial infarction reveals a role of miR-29 in cardiac fibrosis. Proc Natl Acad Sci U S A. 2008 Sep 2;105(35):13027-32. doi: 10.1073/pnas.0805038105

CHAPTER 4. SELF-CROSSLIKING NITRIC OXIDE RELEASING COATING FOR ANTIMICROBIAL TRAQUEAL STENTS

4.1 INTRODUCTION

Nitric oxide has been presented as a key signaling molecule of mammalian biochemistry playing crucial roles in vascular and neural tissues. Previous chapters have been focused in developing co-delivery systems of RNA and nitric oxide, targeting the release patterns of the vascular system and altering the expression profiles. During the development of synthetic non-viral vectors with NO delivery capabilities, several different nitric oxide releasing moieties have been explored. Some of the polymers developed in chapter 1 may have the potential to be used in applications where significantly higher amounts of released nitric oxide find potential use in antimicrobial materials.

During evolution, NO unique chemical properties have been adopted into mammalian biochemistry to play multiple roles under different stimuli and conditions. As a free radical with an unpaired electron, nitric oxide has high reactivity against biomolecules showing ultimately cellular toxicity. Those properties have probably made it useful during evolution to favor defensive roles in the immune system against host organisms. Macrophages express a special isoform of NOS called induced nitric oxide synthase (iNOS) that produces high local concentrations of nitric oxide as a response to inflammatory cytokines or microbial antigens, see Figure 4.1.1. Although the concentrations of NO required to produce a defensive environment are highly toxic, under biological environment toxicity is restricted to approximately 100 microns surrounding the generation site, being a mechanism useful against local infections and pathologic disfunctions like those generated by cancer cells. However, dysregulation of NO production from the immune system have been reported and can be the cause of triggering some autoimmune diseases[1].

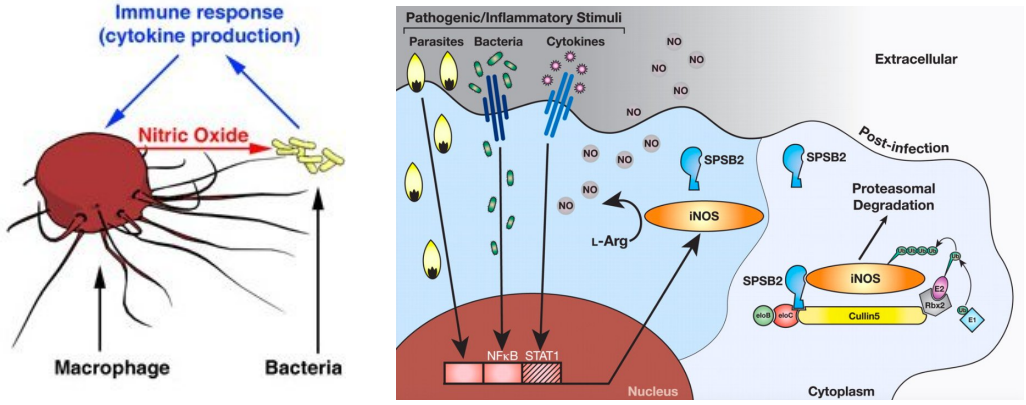

Figure 4.1.1 Role of nitric oxide as response to pathogenic or inflammatory stimuli. Left, scheme of response of macrophages to infection through nitric oxide production [2]. Right, mechanisms of iNOS induction by parasites, bacteria or cytokines to produce nitric oxide and stop iNOS activity when stimuli stop [3].

NO shows interestingly, a high toxicity profile against prokaryotic cells due to the high permeability of nitric oxide trough bacterial cell membranes and lack of specific mechanisms to protect prokaryotic cells from nitric oxide. Nitric oxide mediated toxicity is caused by interaction with Fe-S cluster of ferrodoxin [4], non-haem metalloproteinases, DNA and ribonucleotide reductases among other biomolecules [5]. Besides specific interference of nitric oxide with key proteins, non-specific toxicity is also an important mechanism against host cells. Nitric oxide can also exert toxicity to cells by combination with peroxinitrites or thionitrites that have a broader spectrum of action [6].

Despite the attractive mechanisms of toxicity, local effect and almost negligible degradation footprint, toxicity of NO against microorganisms is highly variable among species being more sensitive to strains of *Staphylococcus aureus* or *Pseudomonas aeruginosa*[7] and less sensitive to other strains like *Escherichia coli or Staphylococcus epidermidis*[8]. Besides the variability, nitric oxide is not only a single species and is presented *in vivo* as a multifactorial set of NO itself, peroxinitrites and s-nitrosothiols with an interesting potential against pathogens, specially nowadays that pathogens with multiple drug resistance are starting to become a significant threat to public health[9].

Nitric oxide releasing materials are an interesting strategy to protect devices that have potential infection associated such as intravascular catheters, wound dressings and potentially any surface that is exposed to an environment with risk to develop contamination.

Many materials with NO release capabilities have been proposed, being the chemical strategies that carry diazeniumdiolates and thionitrites the more commonly synthetic explored to integrate. Lack of dependence over enzymatic pathways to generate nitric oxide avoids tolerance and variability among tissues, making diazeniumdiolates and S-nitrosothiols the preferred strategies for antimicrobial or anticlotting purposes. Using systems to deliver nitric oxide from S-nitrosothiols equivalent to those found in mammalian metabolism has been proposed as an advantage strategy over fully synthetic NO donors[10] such as dizeniumtiolates. Interestingly S-Nitrosothiols can be tuned to deliver NO from very fast molecules with minutes of half-life to quite slow delivery by properly designing the chemical hinderance[11] and hydrophobicity[12] of donor environments.

During the last decades several strategies have been proposed to incorporate S-nitrosothiols to medical devices attempting to incorporate antibacterial and thromboresistant properties. PAMAM dendrimers have modified to link S-Nitrosothiols to the outer shell of the macromolecules gaining efficient antibacterial properties. The release of nitric oxide is efficiently controlled modified by using primary or tertiary thionitrites[13]. Those strategies have the ability to store great quantities of nitric oxide.

Tertiary thionitrites based on penicillamine have been incorporated into polymers by simple swelling and drying techniques allowing sustained effluxes for several days or even weeks accomplishing clot and several log bacterial reductions of polymeric surfaces and intravascular catheters[14][15][16] Dispersion by swelling may lack the ability to reproduce kinetics and may also alter the properties of some polymers and medical devices.

Lutzke *et al*[17] have developed biodegradable polymers such as polyphsophazenes with integrates S-nitrosothiol moieties to sustain delivery of nitric oxide over several days.

Present chapter aims to use the biodegradable polymers developed and apply them as antimicrobial coatings. Those polymers have integrated S-nitrosothiols with the ability to self-polymerize due to the SNO homolysis. Self-crosslinking is an interesting strategy that lacks application of catalyst or additives. Development of coatings has the advantage to be minimally interferent with the bulk mechanical properties of materials and take advantage of well stablished medical devices adding key antimicrobial properties. The coating strategy also favors high drug concentrations over specific sites inhibiting bacterial colonization just in the device surroundings.

Among the many materials with a high burden of infection that could benefit from a bacteriostatic degradable coating, tracheal stents present unacceptably high rates of complications associated to bacterial colonization that ultimately lead to infection[18]. Tracheal stenosis is usually presented clinically by airway obstruction caused from tumors surrounding the vessel leading to resistance in breathing presented as dyphnea.

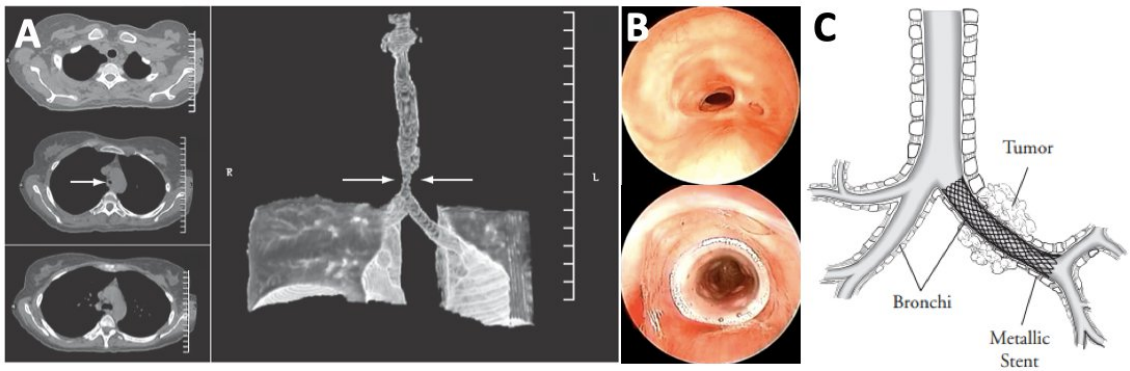

Figure 4.1.2 Treatment of tracheal stenosis with airway stent. A, MRI of an airway system with severe stenosis[19]. B, Example of endoscopic images of pre and post tracheal angioplasty with silicone stent[20]. C, Scheme of the treatment with a self-expanded stent to a tracheal tumor.

The insertion of metallic and polymeric materials into the airway system aiming to restore air flow dates back to the early 1950s. Since then the technique has been growing in use for treatment of severe obstructions. Airway stents are hollow tubes that

come in different shapes and materials such as silicone semirigid tubes or Nitinol self-expandable devices. Although opening of the airway obstructions by stents is nowadays the best in class treatment and contributes significantly to improve patient's quality of life, the technique is considered to be manly palliative. It has unacceptably high rates of bacterial colonization, as high as 70%, of the prothesis and more than 20% of stent-associated respiratory tract infection (SARTI)[21] leading to serious safety events for patients.

Present work will try to apply the novel material to treatment of tracheal stenosis attempting to reduce the level of prothesis colonization and ultimately infections. Potentially nitric oxide delivered from the device may also help to improve pulmonary function[22] of patients with comprised lung function. Being specially indicated for patients with compromised immune function or comorbidities such as chronic obstructive pulmonary disease.

4.2 MATERIALS AND METHODS

4.2.1 Materials: Unless noted all reagents were used from Sigma-Aldrich. CK3 was obtained from GL biochem without further purification, DAF-FM was purchased from Thermofisher) and Tracheal stents were used from Boston Scientific (Wallflex®).

*4.2.2 Synthesis of T64-SNO polymer***:** C32 based pBAE containing thionitrites were synthetized as described in previous chapte. Briefly n-mercaptocarboxilic acid (1 eq) was reacted with tertbutyl nitrite (1.1 eq), reaction quickly evolved and excess solvent was evaporated. C32 was coupled using DCC as coupling agent, DMAP as catalyzer and n-nitrosothiolcarboxilic acids (1.0 eq) at final concentration of 5%. NMR and C32-SNO is presented as example ^{1}H-RMN (400 MHz, CD_3OD, TMS) (ppm): δ= 7.26 (s 1H), 8.23-8.21 (d, 1H), 6.62-6.60 (d, 1H), 4.11 (m, 5H), 3.73 (m, 3.5H), 3.58 (m, 1.9H), 3.13 (s, 2H), 2.8(m, 3.8H), 2.8(m, 3.8), 2.67(m, 1.5H) 2.6(m, 2H) 2.4 (m, 3.5H), 2,32 (m, 2H), 2.04 (s, 1.3H), 1.7-1.4 (m, 9H), 1.25 (m, 11H). UV-Vis: 339 max, 506 max. FTIR-ATR: 1650 cm^{-1} (NO stretch), 1124 cm^{-1} (C=O stretch).

Kept for 6 months at -20 degrees until use.

4.2.3 Stent coating: Tracheal silicone coated braided nitinol stents 25x150mm were activated with atmospheric plasma nozzle at 35mm height and 500ms of plasma exposure (OpenAir®, Plasmatreat). Then dip coating of T64-SNO was performed with acetone while rotating and allowed to dry and evaporate at 37 degrees for 4 hours. Final coating density was fixed at 10 mg/cm^2 determinate by weight difference divided by coated surface.

4.2.4 Crosslinking Rheology: T64-SNO was vacuum rotavaporated to eliminate acetone and added into a rheometer to study the degree of crosslinking (parallel plate, 200µm x 25mm, and sweep angle 1°/s, MCR-2 Anton Paar) to perform a Sweep test for 12 hours. Temperature was fixed at 25 deg Celsius.

4.2.5 Swelling studies: T64-SNO was crosslinked overnight at 34 degree Celsius in an oven and placed into different solvents registering the weight before and after absorbtion. Swelling ratio was determined using the following formula:

$$\text{Swelling ratio} = \frac{\frac{(w_f - w_o)}{\rho} - w_o}{w_o}$$

4.2.6 Interface adhesion of T64-SNO polymer: silicone was prepared flat and with a 10µm rugosity molding surface. Then plasma activation of the silicone was performed by direct contact with atmospheric plasma and dip-coating with T64-SNO (100 mg/mL in Acetone).

Polymer was allowed to cure for 4 hours at 37 degrees and peel tested was checked with a high peel tape (TESA 4651) to ensure that failure mode is based in the polymer-silicone interface (ZwickRowell).

4.2.7 Contact Angle measurement: Contact angle was measured by adding 5uL drops of miliQ® treated water to determine the effectiveness of plasma activation and adhesion

force. Contact angle was determined using (Drop Shape Analyzer 100S, Krüss) within the 30 minutes after treatment.

4.2.8 Nitric oxide release kinetic measurement: T64-SNO was dried from stock solution using a rotatory evaporator protected from light. Then a film was extended using a film applicator of 50µm and left to cure at 37ºC for 4 hours. Then, samples of 4mm in diameter were cut and incubated in PBS at 37ºC at 500rpm protected from light. Liquid was extracted, immediately frozen and changed by new PBS. Finally samples were analyzed using Griess method. Aquose solutions of 2% sulfanilamide in 5% phosphoric acid and 0.2 % naphthylethylenediamine dihydrochloride were prepared and mixed in 1:1 ratio and added to samples and standard sodium nitrite curves.

4.2.9 Coating thickness: Tracheal silicone and T64-SNO coated stents were gold sputtered, coated with T64-SNO, gold sputtered again and embedded in epoxy resin. After polishing thickness was determined by inspection with SEM backscattered electron detector (EVO SEM, Carl Zeiss) and analysis with ImageJ®.

4.2.10 Inhibition halo test: Agar plates confluently seeded with SA MRS and PA were prepared, then 10 uL of polymers T64-SNO and C32-CK3 were added in the center of the plate and left to grow at 37 degrees overnight. Then the halo was inspected and measured.

*4.2.11 Bacterial growth inhibition***:** To study the effect of polymer into bacterial growth, 10uL of previously vaccum dried T64-SNO was deposited in the bottom edge of 48 wp and left for 4h at 37ºC. Then 300uL of LB with an inoculum of Methicillin-resistant *Staphylococcus aureus* and *Pseudomonas aeruginosa* was added and OD was registered continuously during 16h. C32-CK3 was also used as an experimental group. Inoculum of Bacteria with LB was used as positive growth control and LB media was used as negative growth control.

4.2.12 Cell Culture: MDA MB 231 (GFP+) and HDNF have been expanded at least two passages previously to experimental use and HDNF have been used for all experiments between passages 3 and 8. Cells were cultured at 37ºC in a 5% CO_2 atmosphere. The media used consisted in DMAEM supplemented with 10% FBS, penicillin/streptomycin and 1% glutamine. During expansion media was changed every 48h.

4.2.13 Contact cell toxicity: Polymer drops of 10 uL were seeded over confluent cell layers and incubated for 24h at. Following T64-SNO incubation, calcein-AM was added to stain viable cells and subsequent imaged using a fluorescence transilluminator imaging system. Radius of inhibition was obtained by image analysis using ImageJ®. Cells were also stained with propidium iodide to see if dead or apoptotic cells remain in the border.

4.2.14 Non-contact cell toxicity: Toxicity due to elution of nitric oxide or other fragments has been studied by using a transwell plate with a variable amount of T64-SNO in the basket and a fixed amount of cells in the wellplate. Toxicity was obtained by comparing the positive control wellplate treated with ethanol for 30s and the negative control of toxicity (untreated cells). After 24h incubation, cells cultured were washed with PBS,

incubated in 20% of MTS (Celltiter 96, Promega) diluted in culture media for one hour and analyzed by optical absorbance at 490nm in 96 wp (Elx808 Biotek Instruments Ltd).
4.2.15 Intracellular Nitric oxide staining: Cells were washed with PBS and stained with DAF-FM(ThermoFisher) at 5µM in PBS for 30 minutes. Then FBS free media was added and cells were imaged by fluorescent microscopy 495/515 em/ex.

4.2.16 Ex vivo tracheal inhibition growth: Porcine tracheas were obtained from local livestock and immediately refrigerated at 4^{o}C until use. Within 24 hours the stents (Boston Scientific, Marlborough, MA, USA) partially coated with T64-SNO were deployed internally using a deployment catheter and left for 24h at 31^{o}C in a sealed container. Stents used were only half coated to serve as internal negative control. After incubation, tracheas were dissected and frottis from the coated and uncoated zones of the inner stent surface, outer stent surface and luminal trachea. Then, samples were transferred to agar plates to further study the density of microorganisms as colony forming units (CFU) by counting ImageJ®.
4.2.17 Statistical analysis: Data were analyzed using GraphPad® Prism. Comparisons between groups were done by one-way ANOVA using Turkey *post-hoc* test. Differences were considered significant when $p<0.05$ *, $p<0.01$** and $p<0.001$***.

4.3 RESULTS AND DISCUSSION

4.3.1. T64-SNO synthesis

Synthesis of pBAE polymers with integrated nitric oxide release properties through SNO moieties has been accomplished and detailed in chapter 1. During synthesis, gelation reactions were occasionally found encouraging the investigation as self-crosslinking polymers with nitric oxide release properties.

The proposed synthetical scheme (Figure 4.3.1) was found to be compatible with Steglich reactions to derivate hydroxyls but major care was necessary to avoid undesired crosslinking. During synthesis a set of polymers was obtained successfully with extensions comprised between 2 and 16 carbons atoms. Use of primary, secondary and tertiary thiols were also explored and some polymers were obtained successfully with more than three orders of magnitude difference in stability on aqueous media. A proof of concept over stability in water media lead towards selection of primary S-nitroshothiol extenders with more than 10 carbons.

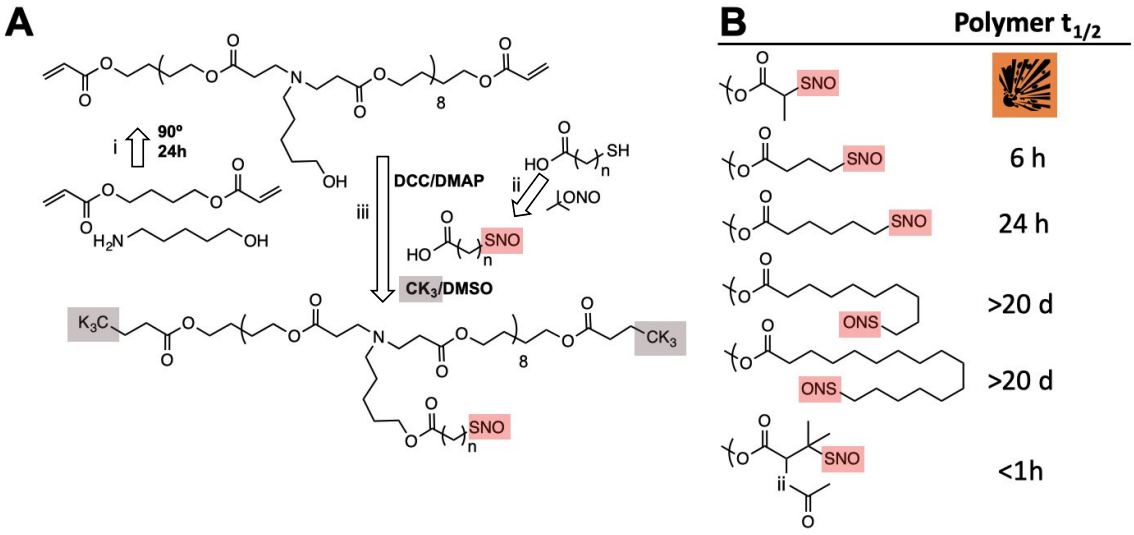

Figure 4.3.1. Synthetic scheme of T64-SNO family of polymers. A, Synthetic scheme of C32 pBAE and further reaction with thiocarboxylic acid to obtain pBAE containing thionitrites. B, Qualitative stability of the polymers synthetized in water media, showing higher stabilities with longer chains.

Synthetic reactions were optimized to limit requirements for workup due to sensitiveness of the polymer to gel. Optimization of the reaction conditions was accomplished using TLC and Griess reaction to analyze the presence of SNO byproducts. From all polymers developed, it was selected an esterification of C32 with S-nitrosomercaptoundecanoic acid named as T64-SNO

4.3.2 Biomaterial characterization

T64-SNO is a polymer specially developed to show antibacterial properties, being biodegradable, self-crosslinkable and potentially co-deliver RNAs. Experiments detailed in Figure 4.3.2.1 summarize the experiments planned to characterize the material and its suitability to coat tracheal stents.

At room temperature the polymer evolves, with time or temperature, from a viscous deep red liquid (Figure 4.3.2.1.I) to a viscoelastic material that loses its characteristic red color over time and becomes rubbery. Crosslinking of T64-SNO was tracked by a sweep analysis at room temperature. It can be observed (Figure 4.3.2.1.C) how elastic modulus increases at a faster rate than viscous modulus suggesting that the material has more ability to store mechanic energy becoming crosslinked. Additional experiments were conducted to ensure that crosslinking was taking place. Incubation of crosslinked material in different solvents was studied observing a clear tendency towards swelling rather than dissolving in all solvents (4.3.2.1.F). Water, DMSO, isopropanol, hexane and acetone have been used to screen the interchain bridge formation. Acetone shows the larger swelling ratio probably because the similarities in polarity between polymer backbone and solvent chemistry, surprisingly color was maintained in all solvents besides hexane that shows a rapid loss of the thionitrite that will be discussed in Figure 4.3.2.2.

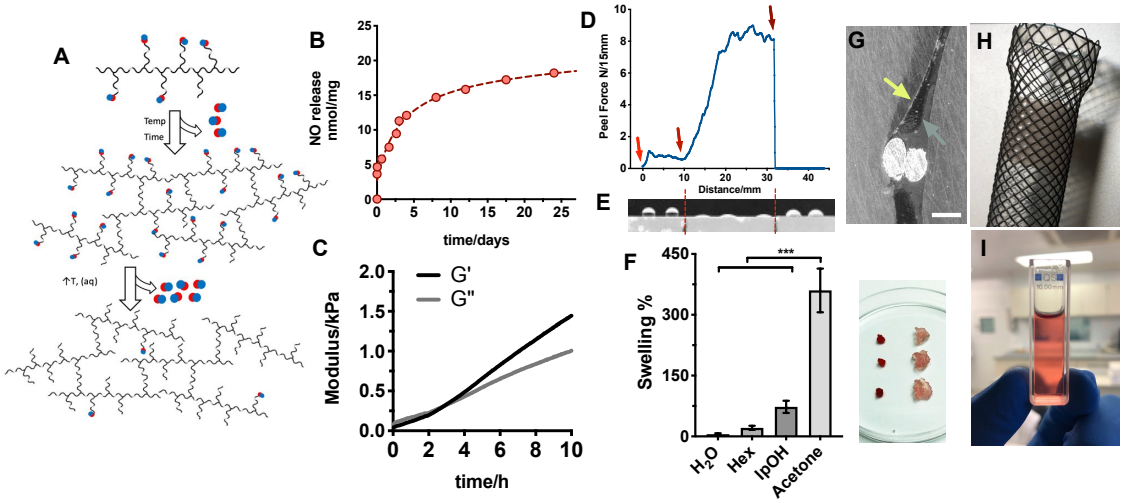

Figure 4.3.2.1 Biomaterial Characterization. A, NO and crosslinking scheme. B, 28 day nitric oxide delivery. C, Crosslinking kinetics measured by shear oscillatory crosslinking. D, Interface energy of silicone rugose (20 um) (left), rugosity + plasma activation (center) and smooth control (right). E, Water contact angle of the previously described zones. F, Swelling results and images. G, Thickness measurement of hydrogel coating, scale bar 250 µm yellow arrow (gold layer T64-SNO), grey arrow (silicone layer) . H, Medical device example and I, Characteristic red color of the primary S-nitrosothiol of T64-SNO. Histograms are plotted as mean ± SEM. Significant differences between the groups: * $p < 0.05$, ** $p<0.01$, *** $p < 0.001$ and ns=non significant.

Considering the wide solubility of uncrosslinked T64-SNO in DMSO or acetone and the rheological results it can be concluded that true self-crosslinking is taking place.

Together with crosslinking, nitric oxide release takes place (Figure 4.3.2.1.A). NO delivery is desired to last longer than 20 days to potentially show clinical benefits in mid or long-term implants. Ideally, kinetics should follow an initial burst release to limit settling of existing microorganisms around the device and a sustained release to block growth. Originally, several short extenders (2-3 carbon atoms) were used having primary secondary and tertiary thionitrites. Surprisingly, short extenders showed a significant instability reporting very limited NO release. In an attempt to extend the delivery of nitric oxide, longer extenders were evaluated showing a significant increase form a few hours up to more than 20 days for a 11-carbon aliphatic extender with a primary SNO T64-SNO. The results of NO release (Figure 4.3.2.1.B) from T64-SNO are sustained for up to 25 days being potentially extended beyond 40 days. Surprisingly the extension of the side chain seems to have a non-linear relationship showing an effect that is beyond the increase in hydrophobicity. Use of T64-SNO depleted from nitric oxide served as negative control for potential interferences.

Once gelation and nitric oxide release properties were stablished, the application to tracheal silicone covered stents was explored. Initially, direct coating of T64-SNO over silicone was found to be poorly anchored being easily peeled and incompatible with the delivery system. To improve the results a dual strategy of increasing the surface roughness of silicone in combination with atmospheric plasma was studied. Results showed that roughness has a higher interfacial energy than flat silicone and plasma treatment increased significantly the surface energy (Figure 4.3.2.1.D). It is hypothesized that the increase in anchoring energy comes from radical based reaction in the interface between thionitrites and surface radicals. Coating of T64-SNO was reproduced over nitinol coated silicone tracheal stents. Although atmospheric plasma was found to be an effective treatment to improve the binding energy, atmospheric plasma treatment over the silicone did not last during more than 60 minutes if uncoated. Coating have an average thickness of 75 ±15 μm (Figure 4.3.2.1.G) being tunable to virtually any value under 500μm. It is proposed that thicker coatings will result in an increase of absolute NO delivery and slightly longer delivery times. The selected thickness gave a desirable balance between toxicity and antimicrobial effect.

Once the characterization was finished, it was desired to study in a deeper way the mechanisms of crosslinking and the extension of NO delivery capabilities. Normally S-nitrosothiols release nitric oxide under physiologic conditions, nonetheless the reaction has been described to be catalyzed by copper ions, heat, light or presence of thionitrites and thiols[23]. Homolysis between thionitrites releasing nitric oxide is one of the possible reactions to allow crosslinking. It is also possible that delivering nitric oxide

allows to have reactions with the acrylate moieties of T64-SNO leading to polymeric chain reactions or cross-reactions with the free side thiols generated after decomposition of SNO groups. Due to the length of side chains and the viscosity increase it is proposed that homolysis is quite limited to no more than 5-10% of total SNO.
To understand the reason of the unusual extension of NO release properties and self-crosslinking mechanisms, a series of experiments were conducted.
The following conditions were examined to understand the role of SNO in crosslink reactions; addition of small molecule thionitrites to displace crosslink, butylated hydroxytoluene to block potential radical reactions, 4-Arm PEG thiol-ended to observe potential over crosslink and glutathione to allow thionitrite transfer. Surprisingly, only treatment with S-nitrosothiolactic acid showed limited alteration of the crosslinking supporting the SNO homolysis hypothesis. The lack of reactivity of the SNO in T64-SNO lead to suggest that the long lipophilic side chain of more than 17 atoms was blocking the reactivity of SNO. Some experiments were planned to check the steric hinderance by the long side chain hypothesis.

Interestingly, it was observed that swelling in all solvents did not affect the presence of SNO group besides hexane or acetone/hexane mixtures rich in hexane. It is proposed that swelling in acetone does not allow side chains to fully extend keeping SNO groups covered by the side chains. Addition of hexane to acetone may destabilize the folded branches and expose the end-groups allowing reactions, enhancing the self-polymerization kinetics and loosing nitric oxide. In Figure 4.3.2.2 the hypothesis of folding protection is exposed. Swelling of T64-SNO in hexane resulted in limited swelling with complete loss of red color and opacity appeared (Figure 4.3.2.2.A), further treatment with acetone yielded a very limited swelling of T64-SNO, suggesting that hexane allows a greater crosslink density by side chain unfolding and favored homolysis reaction.
This behavior has only been observed in polymers with large side chains while short 4-6 carbon atoms destabilize rapidly in acetone and other solvents.
In an attempt to further understand the role of hydrophobicity in degradation kinetics an experiment was conducted by dispersing S-nitrosothio-6-hexanoic acid into hydrophobic polymer, such as PLA, and adding it to water observing that decomposition was almost complete after 24h, similar results were found for S-nitrosomercaptoundecanoic acid dispersions.

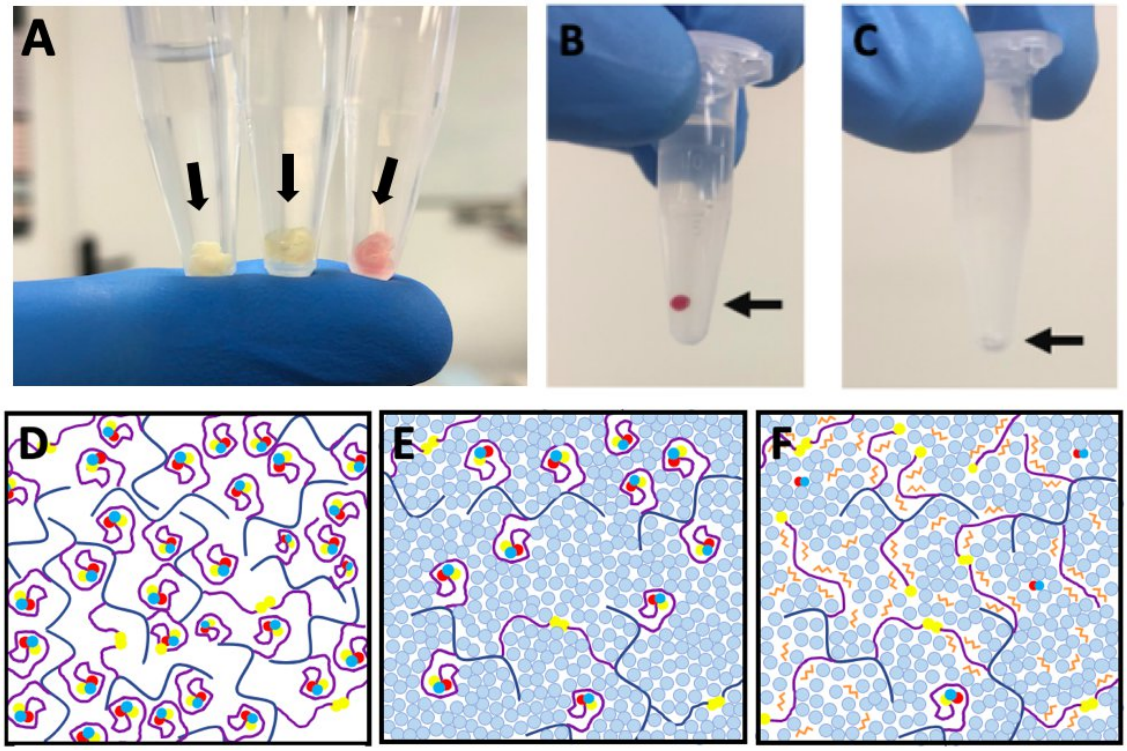

Figure 4.3.2.2 Hypothesis of SNO shielding by long chain extenders. A, Example of hydrogels swollen by left, hexane(observe the pale opaque color), Hexane/Acetone 2:1 mixture and Acetone (right). B, Initial color of PLA-6 hexanoic acid dispersion and B, color after 24h incubation in PBS media. D, T64-SNO in solid form. E, T64-SNO swelled in acetone with some degree of crosslink and side-chains folded. F, addition of hexane allows a complete unfolding allowing a stronger homolysis of end-SNO groups.

Considering that the decomposition of dissolved aliphatic primary thionitrites should be similar it induces to think that sterically hindering by side chains may play an important role in the SNO decomposition.

Finally, a set of self-crosslinking materials with nitric oxide releasing properties beyond 20 days have been synthetized and applied successfully to silicone coated tracheal stents (Figure 4.3.2.1.H). Coatings have been found to highly adhesive when applied after atmospheric plasma treatment of rough surfaces.

4.3.3 Antibacterial properties of T64-SNO

Antimicrobial properties of the material were first studied by observing the effect over inhibition halus of C32, as control polymer, and T64-SNO as experimental group. Furhtermore the effect of the coating and control polymer over bacterial growth in media were evaluated to expand the antibacterial characterization. Attachment of bacteria forming biofilms to polymer coatings has also been studied. Tests were focused in fighting pathogenic *Staphylococcus aureus* MRA and *Pseudomona aeruginosa* PAO1

due to increased sensitiveness to nitric oxide. *Escherichia coli* UPEC and *Klebsiella pneumoniae* resistance against developed polymers was also studied. The mentioned sample of pathogens is intended to represent the more important pathogens in real life infections.

T64-SNO has been found to be highly efficient against *S. aureus* and *P. aeruginosa*. In figure 4.3.2.1 the antimicrobial results are presented, it can be observed how C32 had no effect and T64-SNO completely inhibited the growth of both microorganisms. Apparent reduction of C32 is probably caused by light dispersion artifacts. Inhibition halus smaller than 2 millimeters are consistent with an antimicrobial effect from nitric oxide. While nitric oxide is being delivered from the polymer, it diffuses trough agar killing bacteria. Limited halus are obtained because of the limited half-life of the molecule. Extension of the incubation time in the halus experiment and growth experiment did not show a delayed growth meaning that bacteria has probably being killed by the nitric oxide.

Results of growth inhibition of *K. pneumonia* and *E. coli* have been found to retard growth by 5-10 hours and form significantly smaller or negligible inhibition halus. Previous experiments with an equivalent polymer to T64-SNO but with 6 carbon extension rather than 12 showed complete inhibition of the whole set of pathogens but significantly shorter delivery span of nitric oxide.

Biofilm formation results over T64-SNO have shown a complete inhibition of formation compared to C32 control, biofilm inhibition has also been significantly higher in *K. pneumonia* and *E. coli* probably by the enhanced local effect of the coating (data not shown).

The polymer structure has been chosen considering the balance between antibacterial properties, compatibility with mammalian cells and extension of nitric oxide delivery. It is assumed that current results show a good potential to limit the growth of pathogens in the surroundings of the material/implant while being biocompatible.

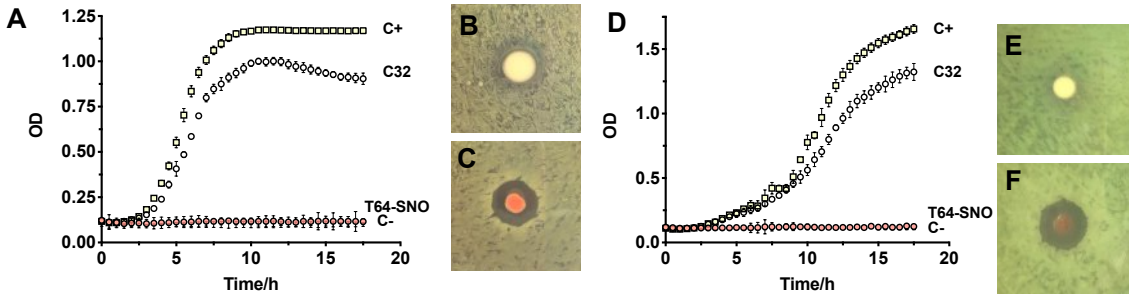

Figure 4.3.3.1 Antibacterial Properties. A, Growth inhibition kinetics of *Staphylococcus aureus* MRA and inhibition halo of C32 B and C32-SNO. Growth inhibition kinetics of *Staphylococcus aureus* MRA and halus inhibition of C32 B and C32-SNO.

In vivo many other cytostatic mechanisms will be combined with the nitric oxide release, allowing hopefully a proper clinical outcome. If a stronger delivery could be necessary,

a coating with multiple layers could be developed or develop a new strategy such as a combination between nitric oxide and local delivery of antibiotics.

4.3.4 Interaction of nitric oxide releasing polymer (T64-SNO) with mammalian cells

As previously mentioned, nitric oxide has also a significant toxicity over mammalian cells. Developing antimicrobial strategies using this agent must consider carefully side toxicity of NO on cells and tissues. To assess the cytotoxicity, non-contact toxicity and halo type experiments were performed over different types of mammalian cells. A cancerous cell line (MDA-MB-231) was chosen as a highly aggressive and resistance cell line plus a Human neonatal fibroblast representing a more sensitive one.
The impact of nitric oxide over mammalian cells was of great interest due to clinical usability is probably determined by a balance of bacterial toxicity and mammalian cell toxicity. Results are presented in Figure 4.3.4.1

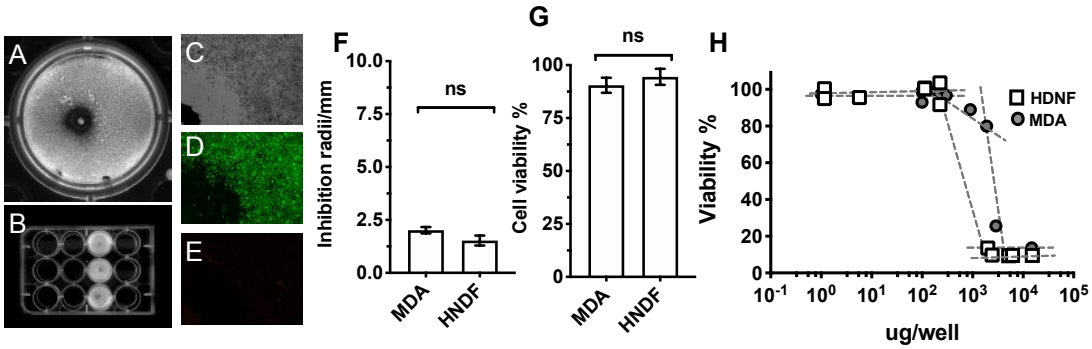

Figure 4.3.4.1 Toxicity of T64-SNO to mammalian cells. A, B, example of confluent endothelial cells stained with DAF T64-SNO added in the center. C, Brightfield image of the inhibition zone. Black spot in the left corner is the T64-SNO. D, Calcein-AM staining of the inhibition radii and E, staining of the inhibition with propidium iodide showing sporadic dells in death in the inhibition zone. F, Average radii of the inhibition halo. G, MTT viability of cells incubated in contact with T64-SNO. H, Contactless cell toxicity of T64-SNO to HDNF and MDA cells by transwell method. Histograms are plotted as mean ± SEM. Significant differences between the groups: * $p < 0.05$, ** $p<0.01$, *** $p < 0.001$ and ns=non significant.

To confluent fluorescent stained cells, polymer was added and incubated to observe effects over surrounding cells. Results showed a very similar inhibition halus between mammalian and bacterial cell lines in absolute values. Probably a monolayer experiment serves as a worst-case situation for mammalian cells due to no vasculature or adjacent tissue is present to dilute the effect of nitric oxide. Viability has been studied by life-dead staining and observing a limited number of necrotic cells within the halo or border and no evidence of cellular damage in the rest of the cell culture. Viability using MTT has also been found to be quite equivalent between cell lines with >90% viability. A contactless toxicity assay was also performed using a transwell method, it was found that fibroblasts are more sensitive than MDA cells and that 5-10 mg/mL is the LC50 of

the T64-SNO material, high sensitivity of the assay was probably influenced by the proximity of the transwell.

Experiments were also planed to explore the role of the polymer on cellular NO uptake. For this purpose, cells were stained with DAF-FM dye and treated with T64-SNO and K72-NO. After a few minutes, cells showed a clear increase in fluorescence in contraposition of K72-NO. Those experiments show the lack of metabolic need to bioactivate the T64-SNO to nitric oxide and could show a potential use of T64-SNO based polymers over highly demanding nitric oxide environments because of high flow, wear or metabolic demand.

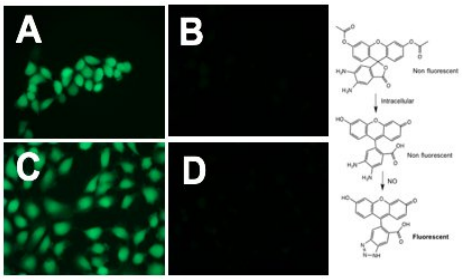

Figure 4.3.4.2 Intracellular levels of nitric oxide treated with T64-SNO. A, COS-7 cells treated with DAF-FM and T64-SNO. B, Control of COS-7 cells treated with DAF-FM and C32-CK3. C, MDA GFP+ cells treated with DAF-FM and T64-64. D, MDA GFP+ treated with DAF-FM and control polymer.

Results of toxicity to mammalian cells encouraged a potential benefit of the antimicrobial properties and toxicity balance.

4.3.5 Ex vivo antimicrobial activity in medical devices.

The validation of the coating system was planned over an *ex vivo* experiment using porcine tracheas and human tracheal stent partially coated with T64-SNO. Due to high variability between tissues it was thought that partially coating the stent would give a better idea of the effectiveness of the system by having internal controls. *Ex vivo* systems have the advantage to expose tracheal stents to a similar flora, similar diffusion of NO and a stronger growth of microorganisms due to decomposition and absence of natural antimicrobial mechanisms. Experiments conducted have been focused on exploring the total growth of microorganisms in tracheal inner surface and inner and outer stent surfaces. Results are presented in figure 4.3.5.1.

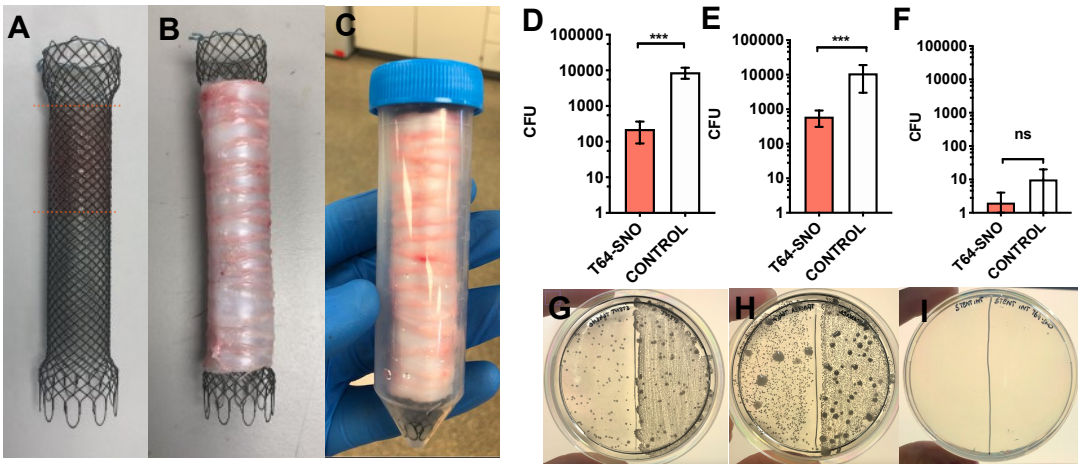

Figure 4.3.5.1 *Ex vivo* evaluation of antibacterial properties. A, Example of a tracheal stent with T64-SNO coating(red coating between dashed lines). B, Stent introduced into porcine trachea explant and inserted into a recipient, C. D, CFU formed into the outer stent surface. E, CFU formed in the tracheal surface and F, CFU in the inner surface of stents. Agar plate examples of outer stent G, tracheal inner surface, H and I, inner stent surface. Histograms are plotted as mean ± SEM. Significant differences between the groups: * $p < 0.05$, ** $p<0.01$, *** $p < 0.001$ and ns=non significant.

Results show a significant reduction of approximately 1-2 logs between the coated and uncovered area. This reduction has been studied over the interior of the stent, the exterior and the interior of the trachea. It is important to note that microorganism's growth is significantly higher *ex vivo* and results *in vivo* could be significantly better. From the translational point of view, improving the treatment using a bacterial strategy may potentially improve significantly the outcomes related to pneumonia and infection. Nonetheless stenosis is treated nowadays as a compassion treatment with the potential to avoid restenosis by developing a strategy that combines mechanical action with pharmacological action. There could arise the temptation to apply a cytostatic drug as was done for vascular stents. However tracheal stenosis is commonly caused by benign and malign tumors were the tissue that generates the compression is at significantly higher distances than equivalent applications such as cardiovascular stents. Meaning that imaginative strategies should be explored to enhance the penetration of drugs beyond epithelial layers of tracheal tissues. Direct injection of RNA loaded nanoparticles prior to the implantation of the antibacterial stent could be a plausible strategy to improve tumor and infection outcomes. Several strategies such as VEGF suppression though a siRNA have been proposed as plausible strategies to limit cancer progression[24].

Drugs to reduce stenosis and/or a broader antibacterial action could in theory be added to the outer and inner surface to improve the clinical outcomes. Up to day some reports have been published showing potential benefits of such therapies[25].

4.4 CONCLUDING REMARKS

Some of the potential non-viral vector proposed in chapter 1 have been found to release high concentrations of nitric oxide. Those materials may not be directly useful as non-viral vectors but can be useful as antibacterials. In present chapter the developed materials with high releasing profile of NO have been directed towards coatings for implants with high infection burden. T64-SNO is highly hydrophobic pBAE with S-nitrosothiols incorporated. The SNO moieties allow the material to show interesting self-crosslinking properties and releasing nitric oxide following a burst release that sustains a milder delivery beyond 25 days.

T64-SNO shows promising inhibition of *Staphylococcus aureus* and *Pseudomona aeruginosa* while being balanced in terms of toxicity to mammalian cells. A set of *ex vivo* experiments have been completed showing encouraging antibacterial properties of the material when applied in a real life medical device. Those antibacterial properties observed in pre-clinical models, although promising, will have to be further investigated to prove its clinical significance in reduction of stent associated-respiratory tract infections.

4.5 REFERENCES

[1] Singh VK, Mehrotra S, Narayan P, Pandey CM, Agarwal SS (2000) Modulation of autoimmune diseases by nitric oxide. Immunol Res. 2000;22(1):1-19. DOI: 10.1385/IR:22:1:1

[2] Dash PR, Whitley GS, Ayling LJ, Johnstone AP & Cartwright JE (2005) Trophoblast apoptosis is inhibited by hepatocyte growth factor through the AKT and beta-catenin mediated up-regulation of inducible nitric oxide synthase. Cell.Signal. 17(5): 571-80

[3] Kuang Z1, Lewis RS, Curtis JM, Zhan Y, Saunders BM, Babon JJ, Kolesnik TB, Low A, Masters SL, Willson TA, Kedzierski L, Yao S, Handman E, Norton RS, Nicholson SE. (2010) The SPRY domain-containing SOCS box protein SPSB2 targets iNOS for proteasomal degradation. J Cell Biol. 2010 Jul 12;190(1):129-41

[4] Ren B., Zhang N., Yang J., Ding H. (2008) Nitric Oxide-Induced Bacteriostasis and Modification of Iron-Sulfur Proteins in *Escherichia coli*. Mol Microbiol. 2008; 70(4): 953–964.

[5] Valence C, (1998) Nitric oxide as an antimicrobial agent: does NO always mean NO? Gut; 1998, 42(3) 334

[6] Kono Y, Shibata H, Adachi K, et al. (1994) Lactate-dependent killing of *Escherichia coli* by nitrite plus hydrogen peroxide: a possible role of nitrogen dioxide. Arch Biochem Biophys 311:153–159

[7] Benjamin J. Privett, Angela D. Broadnax, Susanne J. Bauman, Daniel A. Riccio, Mark H. Schoenfisch (2013) Examination of Bacterial Resistance to Exogenous Nitric Oxide Nitric Oxide. 2012 Mar 31; 26(3): 169–173 DOI: 10.1016/j.niox.2012.02.002.

[8] Fang FC (1997) Perspectives series: host/pathogen interactions. Mechanisms of nitric oxide-related antimicrobial activity. J Clin Invest. 1997 15; 99(12): 2818–2825. DOI: 10.1172/JCI119473

[9] Hernando-Amado S, Coque TM, Baquero F, Martínez JL (2019) Defining and combating antibiotic resistance from One Health and Global Health perspectives. Nat Microbiol. 2019 Sep;4(9):1432-1442. doi: 10.1038/s41564-019-0503-9

[10] Tsikas, D.; Schmidt, M.; Böhmer, A.; Zoerner, A. A.; Gutzki, F.M.; Jordan, J. UPLC-MS/MS Measurement of S-Nitrosoglutathione(GSNO) in Human Plasma Solves the S-Nitrosothiol Concentration Enigma. J. Chromatogr. B: Anal. Technol. Biomed. Life Sci. 2013, 927,147−157.

[11] Roy B; Hardemare AM; Fontecave M. (1994) New thionitrites: Synthesis, stability, and Nitric Oxide Generation. J. Org. Chem 1994, 59, 7019-7026.

[12] Benjamin Meyer, Alessandro Genoni, Ariane Boudier, Pierre Leroy, and Manuel F. Ruiz-Lopez . Structure and Stability Studies of Pharmacologically Relevant S-Nitrosothiols: A Theoretical Approach. The Journal of Physical Chemistry A 2016, 120 (24) , 4191-4200. DOI: 10.1021/acs.jpca.6b02230

[13] Stasko AA, Fisher TH, Schoenfish MH (2008) S-Nitrosothiol-Modified Dendrimers as Nitiric Oxide delivery vehices. Biomcaromolecules 2008,9,3,834-841.

[14] Wang X, Jolliffe A, Carr B, Zhang Q , Bilger M , Cui Y , Wu J , Wang X , Mahoney M , Rojas-Pena A , Hoenerhoff MJ , Douglas J , Bartlett RH , Xi C , Bull JL , Meyerhoff ME. (2018) Nitric oxide-releasing semi-crystalline thermoplastic polymers: preparation, characterization and application to devise anti-inflammatory and bactericidal implants. Biomater Sci. 2018 20;6(12):3189-3201. doi: 10.1039/c8bm00849c

[15] Zhou Y, Zhang Q, Wu J, Xi C, Meyerhoff ME (2018) Synthesis and Characterization of a Fluorinated S-Nitrosothiol as the Nitric Oxide Donor for Fluoropolymer-Based Biomedical Device Applications J Mater Chem B. 2018 Oct 14;6(38):6142-6152. doi: 10.1039/C8TB01814F

[16] Feit CG, Chug MK, Brisbois EJ (2019) Development of S-Nitroso-N-Acetylpenicillamine Impregnated Medical Grade Polyvinyl Chloride for Antimicrobial Medical Device Interfaces. ACS Appl. Bio Mater. 2019, 2, 10, 4335-4345 DOI: 10.1021/acsabm.9b00593.

[17] Lutzke A, Tapia JB, Neufeld MJ, Reynolds MM. Sustained Nitric Oxide Release from a Tertiary S-Nitrosothiol-based Polyphosphazene Coating. ACS Appl Mater Interfaces. 2017 Jan 25;9(3):2104-2113. doi: 10.1021/acsami.6b12888

[18] Vitsas V., Touman A., Agelakis L., Moraitou E., Vogiatzakis E., Koulouris N., Stratakos G. (2017) Bacterial colonization/infection of the airway stents. European Respiratory Journal 2017 50: PA3792; DOI: 10.1183/1393003.congress-2017.PA3792

[19] Germano AL; Kussler D. (2008) anagement of recurrent distal tracheal stenosis using an endoprosthesis: a case report. J. bras. pneumol. vol.34 no.2 São Paulo Feb. 2008.

[20] Left Dutau H. (2013) Endobronchial silicone stents for airway management. Principles and practice of interventional pulmonology. Springer pp.311-321

[21] Agrafiotis M, Siempos II, Falagas ME. (2009) Infections related to airway stenting: a systematic review. Respiration. 2009;78(1):69-74. doi: 10.1159/000213244

[22] Lundberg JO, Settergren G, Gelinder S, Lundberg JM, Alving K, Weitzberg E. Inhalation of nasally derived nitric oxide modulates pulmonary function in humans. Acta Physiol Scand. 1996 Dec;158(4):343-7 DOI: 10.1046/j.1365-201X.1996.557321000.x

[23] Stamler SJ, Toone EJ, (2003) The decomposition of thionitrites. Curr. Op in Chem Biol. 6(6): 770-85. DOI: 10.1016/S1367-5931(02)00383-6

[24] Miwata K, Okamoto H, Nakashima T, et al. Intratracheal Administration of siRNA Dry Powder Targeting Vascular Endothelial Growth Factor Inhibits Lung Tumor Growth in Mice. Mol Ther Nucleic Acids. 2018;12:698-706. doi:10.1016/j.omtn.2018.07.009

[25] Faisal M, Harun H, Hassan TM, Ban AY, Chotirmall SH, Abdul Rahaman JA. **(2016)** Treatment of ultiple-level tracheobronchial stenosis secondary to endobronchial tuberculosis using bronchoscopic balloon dilatation with topical mitomycin-C. BMC Pulm Med. 2016 Apr 14;16(1):53. doi: 10.1186/s12890-016-0209-1

CHAPTER 5. DEVELOPMENT OF ANTIMICROBIAL AND MICROCIRCULATION ENHANCEMENT MATERIALS FOR DERMAL APLICATIONS

5.1 INTRODUCTION

After the evaluation of antimicrobial properties of nitric oxide derived pBAE in epithelial tissues, it was attempted to adapt the material to skin applications. It is well stablished that nitric oxide plays a deep effect in homeostasis and skin repair process.
Human skin is naturally populated of microorganisms such as bacteria, fungi and viruses forming the skin microbiome. Under normal circumstances, the microbiome is innocuous and plays important roles modulating the immune system and balancing homeostasis[1]. Skin is the largest organ in the body providing a highly efficient barrier against chemicals, dehydration or abrasion among other functions.

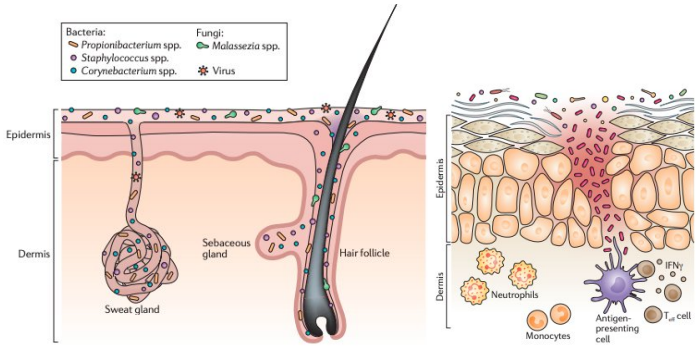

Figure 5.1.1 Structure of human skin and microbiome1. Left, Normal skin with different microorganisms over the exterior layers of skin, sweat glands and hair follicles. Right, compromised skin with microorganisms invasion of inner tissues and subsequent inflammatory response.

Skin also plays essential roles such as thermoregulation, sensation and protecting mesenchymal tissues from contaminants, UV light and microorganisms. Nitric oxide serves as a key factor of dermal regulation. Vasodilatation is strongly influenced by the expression of NOS, enhancing locally nitric oxide levels in the blood flow, allowing more efficient heat exchange or inflammation among other processes. Several experiments have been reported to probe the essential role of nitric oxide in dermal processes. Blocking of NOS through inhibitors like L-NAME has been reported to strongly reduce microcirculation and heat exchange both in animals[2] and humans[3].
Nitric oxide is also involved in the response of human skin to UV irradiation. When exposed to ultraviolet radiation, skin keratinocytes release a cascade of interleukins and cytokines altogether with vasodilation, generating erythema and its characteristic delayed redness. Investigations have been found to inhibit erythema response induced by UV irradiation through local injection of L-NAME, a NOS inhibitor, showing a significant role on nitric oxide and endothelial vasodilation on response to UV induced damage[4].

Nitric oxide concentration on skin exceeding homeostatic levels are associated with inflammation. Either high nitric oxide levels induced by artificial donors or genetic dysregulations induce the autocrine and/or paracrine response by releasing cytokines, the introduction of NOS inhibitors can partially block the signal.

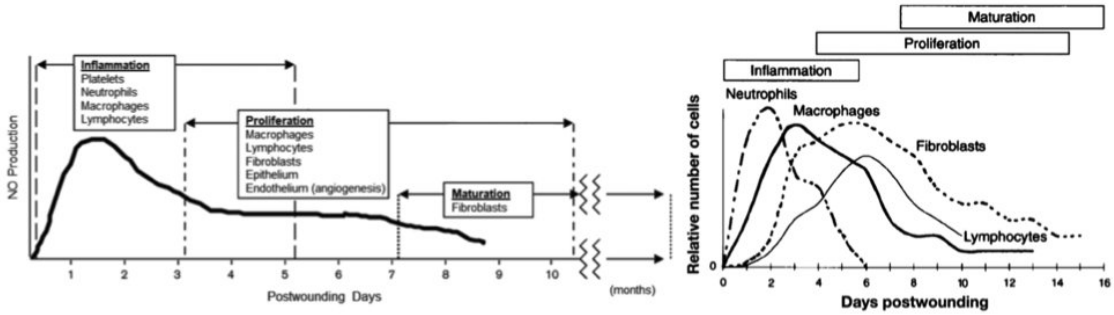

Figure 5.1.2. Nitric oxide and stages of wound healing. A, Relative levels of nitric oxide during the different stages of wound healing[5]. B, Stages of wound healing and relative typology of cells recruited in the wound site[6].

Wound healing in healthy individuals is also related with an increase of nitric oxide production in peri-wound skin. Increase of nitric oxide production after wounding is typically peaked during the first days and can be extended for several weeks[7]. NO helps to increase blood supply, facilitates the permeability of macrophages and lymphocytes improving proliferation of keratinocytes and fibroblasts, ultimately promoting collagen production for scar tissue[8].

High concentrations of nitric oxide exert a strong antibacterial effect that can be induced directly by excretion of keratinocytes and indirectly by conversion of nitrite to nitric oxide due to acidic pH in skin reducing the progression of bacteria, viruses and fungi. Agents that combine an antibacterial effect and promote microcirculation have strong potential to symbiotically protect against opportunistic infections and potentiate intrinsic healing mechanisms. Up to date, no bacterial acquired resistance against nitric oxide has been reported[9] positioning NO as a potential antibacterial agent specially in environments with high risk of bacterial resistance presence. Nitric oxide displays its effect through multiple species such as NO itself, peroxynitrites and thionitrite intermediates making highly complex for microorganisms to develop simultaneous mutations that evolve in resistance.
Multiple dermal compromised situations could take an advantage out of nitric oxide properties. Surgical site infections appear in as much as 2% of all surgical procedures[10]. Burns may also benefit from the proprieties of nitric oxide as large areas require enhancement of regeneration processes and antibacterial properties. Annually more than 60 million injuries are caused from heat burns, with 3 million requiring hospitalizations and 238.000 deaths[11].

Among the most complex dermal injuries are chronic wounds, also known as pressure ulcers, vascular ulcers or diabetic ulcers. While normal wounds typically resolve within a month, chronic wounds are those that enter into a long-term inflammatory stage that can last for months or even remain unresolved[12] in as high as 30% of cases. Chronic wounds are induced by long periods of dermal hypoxia, physical pressure or compromised vascular response in illnesses such as diabetes. Annually as large as 0.5% of population in developed countries can develop pressure ulcers[13], affecting especially elder patients with limited motility. In hospital prevalence of ulcers can appear in as high as 20% of patients hospitalized in first world institutions. Those numbers are accompanied by strong social and economic burden of more than 10 billion dollars each year. Pressure ulcers are the major cause of amputation and are also associated with a 5-fold increase in mortality when associated with other comorbidities.

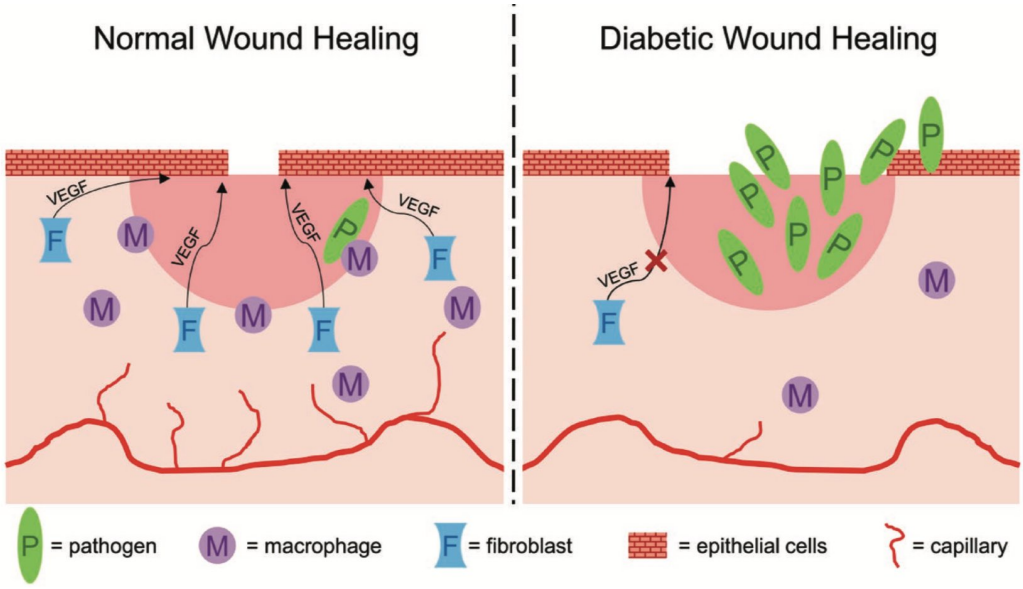

Figure 5.1.3. Mechanisms of normal and diabetic wound healing. In normal tissue(left), neovascularization, inflammation and high growth factor levels directs wound closure. In diabetic wound(left) impaired vascular response limits the inflammatory response and subsequent recruitment of inflammatory response while pathogens populate and expand compromising wound healing[14].

Several applications have been proposed to incorporate exogenous sources of nitric oxide attempting to promote healing, especially in those environments were intrinsic nitric oxide generation is compromised.

First attempts to use nitric oxide were based in applying NO in its natural gaseous state. Ghaffari *et al* reported that treatment with gaseous nitric oxide reduced significantly the burden of *E. coli*, *P. aeruginosa* and *S. aureus* both *in vitro*[15] and *in vivo*[16] suggesting that biomaterials able to locally deliver nitric oxide could take advantage of the antibacterial activity without significant side effects. Although many reports showed

positive outcomes of gaseous nitric oxide, the system is relatively complex and dangerous requiring to be used under professional supervision and hospital location.

Application of nitric oxide locally can also be done by treating ulcers with acidified nitrite to generate locally nitric oxide. Several examples have been reported to significantly reduce bacterial burden *in vitro*[17] and improve chronic wound healing in clinical applications[18][19].

Multiple applications have been based in the introduction of either thionitrites or diazeniumdiolates as nitric oxide donors. Nitric oxide has been covalently linked to gelatin in order to release nitric oxide in an extended manner altogether with light induced photolysis[20]. Kim *et al*[21] developed a chitosan based film with glutathione thionitrite, application of the material to mice wounds showed a significant reduction of bacterial load of 1-2 logs in the wound site and a 3-fold increase in healing rate with two week complete closing.

Bandages based in electrospun fibers with diazeniumdiolates incorporated in the polymeric backbone have been proposed by Lowe *et al*[22], achieving a faster dose dependent healing rate in dorsal mice model and higher capillary density development in wound site.

Observing the multiple applications, present work aims to explore the activity of nitric oxide releasing acrylic adhesive, its influence on microcirculation, antibacterial effects and structural alterations of human skin to make the foundations of potential future translation into clinical practice taking advantage of nitric oxide unique properties in wound healing process and potential combination with RNA delivery.

5.2 MATERIALS AND METHODS

5.2.1 Materials: Unless noted all reagents were used from Sigma-Aldrich. Porcine skin was harvested from local slaughterhouse, dissected and kept at 4 degrees for a maximum of one week until use.

5.2.2 Synthesis of A72-SNO polymer: A72NO was synthetized by radical polymerization of butyl acrylate(1eq) and hydroxyethyl acrylate (2eq) in dioxane at 15% weight using AIBN (6mg/ml) as radical source. polymer was esterified using DCC (2eq), DMAP(0.04eq) as catalyzer and S-nitrosocarboxylic acid(2eq) for 16h at a dilution larger than 5% solids. Once esterified polymer was centrifuged to eliminate DCU, concentrated and AcOEt was added to crystalize DCU and kept at -32 ^{o}C. Polymer was kept at -32 ^{o}C for at least 3 months until use. At room temperature polymer was unstable with a large tendency to gel. FTIR-ATR: 1646 cm^{-1} (NO stretch), 1731 cm^{-1} (C=O stretch), 3367cm^{-1} (OH stretch).

5.2.3 Peel experiments: Samples of adhesives were cut at 20mm with and attached to volunteer forearms and peeled at 10mm/s and an angle degree of 180. Peel force was registered as mean force during the experiment.

5.2.5 Tack characterization: Tack was measured using a rolling ball test inspired in ASTM D3221. Samples of adhesives were placed within final configuration over a flat surface. Then rolling ball was allowed to fall from a specified height and the distance traveled over the adhesive was registered as result. The stainless steel balls were cleaned with acetone and ethyl acetate prior to next use.

5.2.6 MVTR: Permeation of the material was evaluated by the mobile vapor transfer rate method based on the ASTM E96. Samples were placed in stainless steel containers filled with a known quantity of water. Incubation at 37 degree during a specific time and difference in weight served to calculate the water evaporated though the exposed area.

5.2.7 NO delivery over Agar plate: A72-SNO was placed over an agar plate, after 2 hours Griess reagents were added and images were collected.

5.2.8 Ex vivo porcine skin NO delivery: 10x10 mm skin patches of porcine belly were dissected and disinfected with a 70% ethanol wipe prior to adding 100µm A72NO 4 mm patches to the skin and covering with a polyurethane film. Accelerated delivery was tested by incubating the samples during 24 hours at 50 degrees and further analysis of nitrite generation by Griess Method. Skin samples were imaged, were purple color was indicative of nitrite generation supernatant was also measured by UV-VIS spectroscopy to quantify total nitrite delivery.

5.2.9 Ex vivo porcine A72NO antibacterial properties: 10x10 skin parches from belly of young porcine specimens <1 year were dissected and kept in the fridge for up to a week since sacrifice. Specimens were cleaned with saline and disinfected with 70% ethanol wipes. Surface disinfected skin specimens were covered with a polyurethane adhesive dressing and A72NO 4mm patches and control patches to evaluate antibacterial properties. Samples were left at 28 degrees for 24 hours and skin patches were contact

transferred to an agar and agar-blood plate and left overnight at 34 degrees to evaluate inhibition capabilities of skin microbiota imaged and counted.

5.2.10 In vivo Porcine skin experiments: Patches 10247. Histology evaluation of the skin sections treated were dissected and fixed in formaldehyde sent to embed in paraffin sections stained by H&E method and evaluation of the histopathologly (Laboratorio Echevarne. Barcelona, Spain).

5.2.11 TEWL measurements: Trans epidermal water loss were made using a Dermalab TEWL equipment from Cortex Denmark. Measurements were performed in the fore arm of healthy volunteers by setting the TEWL probe into the skin and letting to equilibrate until the measurement was stable with a standard deviation <0.4 g/m^2h. Skin locations were drawn in skin with a marker pen. Skin stripping was performed by stripping tape over skin a single time and 25 times. A skin cream (Nivea for man) was added to skin at approximately 10 $\mu L/cm^2$. Experiments were repeated keeping conditions at 55±10% relative humidity and 22±2°C.

5.2.12 Skin histology: Samples were fixed in formaldehyde for 48h and dehydrated using a sequence of Ethanol concentrations finishing with 100% ethanol. Then samples were incubated in Xylene and finally embedded in paraffin. Sections were sliced using a Leica RM2235 manual microtome and stained with Hematoxilin and eosyn.

5.2.13 Dermal echography: Skin was explored using an echograph (MyLab™25Gold, esaote, Barcelona, Spain) and a flat 4cm dermal probe of 12MHz for structural evaluation and doppler measurement for blood flow inspection.

5.2.14 LDPM measurements: Dermal microcirculation was measured using a Laser Doppler perfusion measurement equipment Periflux 5000 (Perimed, Sweden) coupled with 443 probes. Measurements were carried out by attaching the probe to selected areas of 10 centimeters distal to the cubital fossa in hairless or previously shaved forearms. Measurements were taking with an integration of 1 second and allowed to stabilize for at least 20 seconds. Individuals were asked to stay in a room at 22±2°C WITH RH of 50±10% for 10 minutes with the skin uncovered prior to measurment.

5.2.15 Phase 1 clinical trial: 25 healthy volunteers are being relucted to evaluate the antimicrobial and dermal impact of A72NO to healthy skin. Clinical investigation has passed the CEIC (Clinical ethical Investigation committee) of the University Hospital of Mutua de Terrassa in Barcelona, Spain with approved code (4413). The following criteria were followed. Inclusion criteria: volunteers were required to be adult (>18 years old) by the time of participation and do not present any chronic or serious health condition as inclusion criteria.

Exclusion criteria: volunteers that did not sign of the informed consent, were allergic, hypersensitive to polyurethane or acrylic adhesives or had any other incompatibility such as (were participating in other study, being pregnant or having had previous skin conditions) were used as exclusion criteria to participate in the study.

Healthy volunteers were informed with the information form present in the protocol and asked to sign the informed consent documents previous to any action. Prior to

placement of the patches, skin was disinfected with 70% alcohol wipes. Afterwards control and patches of A72NO were added to the back of volunteers using polyurethane dressing (Oper film protect, IBERHOSPITEX S.A. Lliçà de Vall, Spain) as fixative. After three days, the dressings were removed, and samples were collected using a cotton swap previously humidified to transfer skin microbiome to an agar plate. Swaps were made for 30 seconds pressing in the treated area and then transferring for 30 seconds in the agar plate. After it, images of the treated areas were taken with a dermal stereomicroscope and finally microcirculation LDPM and TEWL measurements were carried out as previously described. Upon medical special requirement biopsies and OCT images of the treated areas were taken and analyzed.

5.2.16 Statistical analysis: Data were analyzed using GraphPad® Prism. Comparisons between groups were done by one-way ANOVA using Turkey *post-hoc* test. Differences were considered significant when $p<0.05$ *, $p<0.01$**, $p<0.001$*** and ns=non significant.

5.3 RESULTS AND DISCUSSION

5.3.1. Material characterization

Synthesis of A72NO was inspired in widely used hydrophobic acrylic polymers used as skin adhesives for tapes and wound dressings. Typically, those polymers are composed of hydrophobic acrylate monomers such as 2-ethylhexylacrylate, butyl acrylate or octyl acrylate among others. Those monomers have low glass transition temperatures allowing mechanical energy dissipation necessary for room temperature pressure-sensitive adhesive behavior. A72NO has been developed to be adhesive, release nitric oxide and be permeable to water vapor. The polymeric backbone of A72NO was produced from poly butyl acrylate copolymerized with hydroxyethyl acrylate, p(BAcoHEA) was developed to have limited cohesion with a short molecular weight of 40-60kDa (data not shown). Further extension of alcohols with S-nitrosomercaptoaliphatic acids and subsequent crosslink increased the elastic modulus producing a viscoelastic adhesive material dependent on the degree of crosslink. In Figure 5.3.1.1.A the typical absorbance spectra of primary SNO is observed as well as partial esterification of p(BAcoHEA) leaving free hydroxyl moieties. Material was found to have a characteristic deep red color characteristic of SNO moietites.

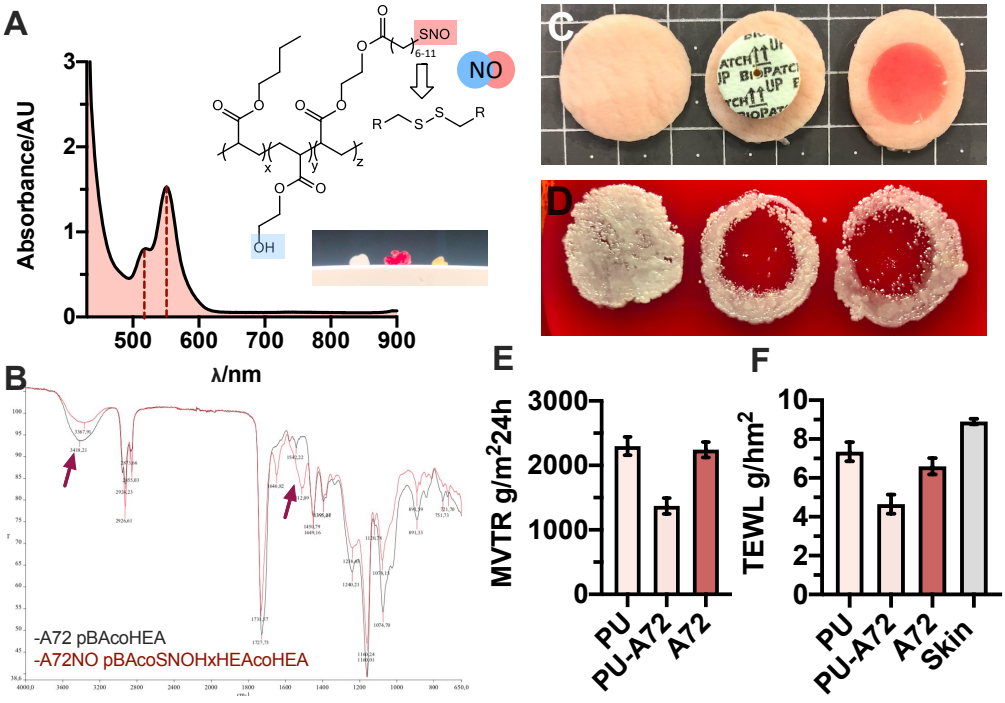

Figure 5.3.1.1. Characterization of A72NO properties. A, UV-VIS spectra of the polymer containing the primary showing the characteristic SNO absorption bands and structure. Image shows; p(BA-co-HEA) (white), A72NO (red) and A72NO after releasing all the nitric oxide (yellow). B, FTIR spectra of p(BA-co-HEA) and A72NO. C, study of antimicrobial properties in *ex vivo* porcine model models of Control, CHG and A72NO and growth in an agar plate D. E, evaluation of the permeability of A72NO *in vitro* and F, on line trans epidermal water loss.

Adhesive properties were dependent on the degree of crosslink between thionitrite moieties evolving from an elastic viscoelastic material to a crosslinked flexible material elastomer with very limited tack (data not shown). Adhesiveness of the material was important to allow for intimate contact and enhancement of local NO concentration in the skin-adhesive interface.

The partial modification of hydroxyethylacrylate (HEA) was observed by a reduction in the FTIR band of OH stretching band beyond. Leaving unesterified alcohols allows for higher hydrophilicity (Figures 5.3.1.1E-F) MVTR and subsequent higher release of NO make the material responsive to accumulation of liquids that usually are accompanied by bacterial expansion.

Although extensively used together with antimicrobial surface decontamination, most adhesives used nowadays fail to protect against opportunistic microflora that remains in inaccessible skin reservoirs such as sweat glands and follicles. Those hidden bacteria repopulate extensively after 3-5 days enhancing the risk of suffering infections[23]. It is described that more than 60% of infections are related to strains from skin microflora[24], suggesting that migration from skin to vasculature causes the infections. Chain extension length of the carboxylic acid was studied to adapt a short release rate to 2-7 days following the guidelines of film dressing use[25]. Final samples were selected with S-nitroso-hexanoic acid due to faster release rates than longer chain extenders although release rate seemed to be heavily influenced by the presence of hydrophilic monomers. Antimicrobial effect in porcine belly *ex vivo* model (Figure 5.3.1.1.C-D) was found to be similar to commercial patches containing CHG.

5.3.2 Ex vivo and in vivo animal studies

A series of experiments were planned to assess the delivery of nitric oxide, reduction of bacterial load and dermal response to release nitric oxide from A72NO, see Figure 5.3.2.1. First, porcine skin was selected as an *ex vivo* model to evaluate the delivery of nitric oxide to the skin. An accelerated model was developed incubating patches of material and skin at 50 degrees Celsius to avoid tissue decomposition. In Figure 5.3.2.1.A-C a series of A72NO patches with different doses of nitric oxide show a dose-dependent release of nitric oxide to the skin and solution. Delivery of nitric oxide was also stablished by exploration of dermal response in porcine skin and incubating the material in an agar plate and reacting with Griess reagents (data not shown) showing a local effect only due to short NO half-life.

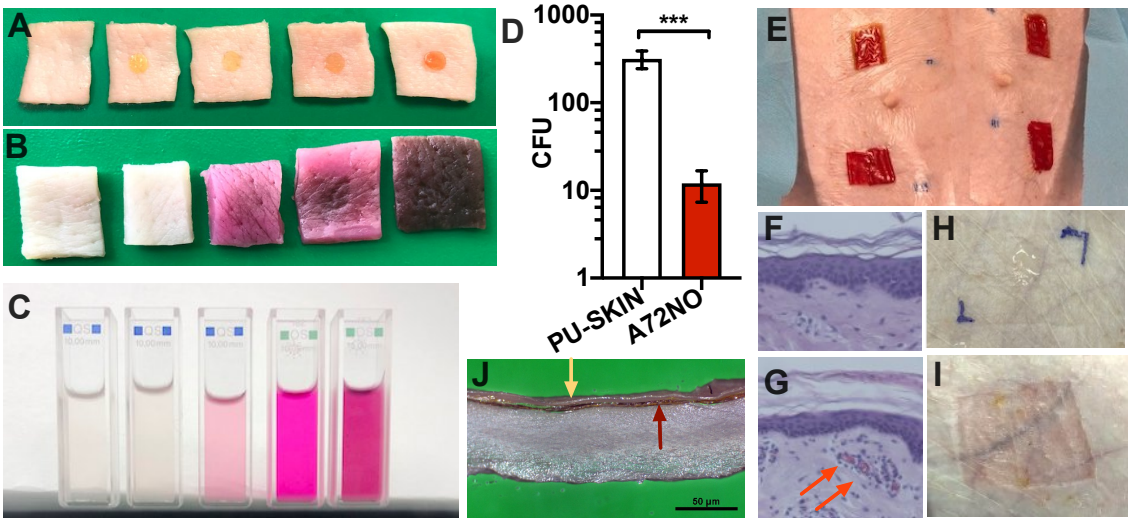

Figure 5.3.2.1. Evaluation of nitric oxide delivery to skin models, skin microorganisms and histologic response. A, Porcine skin sections with A72 sections with variable increasing NO content (left to right). B, Results after incubation and immersion in Griess solution of the skin sections and remnant solution, C. D, Evaluation of skin microbiota of sections placed over porcine belly and controls, E. F,G Histologic sections of controls and treated sections, arrows suggest dilated blood vessels in the treated section. H, example of topical reaction to A72NO low dose and high dose I. J Histologic cut showing the polyurethane (clear layer pointed by the yellow arrow), the A72NO (red layer, pointed by red arrow) and epidermal and dermal tissues.

Application of the materials to porcine belly skin showed a significant reduction of bacterial burden of 1.5 log in the application site (Figure 5.3.2.1.D). Dermal response showed no pathological signs rather than a slight hyperemia consistent with the local delivery of nitric oxide, larger doses of nitric oxide produced a stronger delivery a higher hyperemia reaction (Figure 5.3.2.1.I). Histology showed no noticeable events and a possible higher vasodilation in the A72NO treated group, see Figure 5.3.2.1.F-G. Experiments served to set up and validate the safety and efficacy and local response to A72NO as a first step towards evaluation in human skin. Similar results have been reported by Nye *et al*[26] showing and equivalent reduction of bacterial burden. Nitric oxide load and kinetics can be modified by preheating the samples or using a diffusion control barrier. As shown, nitric oxide load did not show significant short-term side effects.

5.3.3 Validation of methods to evaluate safety and efficacy

Prior to clinical evaluation of the A72NO material, all non-invasive methods intended to be used were validated with experimental controls to avoid method related inaccuracies. Laser doppler perfusion measurements (LDPM) was selected as microcirculation measuring technique due to its non-invasiveness and suitability to evaluate local effect of nitric oxide in skin. Structural alterations of skin were evaluated

by trans epidermal water loss (TEWL) due to its non-invasiveness and indirect information given to evaluate the stratum corneum.

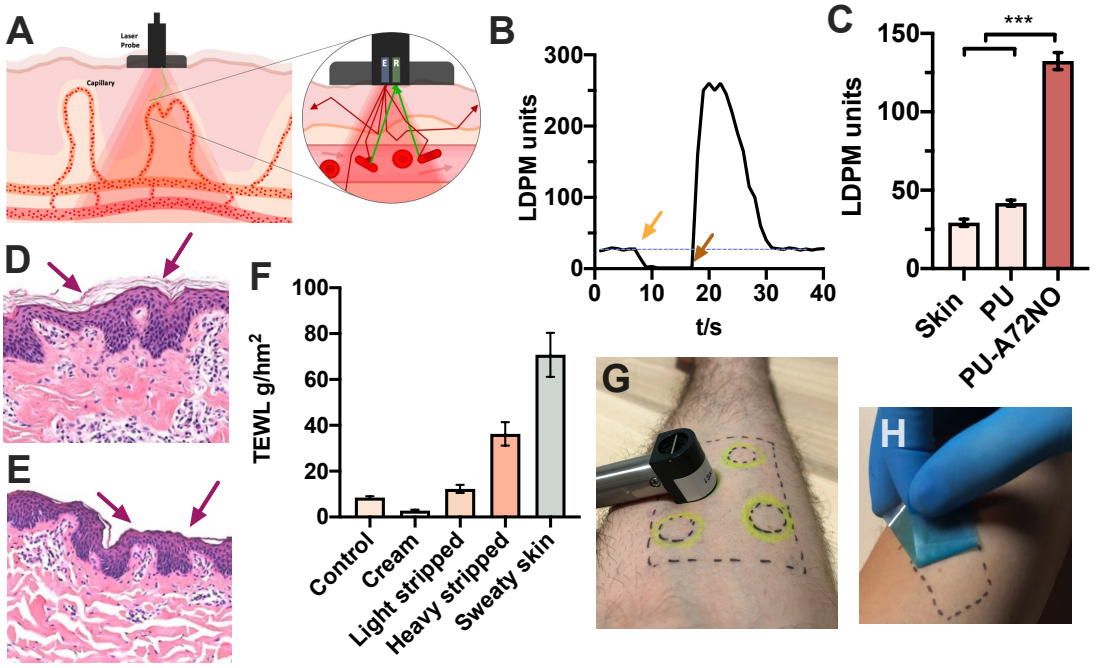

Figure 5.3.3.1. Validation of experimental techniques used in skin characterization. A, scheme of the measurement of dermal microcirculation by laser doppler perfusion technique of scattered erythrocytes of skin capillaries. B, validation experiment of microcirculation, blocking of blood flow by a cuff (yellow arrow) and liberation (brown arrow) correlates with microcirculation. C, Proof of concept experiment of LDPM of A72NO for 24h. D and E, examples of normal skin(D) and stratum corneum stripped(E). F, Trans epidermal water loss of several groups to validate the method. G, Example of TEWL measurement into human skin. H, Skin stripping method used. All results are shown as mean plus minus the standard error mean. * $p<0.05$, ** $p<0.01$, ***$p<0.001$.

LDPM validation was carried out by measuring the forearm skin and blocking the circulation with a cuff (Figure 5.3.3.1), measurement dropped to 0 after a few seconds after blocking until the cuff was freed, increasing drastically the blood flow for some seconds and recovering after a few seconds initial values. After LDPM gave consistent results a first preliminary study with A72NO was evaluated (Figure 5.3.3.1.C). The NO releasing patch was fixed with a polyurethane film adhesive and kept for 48h in an equivalent manner following the method described in the protocol. Skin covered with PU gave a slightly higher value, probably caused by the removal of the adhesive dressing, in contrast A72NO gave a 3-fold increase in blood perfusion that is associated with the local effect of nitric oxide. As results were consistent with similar experiments[27].

Trans epidermal water loss results were consistent with literature[28] and presence of structural stratum corneum in the skin. Skin treated with oily cream was the lowest value and stripping gave results consistent with the degree of skin removal of oily layers leading to further water loss as indicated by the porcine histological sections (Figure 5.3.3.1.D-E).

5.3.4. Phase I clinical results

A total of 8 healthy individuals have been recruited until present date to participate in the INFUSE-NOx phase I clinical trial aiming to evaluate the A72NO antibacterial properties and dermal response. The volunteer sample was attempted to represent a real world population with unbiased age, gender and previous skin conditions representing the population of a southern European country. Study scheme can be observed in Figure 5.3.4.1.A

During the experiment, no major dermal events have been reported and only minor responses, such as slight itching or slight erythema, have been observed while none of the events required medical attention. Dermal response has been observed to be stronger in younger than older volunteers.

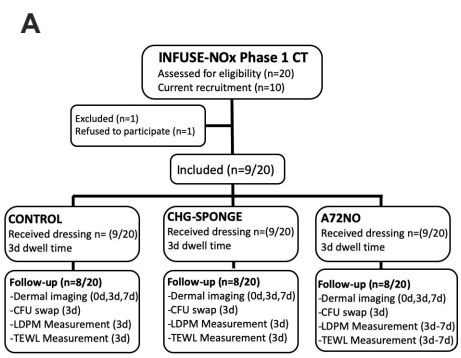

B SUMMARY

Participants	8/20
Age	49 (36-84)
Sex (% females)	38%
Previous skin condition	
Carcinoma	25%
Melanoma	13%
Other	12%
Skin tone*	2.6
Skin condition	
Normal	64%
Dry	24%
Highly dry	12%
**Fritzpatrik scale*	

C CLINICAL FOLLOW-UP

	CONTROL	A72NO	CHG	p
Skin Injury				
Erhytema Score	0	1.1	0.1	n/a
Delayed Erythema (1d)	0	1-100%	0.1	n/a
Delayed Erythema (7d)	0	0	0	n/a
Blanchable	n/a	YES	n/a	n/a
Blanchable (7d)	n/a	YES	n/a	n/a
Develops tan	0%	75%	0%	n/a
SC discamation (7d)	0%	0%	0%	n/a
Swelling	0%	0%	0%	n/a
Blistering	0%	0%	0%	n/a
Pruritus				
None	0%	80%	75%	n/a
Unlocaliced	0%	20%	15%	n/a
Rash	0%	0%	10%	n/a
Major dermal events	0%	0%	0%	p=1

Figure 5.3.4.1. Summary of volunteer's clinical parameters and preliminary results of clinical follow-up of the patches.

Preliminary results show a significant reduction larger than 10 times in the reduction of skin bacteria comparable to well stablished antibacterial dressings containing chlorhexidine digluconate (Figure 5.3.4.2.A-C). The antibacterial effect is highly influenced by multiple factors such as the microflora level, physical activity or skin dryness among patients, but the reduction was sustained in all cases.

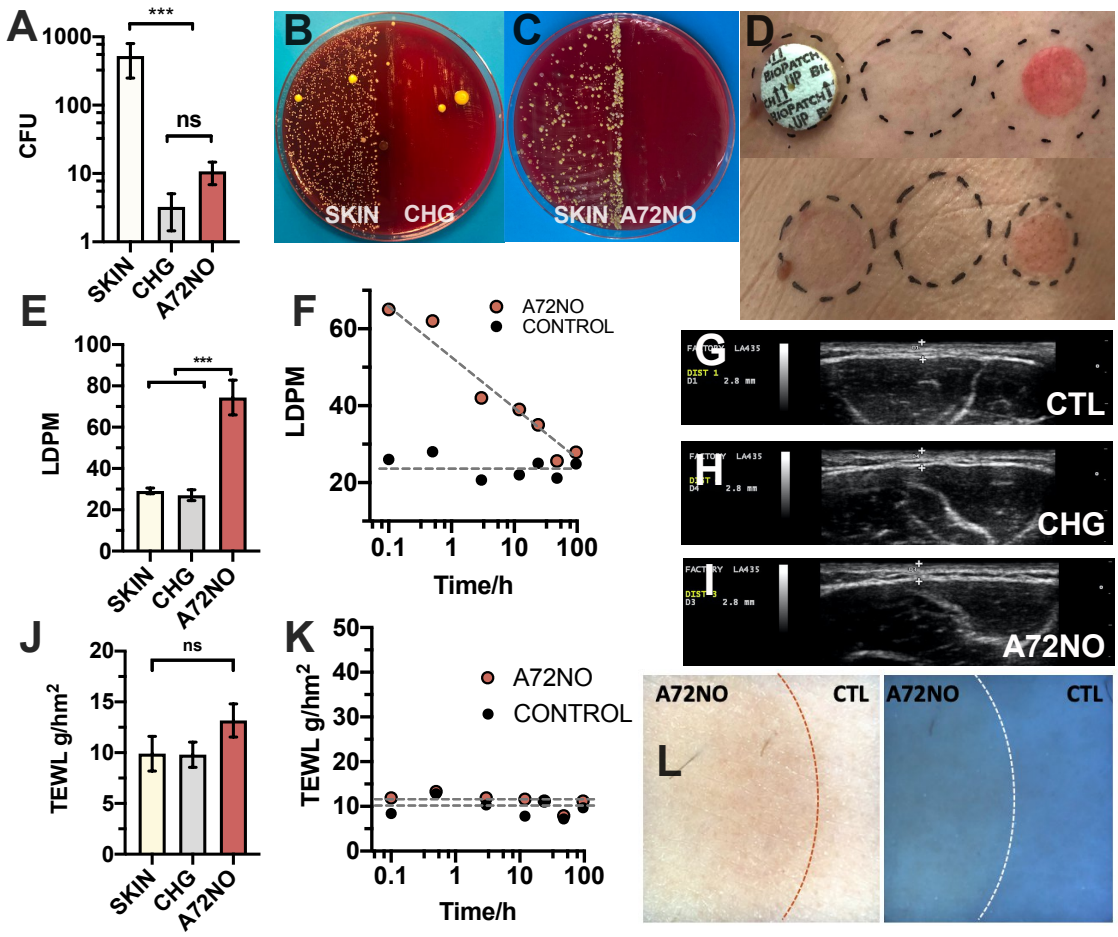

Figure 5.3.4.2. Summary of experimental preliminary results of the phase I clinical trial. A, Bacterial reduction of skin treated with experimental group and control. B-C, examples of petri dishes showing microorganism growth of untreated skin and CHG or A72NO. D, example of the experimental groups on a volunteer. E, microperfusion experiments performed at dressing removal and LDPM evolution over time after removal F. G-I dermal echography of skin with the different dressings before removal. J, evaluation of TEWL after dressing removal and evolution with time K. L, Evaluation of macroscopic epidermal response under visible light and Wood lamp (365nm). Histograms are plotted as mean ± SEM. Significant differences between the groups: * $p < 0.05$, ** $p<0.01$, *** $p < 0.001$ and ns=non-significant.

Nitric oxide releasing A72NO, has been found to significantly increase microcirculation of surface vessels such as dermal papillae or loops, and potentially deeper micro-vessels, such as dermal and subdermal plexus (Figure 5.3.4.2.E-F), exploration with doppler effect echography did not show significant blood flow in deeper tissues suggesting that the effect was limited to superficial epidermal layers. The increase in microcirculation is gradually loosed during the following days showing a delayed and sustained effect for up 2 to 4 days. This effect is consistent with slight erythema that was observed in some volunteers caused by local hyperhemia, similar results have been observed in other systems to develop topically nitric oxide[29].

The reduction of the bacterial load and increase of microcirculation has not been observed to alter alteration the structure of skin in any of the experimental groups after exploration by TEWL and dermal echography (Figure.5.3.4.2.G-K), none of the patients have been observed to peel skin in the treated zones. Imaging of skin did show moderate erythema formation in the A72NO group, (Figure.5.3.4.2.L). The local inflammation was susceptible to blancheability after applying pressure supporting the response related to increased local blood flow induced by local nitric oxide effect.

It was also observed that some patients developed a slight tanning response after hyphemia decreased in a manner similar to sunlight exposure but without developing skin peeling. Exposure of skin to UV sunlight is usually followed by delayed erythema, tanning and ultimately peeling of stratum corneum. Irradiation of skin with UV light generates a stimulation of NOS and enhanced NO production altogether with prostacyclin expression, it is suggested that an external dose of NO may induce a similar reaction leading to tanning of skin without peeling due to no irradiation related damage has been induced[30]. A72NO was also studied previously heating overnight at 80^{o}C losing all the NO. It did not show any erythema, LDPM increase or dermal response assuming that all the dermal effect was associated to nitric oxide release only.

Recruitment has been altered by the COVID-19 pandemic limiting the recruitment date, but the study continues up to date.

This kind of novel adhesive, antimicrobial and enhancer of blood flow could be highly beneficial to treatment of skin or health disorders that alter natural healing mechanisms such as vascular disorders, neuropathy or diabetes.

The developed material could also be adapted to be administered together with oligonucleotides and pBAE for the treatment of wounds. It could combine the potential effect of nitric oxide reducing the harm of opportunistic microorganisms, the microcirculation boost and the specific effect of siRNA or miRNA altering temporarily the expression patterns of pro-healing pathways. In that sense a series of proof of concept experiments have been done to evaluate adhesion over skin, obtaining a high adhesiveness in a similar way than epithelial surfaces explored in previous chapters. How viable is the direct administration of RNA and pBAE over open wounds would have to be addressed in the future.

5.4 CONCLUDING REMARKS

A nitric oxide releasing adhesive has been found to be permeable to water moisture, improve local circulation and inhibit bacterial growth in several models. The material, A72NO, is based on an amphiphilic polyacrylate combining free hydroxyls, hydrophobic and thionitrite side chains.

The combination of side chains allows the material to be highly permeable, self-crosslink due to the tendency of the SNO side chains to generate disulfide bonds while releasing nitric oxide and producing antimicrobial effects. It has been found both *ex vivo* and *in vivo* that the antimicrobial effect is comparable to well stablish antimicrobial agents. Besides the effect of nitric oxide in bacteria, a vasodilation effect has been found in a dose-dependent manner.

Finally, preliminary results in a phase I voluntary clinical trial seem to confirm that in a real-world population A72NO induces a slight erythema being attributed to nitric oxide alone due to its vasodilation capabilities. The treatment does not induce an alteration of dermal structure both confirmed by ultrasound and trans-epidermal water loss.

Results lead to suggest that its benefits could lead to further developments combining the potential nitric oxide responses with increasing the expression of healing pathways of skin disorders and potentially even with RNA therapeutics.

5.5 REFERENCES

[1] Byrd, A. L., Belkaid, Y., & Segre, J. A. (2018). The human skin microbiome. Nature Reviews Microbiology, 16(3), 143–155. doi:10.1038/nrmicro.2017.157

[2] E. Lawrence, SD Brain, (1992) Responses to endothelins in the rat cutaneous microvasculature: a modulatory role of locally-produced nitric oxide. Br. Pharmacol. 106 (1992) 17-21

[3] JD Coffman,(1994) Effects of endothelium-derived nitric oxide on skin and digital blood flow in humans. Am J. Physiol 267 (1994) H2087-H2090

[4] JB Warren, RK Loi, ML Coughlan. (1993) Involvement of nitric oxide synthase in the delayed vasodilator response to ultraviolet light irradiation of rat skin in vivo. Br. J . Pharmacol. 109 (1993) 802-806

[5] Efron DT, Most D, Barbul A. Role of nitric oxide in wound healing. Curr Opin Clin Nutr Metab Care. 2000;3(3):197-204. doi:10.1097/00075197-200005000-00006'

[6] Witte MB, Barbul A. General principles of wound healing. Surg Clin North Am. 1997;77(3):509-528. doi:10.1016/s0039-6109(05)70566-1

[7] MR Schaffer, U. Tantry, RA van Wesep, A. Barbul (1997) Nitric oxide methabolism in wounds. J. surg. Res. 71 (1997) 25-31.

[8] Frank S, Kämpfer H, Wetzler C, Pfeilschifter J. Nitric oxide drives skin repair: novel functions of an established mediator. Kidney Int. 2002;61(3):882-888. doi:10.1046/j.1523-1755.2002.00237.x

[9] Malone-Povolny MJ, Maloney SE, Schoenfisch MH. Nitric Oxide Therapy for Diabetic Wound Healing. Adv Healthc Mater. 2019;8(12):e1801210. doi:10.1002/adhm.201801210

[10] Gómez-Romero FJ, Fernández-Prada M, Navarro-Gracia JF. Prevention of Surgical Site Infection: Analysis and Narrative Review of Clinical Practice Guidelines. Prevención de la infección de sitio quirúrgico: análisis y revisión narrativa de las guías de práctica clínica. Cir Esp. 2017;95(9):490-502. doi:10.1016/j.ciresp.2017.09.004

[11] Haagsma JA, Graetz N, Bolliger I, et al. The global burden of injury: incidence, mortality, disability-adjusted life years and time trends from the Global Burden of Disease study 2013. Inj Prev. 2016;22(1):3-18. doi:10.1136/injuryprev-2015-041616

[12] Bjarnsholt T, Kirketerp-Møller K, Jensen PØ, et al. Why chronic wounds will not heal: a novel hypothesis. Wound Repair Regen. 2008;16(1):2-10. doi:10.1111/j.1524-475X.2007.00283.x

[13] Richmond NA, Maderal AD, Vivas AC. Evidence-based management of common chronic lower extremity ulcers. Dermatol Ther. 2013;26(3):187-196. doi:10.1111/dth.12051

[14] Kasiewicz LN, Whitehead KA. Recent advances in biomaterials for the treatment of diabetic foot ulcers. Biomater Sci. 2017;5(10):1962-1975. doi:10.1039/c7bm00264e

[15] Ghaffari A, Neil DH, Ardakani A, Road J, Ghahary A, Miller CC. A direct nitric oxide gas delivery system for bacterial and mammalian cell cultures. Nitric Oxide. 2005;12(3):129-140. doi:10.1016/j.niox.2005.01.006

[16] Ghaffari A, Jalili R, Ghaffari M, Miller C, Ghahary A. Efficacy of gaseous nitric oxide in the treatment of skin and soft tissue infections. Wound Repair Regen. 2007;15(3):368-377. doi:10.1111/j.1524-475X.2007.00239.x

[17] Major TA, Panmanee W, Mortensen JE, Gray LD, Hoglen N, Hassett DJ. Sodium nitrite-mediated killing of the major cystic fibrosis pathogens *Pseudomonas aeruginosa*, *Staphylococcus aureus*, and Burkholderia cepacia under anaerobic planktonic and biofilm conditions. Antimicrob Agents Chemother. 2010;54(11):4671-4677. doi:10.1128/AAC.00379-10

[18] Edmonds ME, Bodansky HJ, Boulton AJM, et al. Multicenter, randomized controlled, observer-blinded study of a nitric oxide generating treatment in foot ulcers of patients with diabetes-ProNOx1 study. Wound Repair Regen. 2018;26(2):228-237. doi:10.1111/wrr.12630

[19] Phillips R, Adjei O, Lucas S, Benjamin N, Wansbrough-Jones M. Pilot randomized double-blind trial of treatment of Mycobacterium ulcerans disease (Buruli ulcer) with topical nitrogen oxides. Antimicrob Agents Chemother. 2004;48(8):2866-2870. doi:10.1128/AAC.48.8.2866-2870.2004.

[20] Vogt C, Xing Q, He W, Li B, Frost MC, Zhao F. Fabrication and characterization of a nitric oxide-releasing nanofibrous gelatin matrix. Biomacromolecules. 2013;14(8):2521-2530. doi:10.1021/bm301984w

[21] Kim JO, Noh JK, Thapa RK, et al. Nitric oxide-releasing chitosan film for enhanced antibacterial and in vivo wound-healing efficacy. Int J Biol Macromol. 2015;79:217-225. doi:10.1016/j.ijbiomac.2015.04.073

[22] Lowe A, Bills J, Verma R, Lavery L, Davis K, Balkus KJ Jr. Electrospun nitric oxide releasing bandage with enhanced wound healing. Acta Biomater. 2015;13:121-130. doi:10.1016/j.actbio.2014.11.032

[23] Callahan JL, Wesorick B. Bacterial growth under a transparent dressing. Am J Infect Control. 1987;15(6):231-237. doi:10.1016/0196-6553(87)90116-7

[24] Safdar N, Maki DG. The pathogenesis of catheter-related bloodstream infection with noncuffed short-term central venous catheters. Intensive Care Med. 2004;30(1):62-67. doi:10.1007/s00134-003-2045-z

[25] Guidelines for the Prevention of Intravascular Catheter-Related Infections, CDC Centers for Disease Control and Prevention Department of health and human services-USA 2011.

[26] Nye R, Robinia K, Peterson P, et al. Efficacy of a nitric oxide dressing in decreasing bacterial counts on human skin. J Wound Care. 2018;27(Sup7):S19-S25. doi:10.12968/jowc.2018.27.Sup7.S19

[27] Seabra AB, Fitzpatrick A, Paul J, De Oliveira MG, Weller R. Topically applied S-nitrosothiol-containing hydrogels as experimental and pharmacological nitric oxide donors in human skin. Br J Dermatol. 2004;151(5):977-983. doi:10.1111/j.1365-2133.2004.06213.x

[28] Alexander H, Brown S, Danby S, Flohr C. Research Techniques Made Simple: Transepidermal Water Loss Measurement as a Research Tool. J Invest Dermatol. 2018;138(11):2295-2300.e1. doi:10.1016/j.jid.2018.09.001

[29] Mowbray M, Tan X, Wheatley PS, Rossi AG, Morris RE, Weller RB. Topically applied nitric oxide induces T-lymphocyte infiltration in human skin, but minimal inflammation. J Invest Dermatol. 2008;128(2):352-360. doi:10.1038/sj.jid.5701096

[30]Lassalle MW, Igarashi S, Sasaki M, Wakamatsu K, Ito S, Horikoshi T. Effects of melanogenesis-inducing nitric oxide and histamine on the production of eumelanin and pheomelanin in cultured human melanocytes. Pigment Cell Res. 2003 Feb;16(1):81-4. doi: 10.1034/j.1600-0749.2003.00004.x.

CHAPTER 6: CONCLUSIONS

Non-viral vectors based on pBAE with NO releasing properties have been developed and studied for local delivery therapies. Those vectors have been found to be safe and effective *in vitro* and in preclinical models.

Firstly, objective 1 and 2 have been fulfilled by developing pBAE containing nitric oxide delivery capabilities. This objective has been achieved by adding nitric oxide donors to the backbone of previously well stablished pBAE, forming safe and effective non-viral vectors.

- Derivatization of pBAE with organic nitrates have been found to be viable strategy to obtain stable nitric oxide releasing molecules with minimal cross-reactivity. Thionitrite introduction yielded slightly fewer stable polymers and introduction of diazeniumdiolates and organic nitrites was not found to be a viable strategy.
- Synthetized non-viral vectors containing nitrooxy moieties have been found to form stable nanoparticles with a broad variety of nucleic acids, being at least as stable as equivalent pBAE. Nanoparticles have been also able to modify protein expression *in vitro* through siRNA, mRNA and DNA transfection.
- Infusion of nanoparticles in rats have been found to significantly induce a sustained decrease in blood pressure due to the introduction of nitric oxide donors. The mechanisms that induce the pressure decrease have not been unravel, but high adhesion to blood vessels have been observed *in vivo*.

Secondly, objective 3 has been fulfilled by developing several strategies to locally deliver non-viral vectors. Applications have been focused to several cardiovascular therapies in an attempt to take advantage of the iRNA technology and NO therapeutic potential within the vascular environment.

- A perfusion balloon has been developed to locally deliver nanoparticles to target lesions of the cardiovascular system, being able to track the release of nanoparticles to tissues.
- Drug eluting balloons, and drug eluting stents have been developed including the nanoparticles developed containing pBAE, RNA and NO.
- An intravascular system to locally inject nanoparticles in the myocardium or other locations, has been found to be an effective way to locally inject nanoparticles.

Lastly, objective 4 has been achieved by dedicating polymers containing thionitrite moieties towards applications where antibacterial effects may be needed taking an

advantage of the straightforward delivery of nitric oxide without requiring enzymatic activity.

- T64SNO, a SNO containing pBAE has been found to self-crosslink due to homolysis and sustain the release of NO during months.
- A coating system has been developed to coat silicone covered airway stents using atmospheric plasma to improve adhesion.
- The coating system has been found to effectively limit the growth of pathological *S. aureus* and *P. aeuruginosa in vitro,* while showing equivalent levels of toxicity towards bacteria and mammalian cells.
- In *ex vivo* models, it has been observed that the introduction of the coating allowed a limit of the bacterial growth in the surface of the prothesis.
- Additionally, a polymer inspired in PSA acrylates have been developed and studied for dermal applications. It has been found to limit the growth of bacteria in skin, in an equivalent way to well stablished antibacterial systems. It has also been found that the NO delivered is the cause of the antibacterial effect and a higher blood perfusion is also induced. Those results have been found *ex vivo*, in preclinical models and in phase I clinical trials.

Although current work shows promising results limiting the growth of microorganisms mediated by NO, further research needs to be completed to prove if those preliminary findings can be translated into relevant clinical outcomes.

ANNEX I. DEVELOPMENT OF A HIGH PRESSURE REACTOR FOR DIAZENIUMDIOLATE SYNTHESIS

AI.1 INTRODUCTION

Since its discovery in 1965 diazeniumdiolates have been sequentially increasing its interest to the scientific community due to its ability to store chemically nitric oxide and released in aqueous media and under temperature and especially acidic conditions. Those unusual moieties with three consecutive nitrogen atoms bonded, have been obtained since its discovery[1][2] by treating secondary amines with nitric oxide under basic and high pressure of nitric oxide. The importance of diazeniumdiolate synthesis increased dramatically in the late 80s when nitric oxide was discovered to be a critical signaling molecule in the maintenance of vascular homeostasis, antibacterial mechanisms and neural signaler [3,4,5].

Synthesis of diazeniumdiolates have been successfully obtained by the use of Parr reactors involving high pressure. At present work a dedicated reactor with multiple features of control is expected to be constructed for the synthesis of non-viral vectors with nitric oxide adducts incorporated. Having a properly controlled system allows to extrapolate the reaction evolution by controlling the amount of gas that has been reacted with the secondary amines, being able to control pressure, temperature or mechanical stirring.

AI.2 MATERIALS AND METHODS

AI.2.1 Vessel design and construction: The reactor vessel and lid were machined out of 304 stainless steel in the local workshop by means of a manual Lathe and Milling machine. An openable sight glass was incorporated for observation of reaction development. Sight glass mounting was TIG welded and checked for porosity in the weld, and silicone O-rings were used to keep tightness. Valves included were needle-type 1/8 NPT, manufactured out of 316 stainless steel from Swagelok (Ohio, USA).

The temperature is controlled using a digital programable controller (OMRON-E5CB system), one 100W resistance and a dual Pt-100 system to control vessel body and the internal temperature of the reactor. Heating system worked in loop to control the temperature.

Pressure was monitored using a digital pressure transducer with 0-20 Bar range, 0-5V digital response, an accuracy of ±1%, 0-80°C and one external mechanical pressure gauge 0-25 bar (Genebre, Hospitalet, Spain). All electronics were processed using an Arduino system. An electromagnetic steering system was mounted under the main vessel to be compatible with Teflon coated magnet stirrers.

AI.2.2 Vessel resistance validation: Vessel leak resistance was studied by introducing nitrogen during a week at 50°C and evaluation of the pressure in a daily basis.

AI.2.3 Synthesis of NO: Nitric oxide was obtained by reacting 25g of Ferrous sulfate heptahydrate (Sigma-Aldrich) with sodium nitrite (Panreac), 10 grams of H_2SO_4 and

heating at 100°C. The obtained gas was bubbled through a 30% solution of sodium hydroxide and a trap of anhydrous calcium chloride. The obtained gas was stored in a double balloon and injected into the vessel by a multiple syringe injection.

AI.2.4 Proof of concept of NO reaction and evolution: To check the suitability to react with nitric oxide, a series experiments was planned with simple secondary amines such as DETA.

AI.3 RESULTS AND DISCUSSION

AI.3.1 Vessel construction

Construction of the equipment was performed in stainless steel and high-quality borosilicate glass to avoid potential corrosion problems. In Figure AI.3.1, several sketches and images of the reactor are presented. The vessel was welded using tungsten inert gas technique and further checking the tightness under 5 times as much as positive pressure and under vacuum, without leak detection. The heat control system was constructed using two resistances and two Pt-100 sensors to avoid heating inertia.

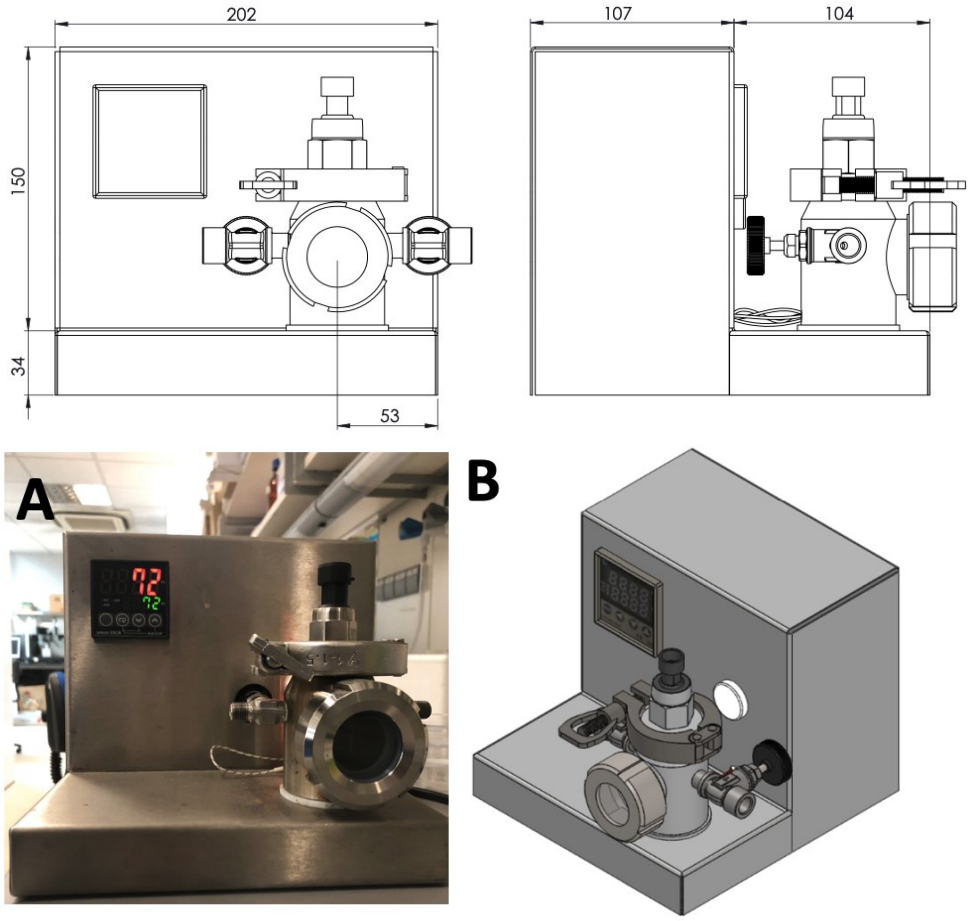

Figure AI.3.1. High pressure vessel reaction for the synthesis of diazeniumdiolate. Top, images of the sketches and bottom, Images of the constructed

The disposition of the temperature sensors was placed immediately close to the heating resistances and in an intermediate zone using both average and independent signals to tune the system. During experiments a neoprene cover was used as insulator. Although not implemented for the experiments, a refrigeration system was also incorporated using a peltier module directly under the vessel to cool down the system. Under the reactor vessel a stirring magnet was also installed to allow stirring during reactions using a magnetic stirrer. In Figure AI.3.1, several sketches and images of the reactor are presented.

AI.3.2 Vessel validation

Prior to experiments, a brief validation was conducted to ensure that the vessel could keep pressures and responses of the pressure monitoring system were linear. To evaluate the pressure stability and potential leaks, the reactor was set at a constant temperature at 10 bar using nitrogen and kept recording the pressure and temperature values for a week. In Figure AI.3.2. the results are presented.

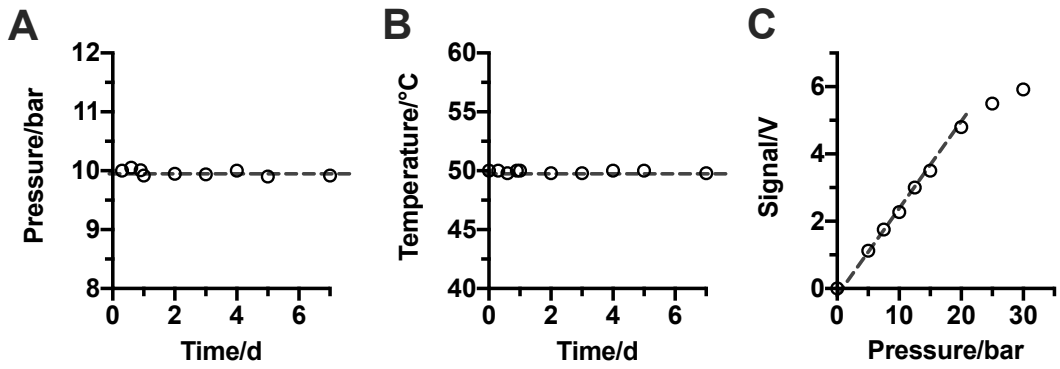

Figure AI.3.2. High pressure reactor validation. A, Pressure against time stability B, temperature stability and C, sensor linear response to pressure

Signal response was found to be linear in the 0-20 bar range, validating that the reductions in pressure will be caused by chemical reactions.

AI.3.3 Proof of concept reaction

Finally, a proof of concept was conducted to study the reaction of nitric oxide and secondary amines to generate diazeniumdiolates in the developed reaction vessel. In Figure AI.3.3 the results are presented.

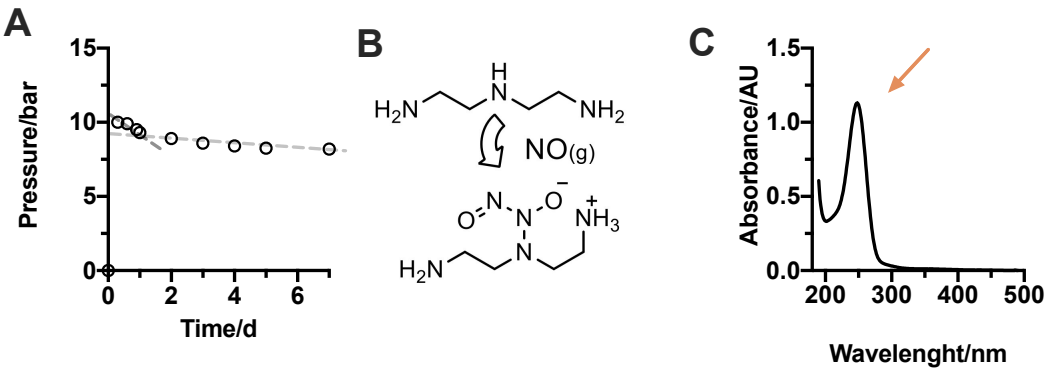

Figure AI.3.3. Proof of concept reaction in the reactor. A, pressure evolution. B, Scheme of the chemical reaction. C, Spectra showing the typical NONOate absorbance at 280nm pointed by the orange arrow.

It can be observed that the reduction in pressure is attributed to the reaction with the secondary amine, forming the NONOate validating the system for further reactions.

AI.4 CONCLUDING REMARKS

The construction of a reactor capable of keeping high pressures, inspect reactions, monitoring pressure and temperature has been fulfilled. The method was found to be useful for generation of small diazeniumdiolates molecules being a reliable tool to follow-up NO fixation reactions.

AI.5 REFERENCES

[1] Drago, R. S., and Karstetter, B. R. (1961) The reaction of nitrogen(II) oxide with various primary and secondary amines. J. Am.Chem. Soc. 83, 1819–1822.

[2] Hrabie, J.A., Klose J.R. (1993) New nitric oxide-releasing zwitterions derived from polyamines. J. Org. Chem. 1993, 58, 1472-1476.

[3Palmer, R. M. J., Ferrige, A. G., Moncada, S. (1987) Nitric oxide release accounts for the biological activity of endothelium-derived relaxing factor. Nature 327, 524–526.

[4] Garthwaite, J., Charles, S. L., Chess-Williams, R. (1988) Endothelium-derived relaxing factor release on activation of NMDA receptors suggests role as intercellular messenger in the brain. Nature 336, 385–388.

[5] Marletta, M. A., Yoon, P. S., Iyengar, R., Leaf, C. D., Wishnok, J. S. (1988) Macrophage oxidation of L-arginine to nitrite and nitrate: nitric oxide is an intermediate. Biochemistry 27, 8706–8711.

[6] Konter J,El-Emam A., Abubo-Rahma G., Lehmann J.(2005). The Notizer- A device for the convenient preparation of diazen-11-um-1,2-diolates. Methods Enzymol.396:17-26